Die Expedition ANTARKTIS VIII/1-2, 1989 mit der Winter Weddell Gyre Study der Forschungsschiffe „Polarstern" und „Akademik Fedorov"

The Expedition ANTARKTIS VIII/1-2, 1989 with the Winter Weddell Gyre Study of the Research Vessels „Polarstern" and „Akademik Fedorov"

Herausgegeben von
Ernst Augstein, Nikolai Bagriantsev und Hans Werner Schenke
unter Mitarbeit der Fahrtteilnehmer

Ber. Polarforsch. 84 (1991)
ISSN 0176-5027

ANT VIII/1 (H.W. Schenke)

1.1 Wissenschaftliche Ziele und Fahrtverlauf

Die *Polarstern*-Expedition ANT VIII/1 vom 5.8. bis 5.9.1989 gliedert sich in zwei Teilabschnitte. Im ersten Teil von Bremerhaven nach Vigo, Spanien, wurden die im Juli 1989 installierten hydroakustischen Vermessungssysteme *Hydrosweep* und *Parasound* kalibriert und anschließend in der Tiefsee-Ebene der Biskaya und am französischen Kontinentalhang erprobt. Die Tiefsee-Erprobung von *Hydrosweep* erfolgte durch Vergleiche der gewonnenen Meßdaten mit den Ergebnissen früherer Fächersonarvermessungen mit *Seabeam* und *Hydrosweep*. Die innere Meßenauigkeit der Fächersonardaten wird durch Wiederholungsmessungen auf ausgewählten Testprofilen abgeleitet.

Schwerpunkte des zweiten Fahrtabschnittes von Vigo nach Puerto Madryn, Argentinien, waren Reichweitenüberprüfungen von *Hydrosweep* und *Parasound* in der Romanche Bruchzone, luftchemische Untersuchungen und Messungen des Ozongehaltes in der unteren Atmosphäre.

Zur Überprüfung der neuen *Hydrosweep*-Anlage wurden unabhängige Vergleichsdaten aus *Seabeam*-Messungen des französischen Forschungsschiffes *Jean Charcot* sowie *Hydrosweep*-Daten der *Meteor* herangezogen. Ein weiteres Ziel der Reise war die Überprüfung und Analyse der Kreuzfächer-Kalibrierung zur Wasserschallkorrektur von *Hydrosweep*-Messungen. Die hierzu notwendigen Spezialuntersuchungen erfolgten in der Tiefsee-Ebene der Biskaya. Zur Überprüfung der aus der Kreuzfächer-Kalibrierung bestimmten mittleren Wasserschallgeschwindigkeit wurden in den Testgebieten CTD- und XBT-Messungen durchgeführt. Vergleiche zwischen den unabhängig bestimmten Schallgeschwindigkeiten ergaben maximale Abweichungen von ±5 m/s. Dieser Wert liegt innerhalb der Meßgenauigkeit von *Hydrosweep*.

Wichtigste Voraussetzung zur Durchführung genauer Meeresbodenvermessungen ist die präzise Navigation und Positionsbestimmung des Schiffes. Hierzu wurde die Methode der relativen Positionsbestimmung mit dem Global Positioning System GPS/NAVSTAR angewendet. Die Referenzstation wurde auf dem Gelände des französischen Meeresforschungsinstituts IFREMER in Brest installiert.

Nach Beendigung der Tiefsee-Tests und der Vergleiche mit *Seabeam*-Daten erfolgte die Abnahme von *Hydrosweep* und *Parasound*. Der erste Teil der Expedition endete am 14. August 1989 in Vigo. 20 Wissenschaftler und Ingenieure wurden dort ausgeschifft.

Während der folgenden Anreise zur Romanche Bruchzone wurden weitere Überprüfungen und Tests mit beiden Sonarsystemen durchgeführt. Ziel war es, den Einfluß unterschiedlicher Morphologie und Meeresbodenstruktur auf die Messungen zu untersuchen. Der kontinuierliche Meßbetrieb während der gesamten Anreise zeigte, daß *Hydrosweep* und *Parasound* bei Einsatz erfahrener Operateure auch unter schwierigen Meßbedingungen und ungünstigen hydroakustischen Verhältnissen gute Meßdaten liefern.

Im Bereich der Romanche Bruchzone wurden zunächst wie geplant die zwölf orthogonal über den Zentralgraben angeordneten Testprofile abgefahren. Diese Profile wurden erstmals 1984 während der *Polarstern*-Fahrt ANT III/1 mit *Seabeam* vermessen. Die zweite Vermessung der Profile erfolgte im Zuge der *Hydrosweep*-Überprüfung auf der *Meteor* während der Expedition M6/4 vom 28. Dezember 1987 bis 12. Januar 1988. Die bisher durchgeführten Teilauswertungen und Vergleiche ergaben gute Übereinstimmungen zwischen den Ergebnissen der verschiedenen Anlagen. Auch großmaßstäbige Karten zeigten selbst in kleinen Strukturen und Details sehr gute Übereinstimmungen.

Die Romanche Bruchzone ist mit 920 km Länge der größte Versatz im Verlauf des mittelatlantischen Rückens. Umfangreiche geowissenschaftliche und ozeanographische Untersuchungen in den letzten Jahren weisen auf das große Interesse hin, das diese Bruchzone international hervorruft. Fächersonarmessungen aus diesem Gebiet liegen auch von der französischen *Jean Charcot* vor. Umfassende physiographische und morphologische Untersuchungen wurden auf der Grundlage dieser *Seabeam*-Messungen und mit *Side-Scan-Sonar*-Messungen des *GLORIA*-Systems von englischen und französischen Instituten durchgeführt.

Verstärktes wissenschaftliches Interesse findet die Romanche Bruchzone neuerdings als vermutetes Durchflußgebiet des kalten antarktischen Bodenwassers in die Nordhemisphäre. Als Beitrag zu diesen Untersuchungen wurde das ursprüngliche Vermessungsgebiet im Westen bis 19° 30´W erweitert. Für das gesamte Gebiet zwischen 17° 30´W und 19° 30´W entlang der Romanche Bruchzone liegen bei sehr guter Überdeckung genügend Fächersonarmessungen vor, um ein großmaßstäbiges Kartenwerk zu erstellen. Hierzu ist jedoch ein sehr zeitaufwendiges Postprocessing der *Hydrosweep*- und Navigationsdaten notwendig.

Die für die Meereis-Fernerkundung zur Registrierung von AVHRR-Daten der Satelliten NOAA 10 und 11 auf *Polarstern* installierte Satellitenempfangsanlage wurde im Verlauf des ersten Fahrtabschnittes erprobt. Weiterhin sollten verbesserte Methoden zur Datenreduktion und -speicherung entwickelt werden. Während der Satellitendurchgänge wurden die für die Auswertung benötigten physikalischen Größen zur Atmosphärenkorrektur gemessen. Alle

gewonnenen Daten wurden zusammen mit den Zeit- und Navigationsdaten für die spätere Bearbeitung im Institut abgespeichert.

Während des gesamten Fahrtabschnittes wurden von mehreren Arbeitsgruppen luftchemische Messungen durchgeführt. Sowjetische Wissenschaftler befaßten sich zur Vorbereitung auf den folgenden Fahrtabschnitt mit der Bestimmung der atmosphärischen Ozonkonzentration nahe der Meeresoberfläche.

Eine Arbeitsgruppe der Luftchemie führte routinemäßig während des gesamten Fahrtverlaufes in-situ Messungen zur Bestimmung der Konzentration leichter Kohlenwasserstoffe in der oberflächennahen Atmosphäre und im Seewasser durch. Im Stundenintervall wurden die atmosphärischen Mischungsverhältnisse von Perocyacetylnitrat (PAN), CO und H_2 bestimmt. Die vorläufige Analyse der Meßdaten bestätigt im wesentlichen die Ergebnisse der Vorjahres-Expedition ANT VII/1. Die Meßwerte in der Atmosphäre zeigten, daß die Luft über dem Atlantik über weite Strecken extrem sauber war.

Mittels der Laser-Photolyse-Fragment-Fluoreszenz-Methode (LPFF) wurden mit hoher zeitlicher Auflösung Messungen der Konzentration von gasförmigem Ammoniak und gasförmiger Salpetersäure durchgeführt. Die Auswertung der gewonnenen Daten unter Einbeziehung der Navigationsdaten und zusätzlicher meteorologischer Parameter wird mehrere Monate in Anspruch nehmen.

Umfangreiche Messungen und Untersuchungen erfolgten zur Erfassung biogener Schwefelverbindungen und ihrer Reaktionsprodukte in der Atmosphäre und im Seewasser.

Luftchemische Untersuchungen in der Grenzschicht Ozean-Atmosphäre erfolgten mit Hilfe hochentwickelter Filtersysteme zur Bestimmung eines Konzentrationsprofiles reaktiver Stickstoffkomponenten entlang der Fahrtroute im Atlantik.

Nach Verlassen des Ärmelkanals wurden in Abstimmung mit der Bordwetterwarte täglich bis zu vier Radiosondenaufstiege durchgeführt. Insgesamt wurden 96 Sonden gestartet, wobei die Aufstiegshöhen zwischen 8000 und 29500 m lagen. Radiosondenaufstiege und XBT-Messungen erfolgten auf jedem vollen Breitengrad.

Als Vorbereitung für den folgenden Fahrtabschnitt ANT VIII/2 und zur Kalibrierung der Meßgeräte wurden von sowjetischen Wissenschaftlern während der gesamten Fahrt Ozonmessungen in der Troposphäre durchgeführt. Im Bereich der Biskaya wurde ein weitaus höherer Ozongehalt gemessen als auf der Südhemisphäre.

1.1.2 Summary and Itinerary

The *Polarstern*-Expedition ANT VIII/1 was separated into two sections. During the first part from Bremerhaven to Vigo, Spain, the new hydroacoustic sonar systems *Hydrosweep* and *Parasound*, which were installed in summer 1989, were calibrated in the North Sea and tested in the deep sea of the Bay of Biscay and at the French continental shelf. During the second part of the cruise from Vigo to Puerto Madryn, Argentina, deep sea trials and special tests were performed at the Romanche Fracture Zone with both systems *Hydrosweep* and *Parasound.*

During the entire cruise, various groups carried out air chemistry observations in the Atlantic along the north-south profile. In addition ozone observations in the lower atmosphere and water sampling in the upper water column were performed systematically. Data from radiosondes were collected continuously during the cruise and used for an improved modeling of the atmospheric correction of AVHRR-data from NOAA satellites. CTD-measurements were carried out in the *Hydrosweep* test areas, and XBT's were launched regularly every one degree of latitude.

For the deep sea trials and comparisons with external data, *Seabeam* measurements from the French R/V *Jean Charcot* and *Hydrosweep* data from the German R/V *Meteor* were made available for this project by the originators of the data. For the determination of the internal accuracy, repetitive measurements of selected profiles were carried out.

Another goal was the verification and analysis of the *Hydrosweep* cross-fan calibration technique used for the determination of the mean sound speed value. For these investigations, special profiles were measured in the abyssal plain of the Bay of Biscay. The mean water sound velocity, derived from *Hydrosweep* measurements, was compared to the results from independent CTD-data in the same area. The maximum observed difference was ± 5 m/s, which would create an error of about 3% of the water depth. The general precision for the mean sound velocity from a period of calibrations is ± 1 m/s.

The most important prerequisite for a precise sea floor survey with multibeam sonar is the precise positioning of the ship. Positioning with the Global Positioning System GPS/NAVSTAR can be performed in the single station or in the relative navigation mode. To secure a good position accuracy for the sea trials in the Bay of Biscay, the relative navigation mode was used. A reference station was deployed at the French marine research institute IFREMER near Brest. Relative navigation with GPS/NAVSTAR is based on the technique of pseudo range code corrections.

Simultaneous operation of both systems *Hydrosweep* and *Parasound* was checked in the deep waters of the Bay of Biscay. At the end of the sea trials and performance tests, the acceptance procedure was closed. *Polarstern* arrived in Vigo on the 14 August 1989, and 20 engineers and scientists disembarked.

On the transit from Vigo to the Romanche Fracture Zone, a number of additional tests and trials in shallow and deep sea waters were done with the new hydroacoustic sonar systems. Studies of the system performance in areas with different morphological structures and topographic features were performed en route. Training courses for maintenance, repair and operation of *Hydrosweep* and *Parasound* were given by technicians of the manufacturer. The investigation during the transit confirmed that *Hydrosweep* and *Parasound* produced excellent results, even under difficult hydroacoustic conditions. However, the main requirement is to have a well trained operator to observe and control the measurements.

At the Romanche Fracture Zone, first the re-survey of the 12 test profiles was performed. The parallel profiles are arranged perpendicular to the fracture zone. These profiles were first established and measured in 1984 during the deep sea calibration of *Seabeam* on the *Polarstern*-Expedition ANT III/1. The second survey of these profiles was performed for *Hydrosweep* sea trials on the *Meteor*-Expedition M 6/4 from 28 December 1987 until 12 January 1988. The comparisons between the three surveys on identical profiles indicate an excellent correspondence. Even on large scale maps, small structures and features on the sea floor can be verified from different surveys.

The vast Romanche Fracture Zone (R.F.Z.) is the most prominent depression of the Mid-Atlantic-Ridge (MAR). The 920 km long east-west transverse ridge has its the deepest point at the Vema Depth with nearly 8 000 m. The southern slope has inclinations of up to 45°. The central part of the trench bottom is covered with sediment layers or sediment bridges.

During recent years, intensive marine geophysical and geological studies have been carried out there. Physiographic and geomorphological investigation have been done with *GLORIA* images (*R/V Discovery*) and *Seabeam* bathymetry (*R/V Jean Charcot*). The Romanche Fracture Zone has also attracted the attention of physical oceanographers, since it is assumed that the cold Antarctic Bottom Water passes through this area. For additional investigations in this area, the survey area was enlarged during this cruise in a western direction. The area between 17°30´W and 19°30´W along the Romanche Fracture Zone is now completely surveyed with multibeam sonar. However, prior to the postprocessing of the multibeam data, correction of the GPS-navigation must still be performed in order to produce high precision large scale bathymetric maps.

A new satellite tracking system for AVHRR-data from NOAA-satellites was installed on board *Polarstern* in the summer 1989. The remote sensing data shall be mainly used for sea-ice studies in the polar regions. During the first part of this leg, the system was tested and calibrated. On the Atlantic, more than 15 satellite passes were tracked. The data were recorded on magnetic tapes and will be used for additional investigations at the institute. Measurements of the physical and meteorological parameters, necessary for the atmospheric correction of the satellite data, were obtained from radiosonde ascents and from observations on board.

During this leg, air chemistry and ozone measurements were performed by various groups in continuation of their investigations during the *Polarstern*-cruise ANT VII/1 in 1988. The series of investigations of the marine atmosphere and its chemistry was continued during this cruise. The first results indicate a good agreement with the data from earlier expeditions.

1.1.2.1 Technical and Scientific Prospects

Since 1976, multibeam sonar systems have been used most successfully for scientific bathymetric survey in deep sea waters. Especially the *Seabeam* system, with more than 12 installations worldwide on research and survey vessels, was used for detailed local surveys and has provided valuable information about the sea floor for marine scientists.

Hydrosweep, a new wide-angle multibeam sonar system with 59 preformed beams (PFB), was developed in Germany between 1985 and 1986. A prototype of *Hydrosweep* (Fig. 1) was installed on the new German *R/V Meteor*. Two scientific cruises on the *Meteor* for deep sea trials and performance tests were carried out in 1986 on cruise M4/1 and 1987/88 on cruise M6/4, during which the excellent data quality and reliability could be demonstrated. As a consequence, the new *Hydrosweep* was also installed on *Polarstern* in summer 1989.

The main advantages of *Hydrosweep* are i) its capability for both deep and shallow water operation, ii) the large 90° opening angle with 59 PFB´s, each with 2° aperture, iii) the cross-fan calibration method which allows compensation for variations of the water sound velocity, and iv) the small dimensions of the transducer arrays which are installed flush in the ship´s bottom. *Hydrosweep* and the new sediment penetrating echo sounder *Parasound*, also developed at *Krupp Atlas Elektronik* (KAE), Bremen, were installed at the same time. After the installation, both systems operated immediately without any technical problems.

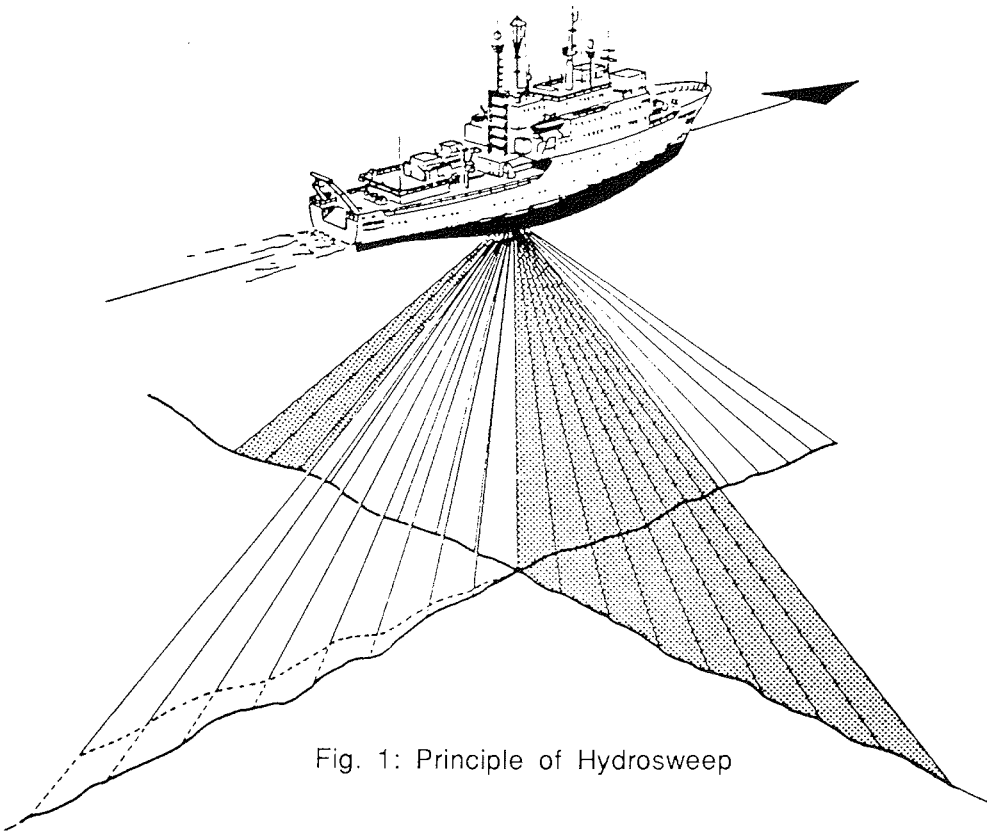

Fig. 1: Principle of Hydrosweep

1.1.3 Preparations (AWI)

Based on experiences with *Seabeam* operation in ice-covered areas and with the *Hydrosweep* system on *R/V Meteor*, a new display and editing program package for multibeam data was developed at the AWI. The program is implemented on a VAX-Station and allows the operator to read, process, edit and plot the *Hydrosweep* measurements immediately on board. The DEC-Workstation MicroVAX II/GPX is linked via a serial interface to the *Hydrosweep* echoprocessor for the on-line processing of bathymetric measurements. Cross-profile editing, contour line plotting and the storing of corrected data can be done parallel to the hydrographic survey. During this cruise, the software package was adapted to the *Hydrosweep* system and tested in-situ with real multibeam sonar measurements.

1.1.3.1 Bathymetry and Hydrography (AWI, KAE)

For the deep sea trials and acceptance tests, several sites and test areas with known sea floor topography were selected in the Bay of Biscay. These areas already had been used for the same purposes by the research vessels *Jean Charcot* and *Meteor* years ago. In preparation for the sea trials, new bathymetric maps from the test areas were compiled from the existing data.

One of the main goals was the verification and analysis of the cross-fan calibration technique, which can be used for the determination of the mean sound velocity. A CTD sensor type Seacat SB19 was used to measure and independently determine sound velocities. This CTD can be easily handled and operated.

1.1.3.2 Navigation and Positioning (IEH, AWI)

As a consequence of the high resolution of *Hydrosweep* measurements, precise ship's positioning is also required. The integrated navigation system INDAS-V with a Magnavox T-Set GPS-receiver was used for ship's navigation. For high precision positioning and ship's attitude control, four GPS-receivers *TI-4100* were installed on *Polarstern*. Their antennas were placed at the bow and stern and on the top mast of the ship. These antennas form two baselines which can be used for precise ship's attitude determination. The relative distance and position between the navigation antennas and the *Hydrosweep* transducer arrays were determined from an engineering survey in the dry dock during the installation of *Hydrosweep* and *Parasound*.

During the *Hydrosweep* tests in the Bay of Biscay, GPS was used in the relative kinematic positioning mode. For this reason, a GPS reference station with two *TI-4100* receivers was installed at the French marine research institute IFREMER in Brest.

1. 3.3 Installation of the Satellite Tracking Station (AWI)

The receiving antenna (two-meter dish) was mounted on the port side of the upper observation deck. The motor control unit, receiver and the computer system were installed one deck below. The computer was connected to the main computer facilities of the ship.

1. 4 Cruise Report of Leg ANT VIII/1 (AWI)

1.1.4.1 Bremerhaven to Vigo, Spain

Polarstern left Bremerhaven on 5 August 1989, 05:20 h, with 32 crew members and 49 scientists, heading for the Bay of Biscay

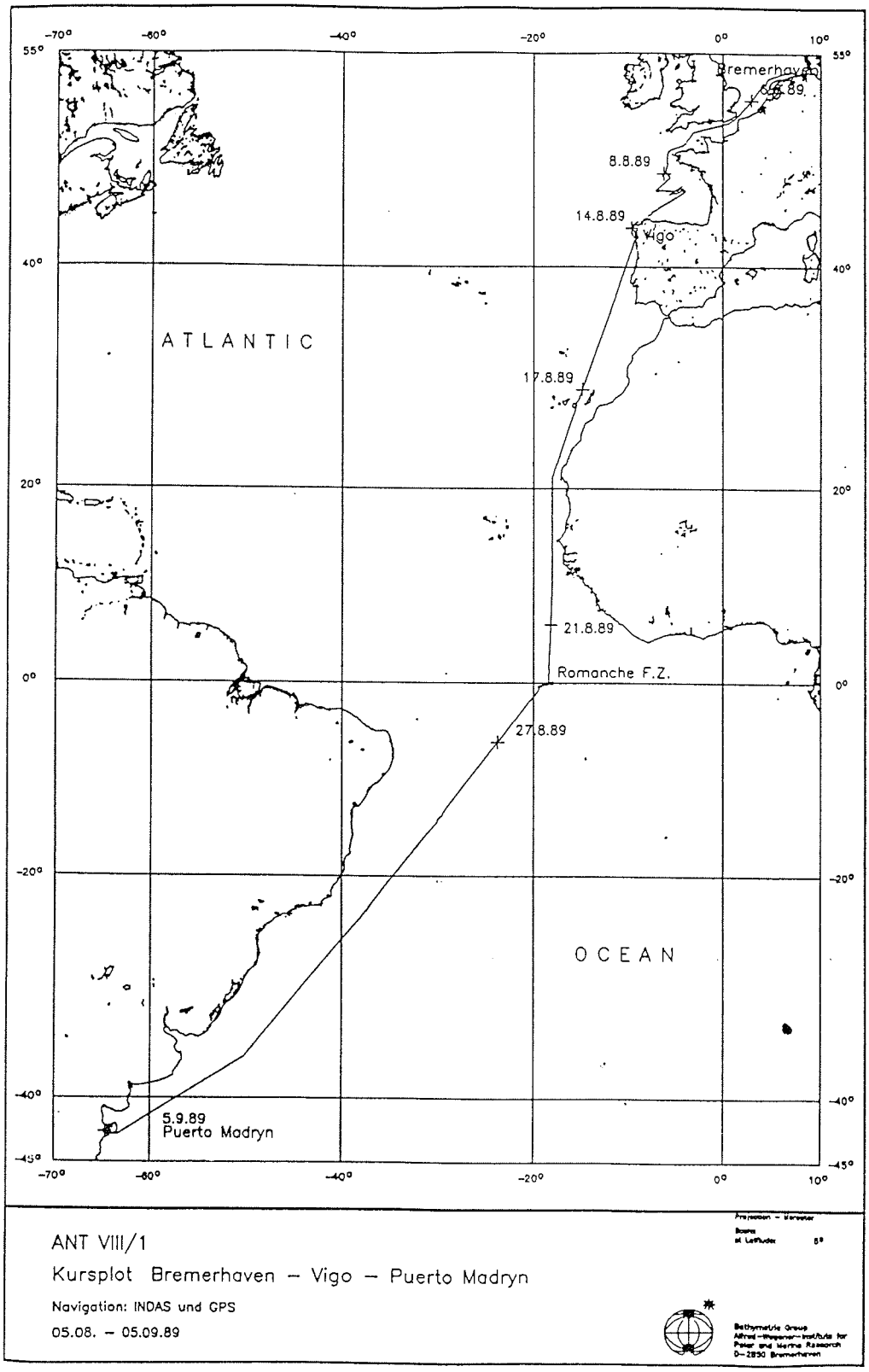

Fig. 2: Trackplot of ANT VIII/1 Bremerhaven - Vigo - Purto Madryn

through the North Sea and the English Channel (Fig.2). The new sonar systems *Hydrosweep* and *Parasound* were switched on immediately after the departure from Bremerhaven. Both systems worked properly from the beginning .

In the English Channel, the known fossil stream ripples covered by 10 to 15 m thick sediment layers were surveyed with *Parasound* and compared to old recordings. The hydroacoustic noise level for *Polarstern* was measured in the shallow waters of the North Sea.

The proper operation and the functionality of the integrated navigation system INDAS-V and the GPS-integration with the program VENUS was tested en route. In addition, detailed investigations and tests were performed with various navigation components. DOLOG was tested in bottom- and water tracking mode. The positions and speeds were compared with results from GPS measurements.

The GPS reference station was installed at the IFREMER, Brest and was in operation from the 5 August 1989 to the 14 August 1989.

On the 7. August 1989, 03:15 UTC, *Polarstern* reached the shallow water test area at 49°05'N, 3°57'W. Sixteen profiles were measured at water depths between 70 to 90 m. The navigation was done with GPS.

The French continental shelf was crossed on 8 August 1989 at the position 47°10'N, 5°40'W (Fig. 3). Two profiles at Location 0 were re-surveyed along known tracks from the *Meteor* cruise M4/1.

Polarstern reached the deep sea test site Location 1 in the Bay of Biscay at the position 45°50'N, 6°40'W on 8 August 1989. In the central part of this test area, a CTD was launched for the independent determination of a sound velocity value (Fig. 14). One test profile, 10 n.m. long, was used for the derivation of the roll and pitch biases.

The complete calibration work with *Hydrosweep* was finished between 8 and 9 August 1989. Following this, tests with *Hydrosweep* were performed during good GPS coverage with at least four visible satellites.

The test profiles in the abyssal plain at Location 1 near position 45°51'N, 6°37'W were measured several times using GPS navigation.

On 10 August 1989, *Polarstern* moved to the test area Location 2B at the French continental slope. This test area was set up during the *Meteor* cruise M4/1. Firstly a CTD was launched on position 45°53'N, 4°40'W (Fig. 14). The eight test profiles were measured twice, with GPS navigation and with integrated navigation. The preliminary

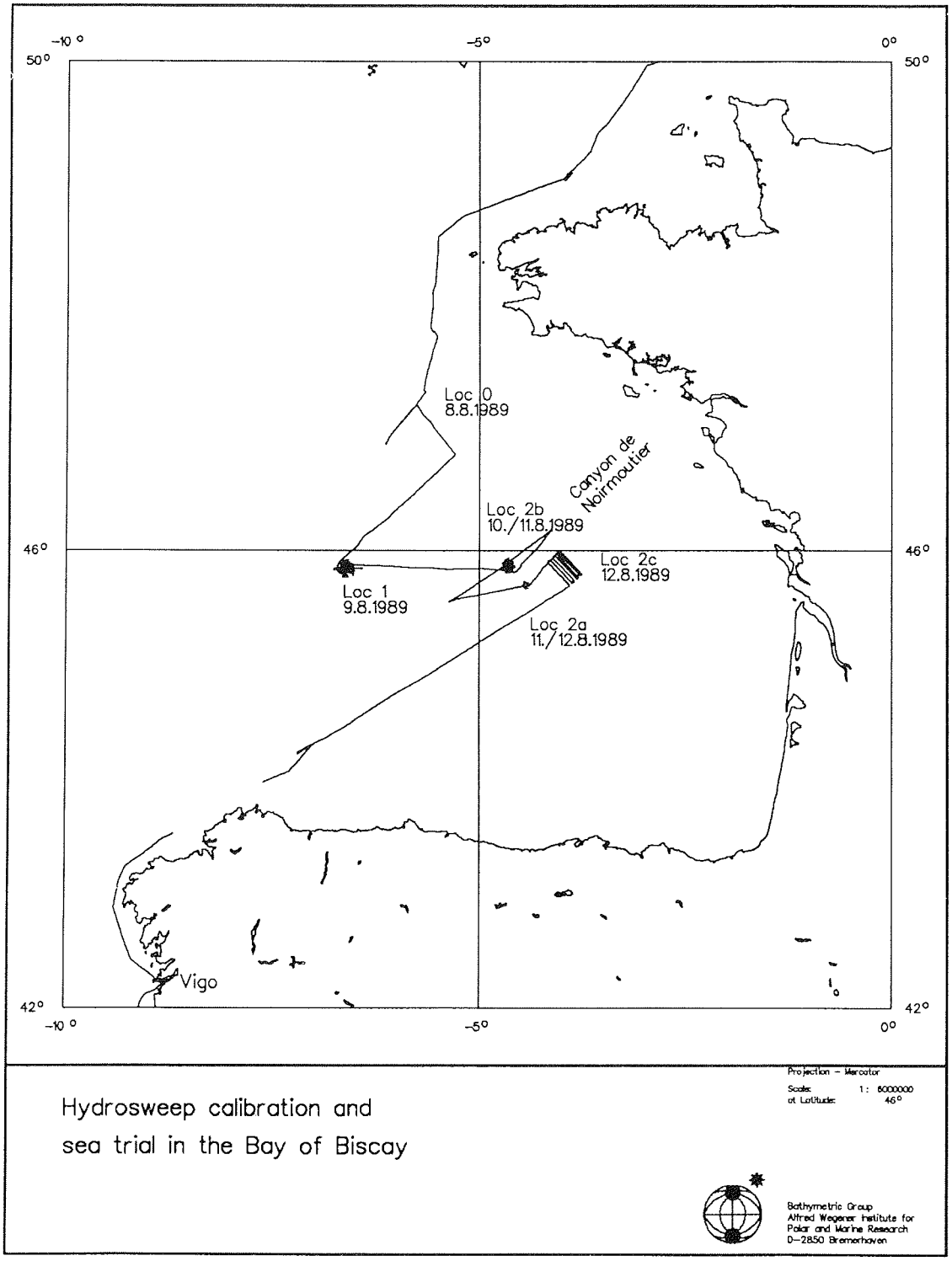

Fig. 3: Trackplot in the Bay of Biscay and Test Locations

results and comparison to *Seabeam* data indicate very good correlation. This survey was finished on 12 August 1989.

Polarstern sailed to the test area at Location 2A at 45°43'N, 4°27'W. On this location two profiles, perpendicular and parallel to the main slope direction, were measured to analyze the influence of the terrain slope. The profiles were also surveyed twice in opposite directions.

At the upper continental slope north of Locations 2A and 2B, an area of about 150 km^2 with depths between 3 000 and 4 300 m was mapped with *Hydrosweep*. *Seabeam* data were also available from this area. The survey followed the same tracks of *Jean Charcot* in order to have comparability with their measurements. A very good agreement between the contour lines is shown from the first comparison of the results.

After the end of this survey on 12 August 1989, 24:00 UTC, *Polarstern* sailed in the direction of Vigo. During this transit, the training course given by the system engineers from the manufacturer was continued for the operators and maintenance engineers on *Hydrosweep* and *Parasound*. After the successful final technical tests and comparison between data from *Polarstern* and from *Meteor* or *Jean Charcot*, the acceptance procedure for *Hydrosweep* and *Parasound* was finished, and the acceptance protocol was signed by the customer's representatives. The harbor of Vigo was reached at dawn of 14 August 1989. Twenty scientists and engineers were disembarked by longboat.

1.1.4.2 Vigo to Puerto Madryn, Argentine

Polarstern left the anchor place off Vigo on 14 August 1989 in the afternoon, heading for additional tests and deep sea trials in the vicinity of the Romanche Fracture Zone (Fig. 2). During the transit, *Hydrosweep* and *Parasound* were operated permanently. The data were recorded and analyzed in part. At each full degree of latitude, an XBT and a radiosonde were launched.

Polarstern reached the test area at the Romanche Fracture Zone (R.F.Z.) on 22 August 1989. The profiles are shown in Fig. 10. In order to determine a water sound velocity profile, a CTD was launched on position 0°12'S, 18°22'W to 2050 m depth (Fig.15), and an XBT was thrown.

Water samples from different depths were taken down to 100 m for air chemistry investigations.

The twelve test profiles across the R.F.Z. were surveyed during good GPS coverage to guarantee optimal coincidence with the previous

swath surveys. During the time with less than three GPS satellites and after finishing the test profiles, the vicinity of the test area was surveyed. East of the main test area, new profiles were measured to close the gap to the *Jean Charcot* survey area of 1988. Following this, ten profiles with a spacing of 5 n.m. were surveyed across the fracture zone. The multibeam sonar survey from 22 to 25 August 1989 covers an area of more than 10000 km^2 with 200 km in an E-W direction and 45 km in N-S direction (Fig. 10). At the end of the survey on 25 August 1989, two CTD´s were launched in the central part of the R.F.Z. at 0°19'N, 18°48'W.

On the route to Puerto Madryn, *Hydrosweep* was operated continually, *Parasound* only sporadically due to some technical problems. The regular launches of XBT´s and radio sondes were continued at every degree of latitude .

On 5 September 1989, 08:00 h, *Polarstern* was docked at Puerto Madryn.

1.1.5 Bathymetry on Board (AWI)

1.1.5.1 Pre- and Postprocessing of *Hydrosweep* Data

The *Hydrosweep* measurements are processed in following steps:

1. Transfer of raw data from *Hydrosweep* to the DEC-Workstation
2. Blunder detection and editing of the *Hydrosweep* measurements
3. Calculation of a digital terrain model (DTM)
4. Clotting contour lines and other products from the DTM.

The *Hydrosweep* measurements are recorded on two different media. The main recording system is the magnetic tape unit, which is part of the *Hydrosweep* hardware. All raw data which are necessary for the complete postprocessing are recorded on this magnetic tape. In addition, the *Hydrosweep* system provides a serial data output, which allows the registration of unfiltered raw measurements on the workstation and a preprocessing of the multibeam data in near real-time on board.

The *Hydrosweep* operator can check the data, detect blunders and eliminate wrong or suspect measurements of the survey profiles. After the corrections, the accepted data are used to calculate a triangulation net for the contour line interpolation. The contour lines are displayed on screen and plotted on a DIN-A0 plotter using a geographic grid. The online mapping is used for data verification and quality checks. In addition this method can serve as an aid for sea bottom navigation and to control the swath coverage during systematic *Hydrosweep* surveys.

For the calculation of a digital terrain model (DTM), all accepted depth measurements and the positions in geographic or UTM coordinates are used. Different program systems for DTM calculations, e.g. TASH (*Topographisches Auswerte System Hannover*, University of Hannover) and *SEABONE* (AWI) are implemented on the DEC- and CONVEX-computers on board *Polarstern*. The calculation of a DTM means the generation of a regularly spaced grid in the ground plane X and Y, and corresponding depths Z from stochastically distributed measurements. TASH uses the method of 'moving surfaces', whereby the terrain around each grid point is approximated by a fitted surface. The equation, which contains as an unknown the depth of the grid point itself, is solved by a least squares adjustment.

The main goal of the cruise was to check the performance and feasibility of *Hydrosweep* and to determine the accuracy of the measurements. For this investigation, several data sets collected during this cruise will be used for comparison with results from other expeditions:

- *Seabeam* data by *R/V Jean Charcot* (CH.139 STRATIGAS, July 1982)
- *Seabeam* data by *R/V Polarstern* (ANT III/1, Oct./Nov.1984)
- *Hydrosweep* data by *R/V Meteor* (M 4/1, October 1986)
- *Hydrosweep* data by *R/V Meteor* (M 6/4, Dec.1987/Jan.1988).

However, detailed conclusions based on the analysis of the numerical results can only be made after the final postprocessing. Beforehand the data reduction of the GPS measurements and the correction of hydroacoustic data must be performed.

1.1.5.2 Training of Users (KAE)

During the first part of the leg, all technicians and scientists, who were responsible for the two sonar systems, were trained by the manufacturer's team (KAE) for operation and maintenance for *Hydrosweep* and *Parasound*, respectively.

1.1.5.3 Ship's Attitude Calibration (KAE, AWI)

The transmitted and received hydroacoustic signals of *Hydrosweep* must be compensated for the ship's attitude, in particular for roll and pitch, in order to avoid wrong swath measurements. Two inertial platforms from *Anschütz* are installed aboard the vessel to measure roll and pitch. Since inertial platforms have different systematic errors, the roll and pitch biases had to be determined for both platforms.

The roll bias can easily be determined in the deep and flat sea floor by surveying the same profile twice in opposite direction. For each profile, the mean slope angle of the terrain along swath must be

determined. The difference between the two mean terrain angles yields the double roll bias of the inertial platform. The pitch bias was measured and determined similar from the forward- and backward looking *Hydrosweep* calibration fan. The roll bias test indicated also that platform No. 2 had a better system behavior and stability than platform No. 1.

	Platform 1	Platform 2
Pitch Bias	-0.27°	+0.37°
Roll Bias	-0.18°	-0.10°

Tab.1: Roll and Pitch Biases for *Anschütz* Inertial Platforms 1 and 2 on *R/V Polarstern*

1.1.5.4 Tests in the Bay of Biscay (AWI, KAE)

1.1.5.4.1 Shallow Water Tests

The tests in shallow water were realized on position 49°5'N, 4°W, 100 km north of Ile de Batz. The water depths varied between 70 and 90 m. The test measurements were performed with an uncalibrated *Hydrosweep* system. However, wrong values for the roll and pitch do not seriously falsify multibeam sonar measurements in shallow water. Postprocessing of these measurements has not yet been performed.

1.1.5.4.2 Deep Sea Plain

Extensive calibration and testing of *Hydrosweep* was done in the deep sea plain of Location 1 (Fig. 4). At this location, special investigations and tests were performed on following topics:

- measurements of the hydroacoustic ship's noise level in deep waters
- adjustment of the beam forming in the *Hydrosweep* system
- determination of the roll and pitch biases
- test and verification of the cross-fan calibration method.

Preliminary results from these tests were obtained on board. A complete analysis can only done after postprocessing of the data.

1.1.5.4.3 Continental Slope

The Locations 2A and 2B were established during *Meteor* cruise M4/1 as special test areas and for the analysis of data quality and accuracy, based on comparison with *Seabeam* data. On the transit between Location 2A and 2B, the Canyon de Noirmoutier (Fig. 5) was surveyed twice. One result is shown as a contour line swath plot at a large scale in comparison with the bathymetric map of the same area

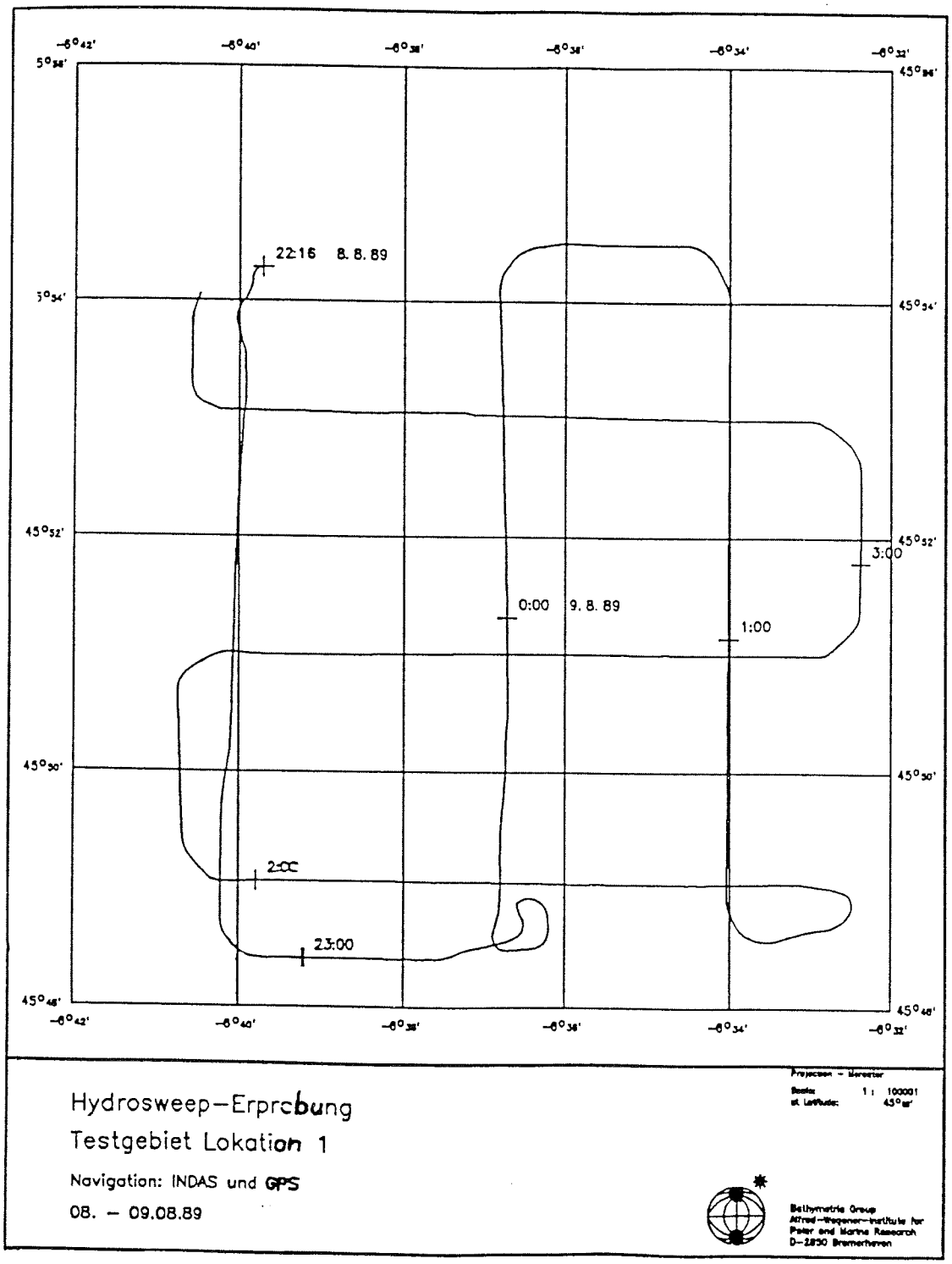

Fig. 4: Trackplot of the Test-Location 1 in the Abyssal Plain

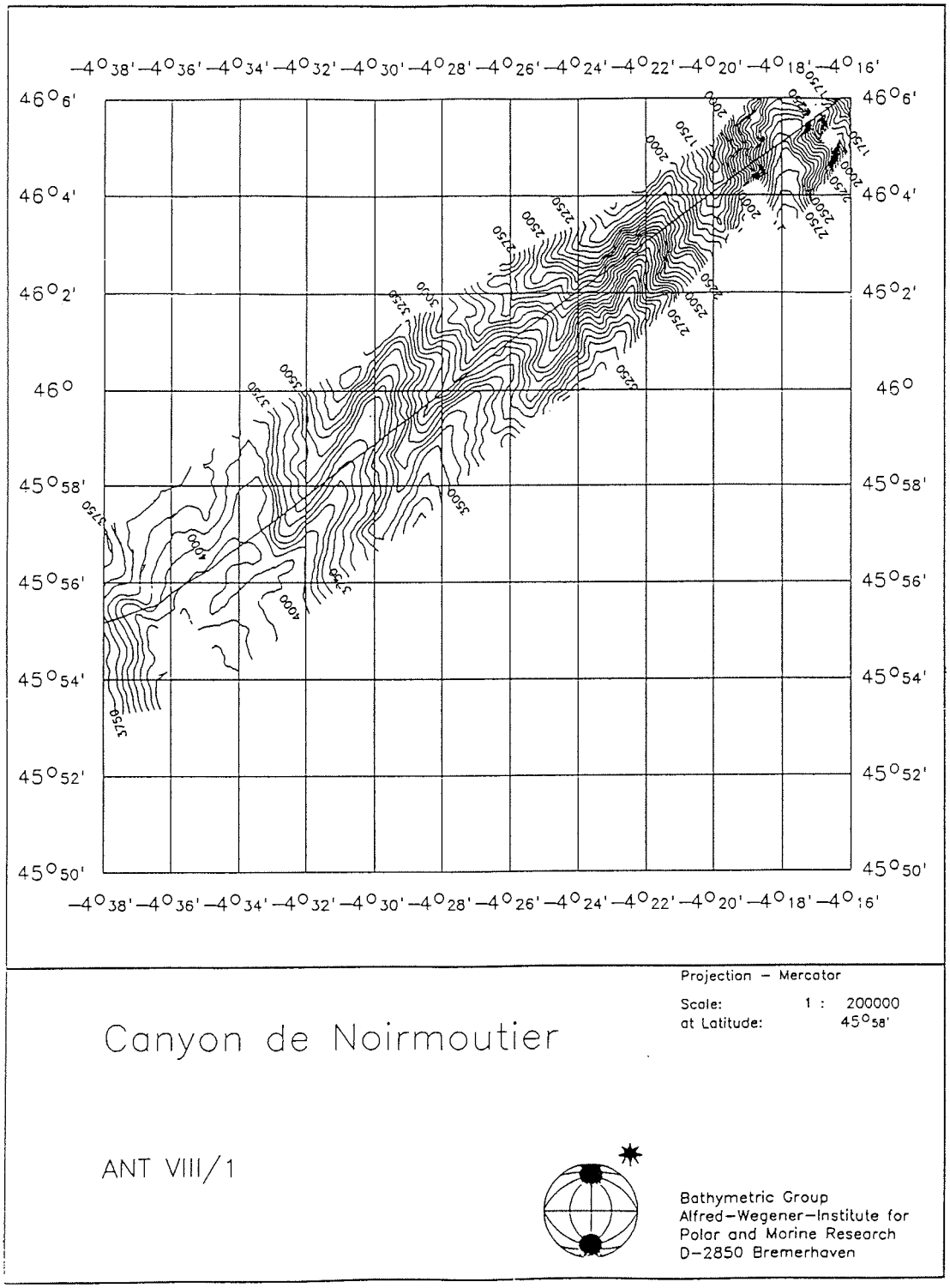

Fig. 5: Online Plot from Hydrosweep in the Canyon de Noirmoutier

Single Swath Track from Hydrosweep Canyon de Noirmoutier

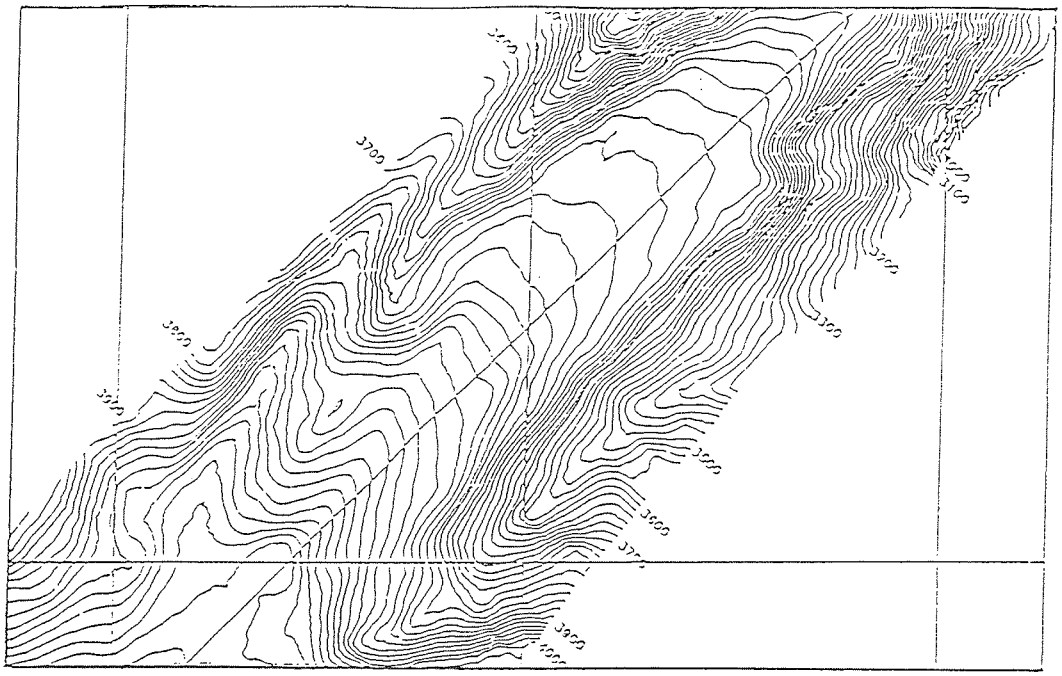

Bathymetric Map from Seabeam Surveys

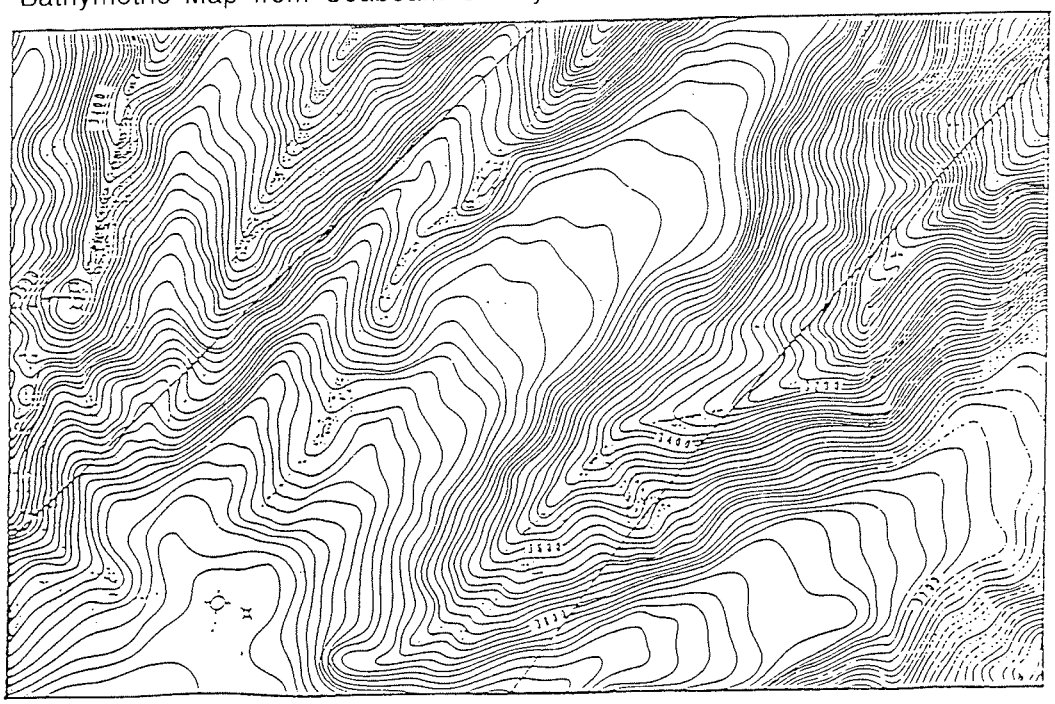

Fig. 6: Comparison between a Bathymetric Map and a Single Hydrosweep Swath

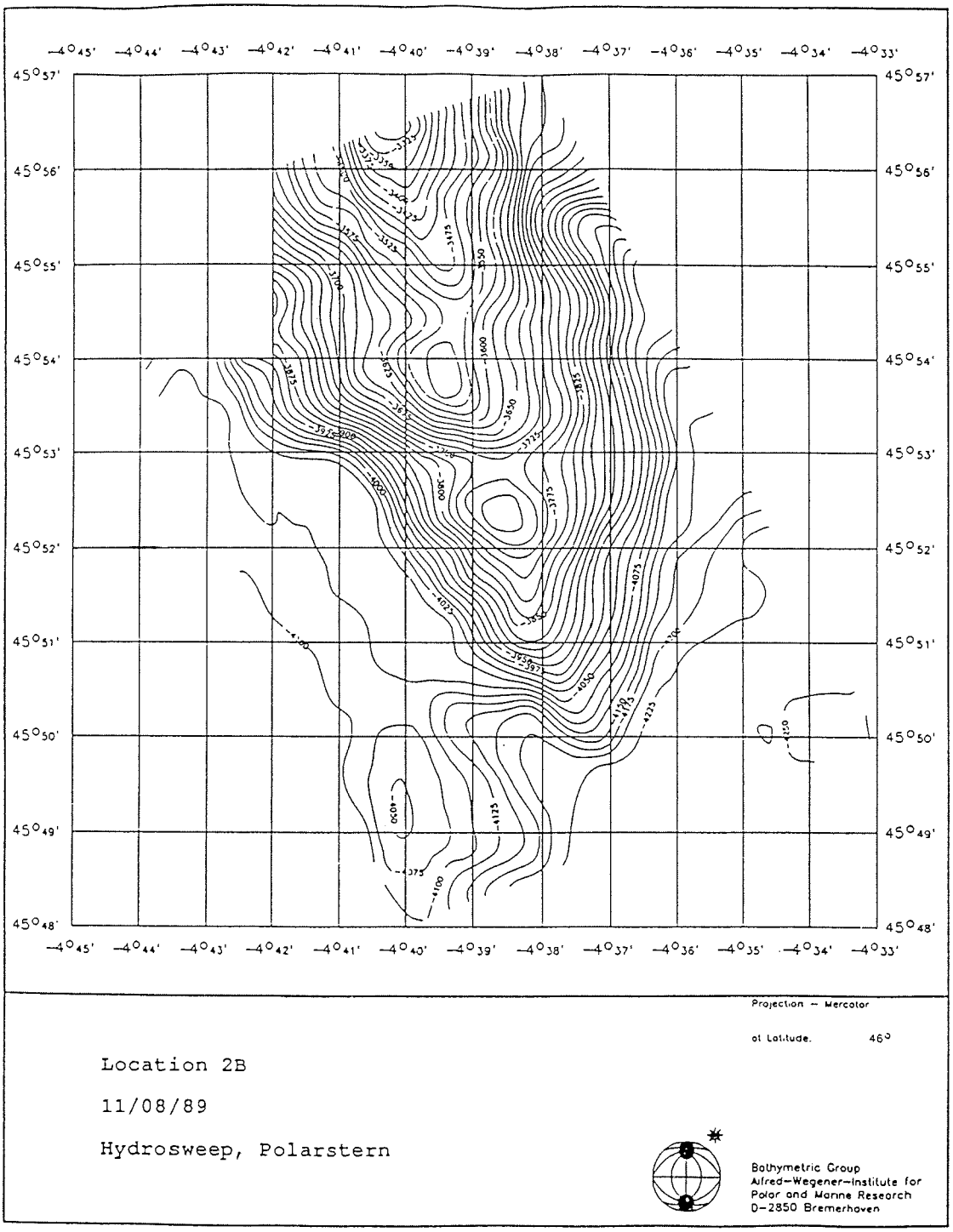

Fig. 7: Contourline Map of Location 2B based on Hydrosweep data from ANT VIII/1

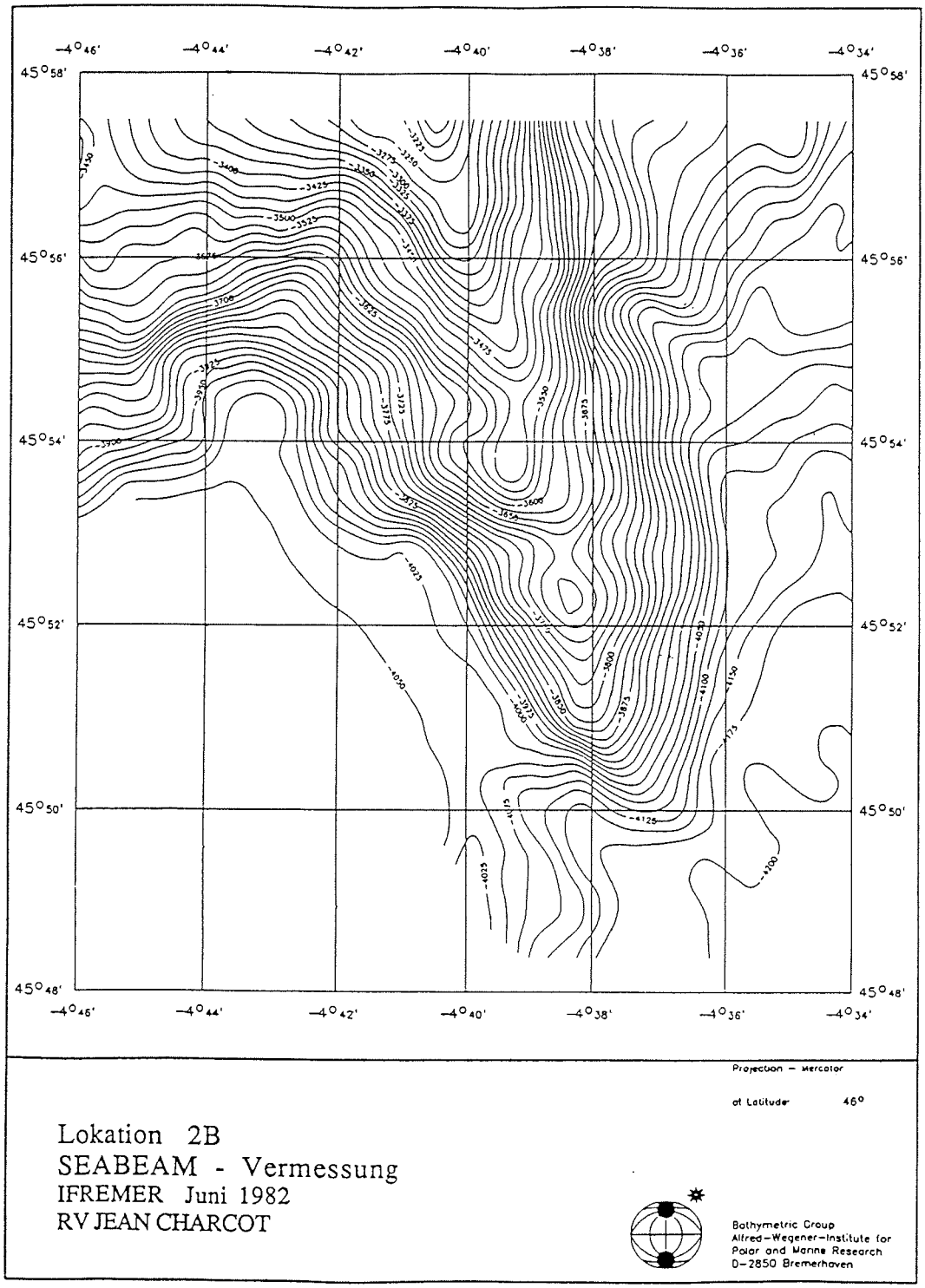

Fig. 8: Contourline Map of Location 2B based on Seabeam data "Jean Charcot"

Location 2B Polarstern

Hydrosweep 10./11.8.89

Demo-File No.2

Bathymetric Group of
Alfred-Wegener-Institute for
Polar and Marine Research
D-2850 Bremerhaven

Fig. 9: Threedimensional Perspective View of the Location 2B

from IFREMER, which is based on *Seabeam* data from the *Jean Charcot* (Fig. 6). An exellent agreement can be confirmed between both plots.

The Location 2B at the base of the continental slope covers a hill area of 10 km by 18 km. The depth varies between 3300 and 4200 m. The eight test profiles were surveyed twice between the 10 and 11 August 1989. The first survey was done during good GPS coverage and the second with integrated navigation only. The spacing of the lines was 2 km. This corresponds to a threefold overlapping of the swathes. The preliminary contour line map (Fig. 7) demonstrates very good agreement with the results from the *Seabeam* survey of the *Jean Charcot* (Fig. 8). The inclinations of the slopes varies between 9% and 14%. A three-dimensional perspective view from the test Location 2B is given in Fig. 9.

Between the 11 and 12 August 1989, the profiles of Location 2A were surveyed. The swathes covers an area of 7 km by 8 km. The steady slope at the lower continental shelf has an inclination of 1.5%. The water depth varies between 3300 and 4200 m. The profiles were measured twice in opposite directions. The combination of two perpendicular tracks indicate very good agreement. The maximum differences in the contour line positions are ±150 m. It could be shown that profiles measured in the direction of the slope gradient are more reliable in topographic details than profiles established parallel to the contour lines.

1.1.5.5 Acceptance of *Hydrosweep* and *Parasound* (AWI, HLTS)

The acceptance procedure of the new sounding systems *Hydrosweep* and *Parasound* was carried out during the first part of the leg between Bremerhaven and Vigo. Hardware problems and software errors, detected during the tests and sea trials as well as recommendations for useful scientific modifications, were enroled in the acceptance protocol. The delivery, installation and the final acceptance of *Hydrosweep* and *Parasound* were performed in four month time only, due to the excellent collaboration between the manufacturer *KAE, Hapag-Lloyd T&S* and AWI. Both systems operate satisfactorily.

1.1.5.6 Deep Sea Trials in the R.F.Z. (AWI)

The twelve test profiles in the central part of the R.F.Z. were surveyed during good GPS coverage in order to guarantee high precision positioning. The spacing of the *Hydrosweep* profiles corresponds to the *Seabeam* survey during ANT III/1. Between the 'GPS windows', additional profiles were measured in the vicinity of the R.F.Z. (Fig. 10).

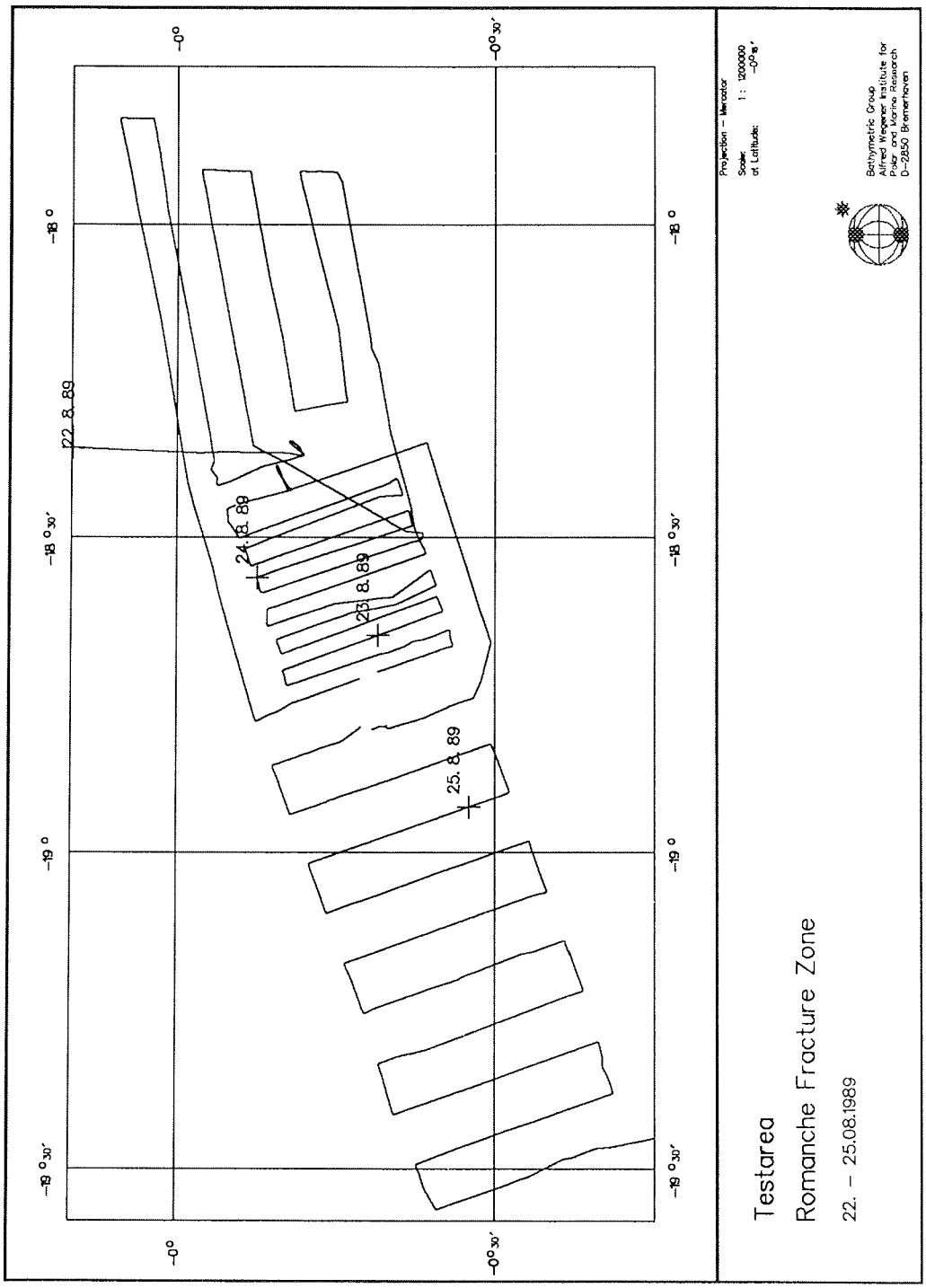

Fig 10: Trackplot at the Romache Fracture Zone Survey ANT VIII/1

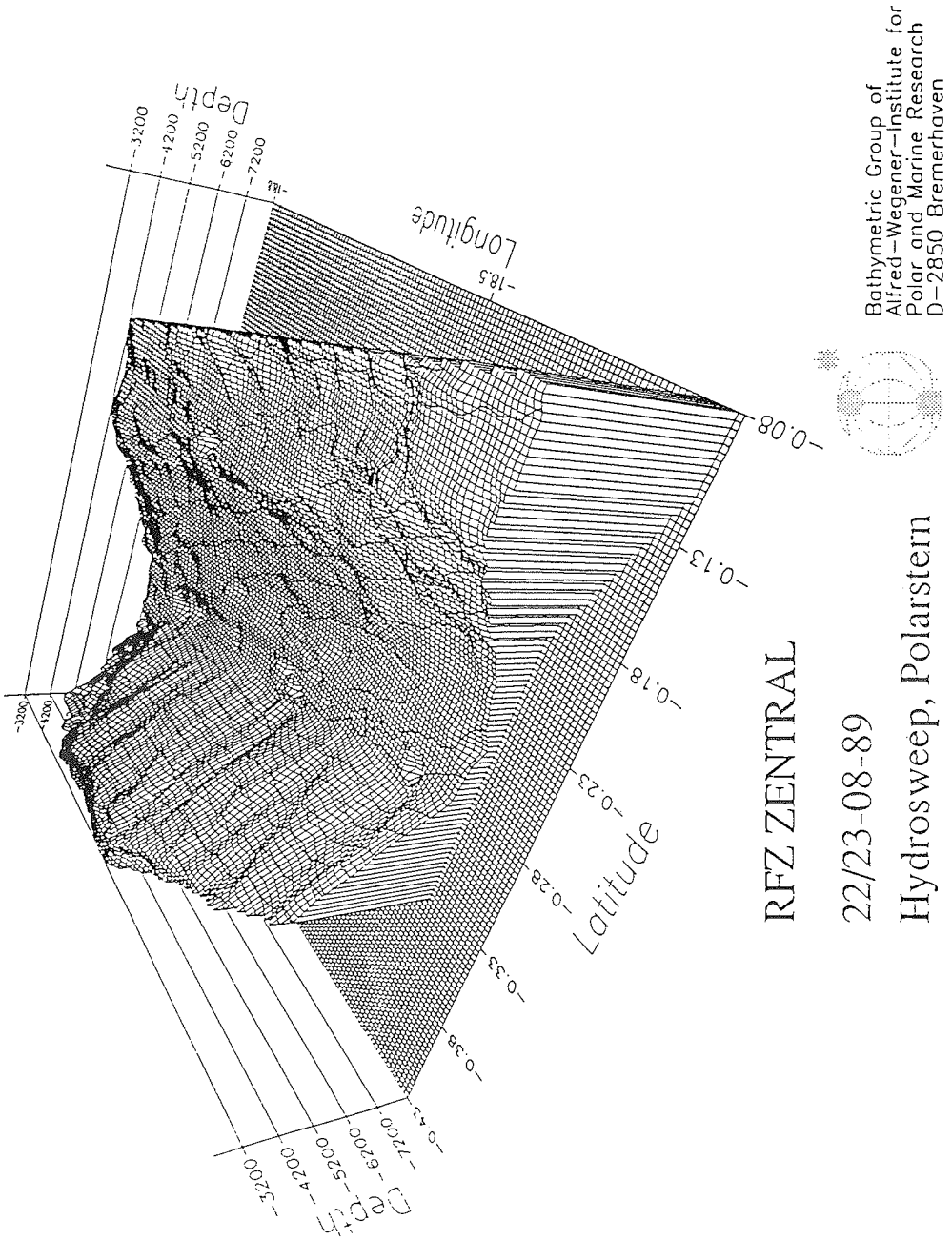

Fig. 11: Threedimensional Perspective View of the Central Part of the Romanche Fracture Zone

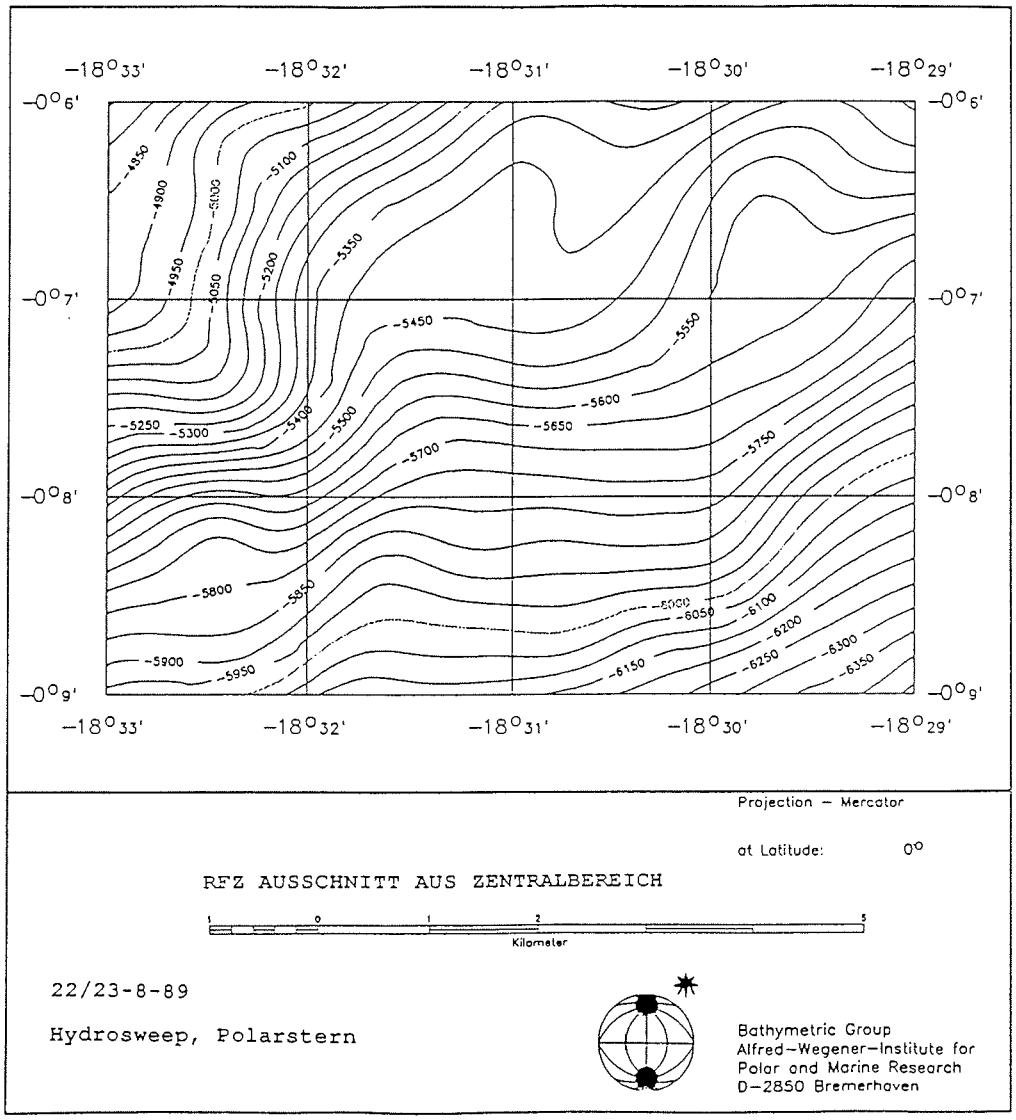

Fig. 12: A Section of the North Slope from the test area in the R.F.Z. from Hydrosweep Measurements on ANT VIII/1

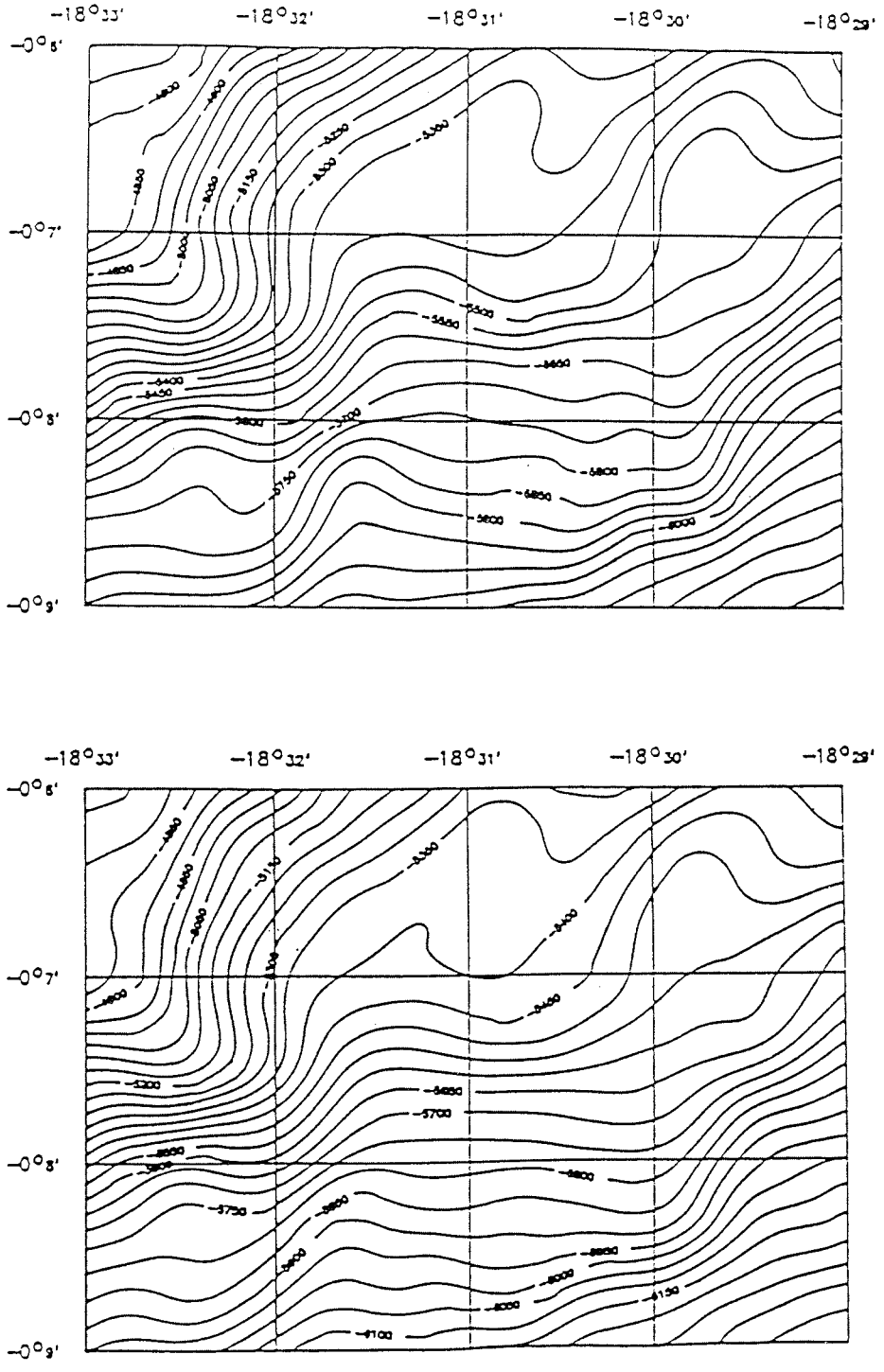

Fig 13: The identical Part of the R.F.Z: surveyed with Seabeam on ANT III/1 (above) and Hydrosweep on M 6/4

After the end of the tests, the survey area was enlarged in the western and eastern directions. The total area surveyed with multibeam sonar covers more than 10 000 km^2. Ship's positioning was carried out with GPS in single station mode, because no reference station could be established in this region. However, it will be possible to determine precise ship's heading as well as roll and pitch from the postprocessing of the GPS phase measurements from the four receivers.

The *Hydrosweep* data measured in the R.F.Z. were analyzed, corrected and transfered to the scientific on-board computer for further processing and map making. A three-dimensional perspective view of the central part of the R.F.Z. is given in Fig. 11.

1.1.5.7 Data Evaluation (AWI)

For the evaluation of the accuracy of adjacent swath profiles, some tracks were compared. The coincidence of contour lines was good, even in the outer beams. Data gaps in the central trench bottom of the R.F.Z. were probably caused by bad hydroacoustic reflectors on the sea floor (sediment bridges).

Digital terrain models (DTM) were calculated with corrected *Hydrosweep* measurements for the central, eastern and western part. The small storage capacities of the scientific on-board computers did not allow processing of the total area. A small part of the test area was processed at a larger scale. The result (Fig. 12) can be compared with plots from the *Seabeam* survey on ANT III/1 and *Hydrosweep* from M6/4 in 1987/88 (Fig. 13). The good agreement can be observed not only for the flat topography in the central fracture zone, but also for the steep slopes. The differences between the positions of contour lines are about ±150 m.

1.1.5.8 Experience with *Parasound* (AWI)

Simultaneous operation of *Hydrosweep* and *Parasound* was performed outside the test areas, in order to avoid interference between both systems. During the transits, the ship's speed was about 15 kts which does not create serious problems. Good results were observed using *'normal Mode'* (HS Master, synchr.) until 3 000 m water depth. However in this mode, a reduced resolution was observed. Following this results, the *'Pilot Mode'* (PS Master, asynchr.) should be used in water depths greater than 1500 m. A good penetration was obtained even in very deep water using this Pilot-Tone-mode. Small interferences were observed in the outer *Hydrosweep* beams in areas with bad hydroacustic reflectors.

1.1.6 Positions with GPS in the Bay of Biscay (IEH, AWI)

For the calibration, the technical inspection and the acceptance tests of the new systems *Hydrosweep* and *Parasound*, a precise positioning of the vessel is important. The creation and compilation of large scale bathymetric maps (1:50 000) from multibeam sonar data requires high accuracy in the ship's position.

This can be achieved by the use of GPS/NAVSTAR. Four GPS receivers *TI-4100* were installed on *Polarstern*. For high precision relative kinematic navigation in the Bay of Biscay, two receivers of the same type were installed on the reference station in Brest. The use of four GPS receivers on *Polarstern* also allowed the ship´s attitude to be determined.

The absolute position accuracy for single stations in kinematic mode with P-Code is about ±10 m. With C/A-Code receivers the accuracy was ±20 to 30 m during the time of the cruise. By using two receivers and tracking the same satellites, the errors at both observation sites are mostly identical. Following from this, the determination of an interstation vector is possible with an accuracy of ±10 m even over long distances of more than 1 000 km. Improved ship´s positions can be determined by adding the measured interstation vector to the known coordinates of a reference point.

The measurement of the carrier phase data allows an increase in the accuracy of the baseline to a few decimeters, even to 1 ppm of the baseline length.

The reference station near Brest was occupied with two *TI-4100* receivers. The *TI-4100* cannot track more than four satellites. The use of two receivers, linked to one antenna, enables the user to observe up to 7 satellites. The observations near Brest were carried out by two observers from the Institut für Geodäsie, Universität Hannover. The observations were stopped on the day of arrival of *Polarstern* in Vigo.

The GPS-tracking was scheduled according to the actual satellite alerts to make sure that the same satellites were observed on the ship and on the reference station. Eight satellites were in orbit, two of which were the new Block II types. Satellite 8 was set unhealthy according to the almanac and therefore not used during this campaign. The observations with four receivers on board *Polarstern* were kindly supported by two Canadian colleagues and members of the AWI-Bathymetry Group.

In the Bay of Biscay, the period of a good GPS coverage with a maximum of 5 satellites in the "GPS-window" was between 21:00 and 11:00 UTC. In the equatorial region of the R.F.Z., the GPS visibility

changed to the time span between 20:00 to 08:00 UTC with a maximum number of 8 satellites.

The GPS-windows were used for precise ship's positioning, as well as for ship's attitude measurements. The time between GPS-windows was used for oceanographic measurements and calibration of *Hydrosweep* and *Parasound*. After leaving the Bay of Biscay, the ship's positioning was done in single station mode only.

For further scientific investigations, the data for speed, heading, roll, pitch and heave from the INDAS-system were recorded on magnetic tapes.

1.1.7 Satellite Remote Sensing (AWI)

During the first leg of the ANT VIII expedition, NOAA-AVHRR images were acquired with the goal of improving the methods of atmospheric corrections for the AVHRR data. This was done by combining these data with in-situ measurements of the atmospheric extinction caused by water vapor and aerosol. Additionally the sea surface temperature was recorded. The ground based measurements were carried out mainly in parallel with the satellite passes.

The tracking activities during the first leg of the expedition were also used as a test for the complete system.

1.1.7.1 Data Acquisition (AWI)

Data from the NOAA 10 and NOAA 11 satellites were acquired. The orbit parameters needed for the precalculation of the antenna navigation were provided by the Met-Office and by the AWI. For the undisturbed tracking of the satellite, the antenna system had to be corrected for the ship's position and heading. It results that for slow changes in the heading, an undisturbed acquisition was possible without any problems. The pitch and roll movement of the ship influenced the acquisition only at very low elevation angles. The main disturbance in data reception was caused by the superstructure of the ship itself. Simultaneous ground measurements of radiation for the determination of the aerosol extinction were made during 15 satellite passes. Subareas of the regions of interest around *Polarstern* were extracted from the raw data sets and stored on magnetic tapes for the postprocessing at the institute.

1.1.7.2 Radiation Measurements (AWI)

For the determination of the aerosol extinction, measurements of the direct solar radiation were carried out during suitable weather conditions (no clouds) by using a portable photometer. The pre-processing of the data on board showed that all desired atmospheric conditions were included in the data set. In parallel to these

atmospheric measurements, the sea surface temperature was recorded using an infrared radiometer, and the water vapor content was estimated from radiosonde profiles.

1.1.7.3 Radiosonde Measurements and XBT-Measurements (AWI)

As usual during the previous north-south cruises of *Polarstern*, operational measurements of atmospheric and oceanic conditions were made using radiosondes and XBT's. Between 40°N and 40°S, these observations were done at every degree of latitude.

The radiosonde observations started at 7 August 1989 after passing the English Channel. Altogether 96 measurements were made. The radiosondes reached altitudes between 8 000 m and 29 500 m. Up to four measurements per day were included into the GTS. All data sets were stored on tapes and are available from the Alfred-Wegener-Institut. The XBT measurements started at 15 August 1989 at 40°N. Altogether 78 profiles were collected from which 73 profiles reached 900 m water depth and five XBT's reached 2 000 m water depth. The deep profiles were combined with CTD profiles obtained in parallel (Fig. 14 and 15).

1.1.8 Light Hydrocarbon, PAN and CO in the Marine Atmosphere and Dissolved Hydrocarbons in the Surface Water of the Atlantic (KFA)

The series of investigation of the marine atmosphere and its chemistry was continued during ANT VIII/1 by measurements of light nonmethane hydrocarbons (NMHC), peroxyacetylnitrate (PAN), CO and H_2 over the Atlantic and measurements of dissolved NMHC in sea water.

The atmospheric measurements were carried out similar to previous cruises on the top deck of the *Polarstern* in a laboratory container. Sea water samples from the continuous pumping system of Polarstern were analyzed in a ship laboratory. The concentrations were measured by in situ gas chromatography in intervals of about 3 hours. The lower limits of detection were about 1 pMol/l NMHC in sea water and 10 ppt of NMHC, 0.5 ppt PAN and 1 ppb CO in the atmosphere.

The NMHC concentrations in the surface sea water were in the range of some pMol/l to several hundreds of pMol/l. This is comparable to previous results obtained during the *Polarstern* cruise ANT VII/1 in 1988. Alkene concentrations were higher by factors of 3 to 10 compared to homologous alkane concentrations, and concentrations generally decreased with increasing molecular weight per compound. No strongly enhanced concentrations of NMHC were found in regions of high biological activity, e.g. the upwelling region of Northwest Africa.

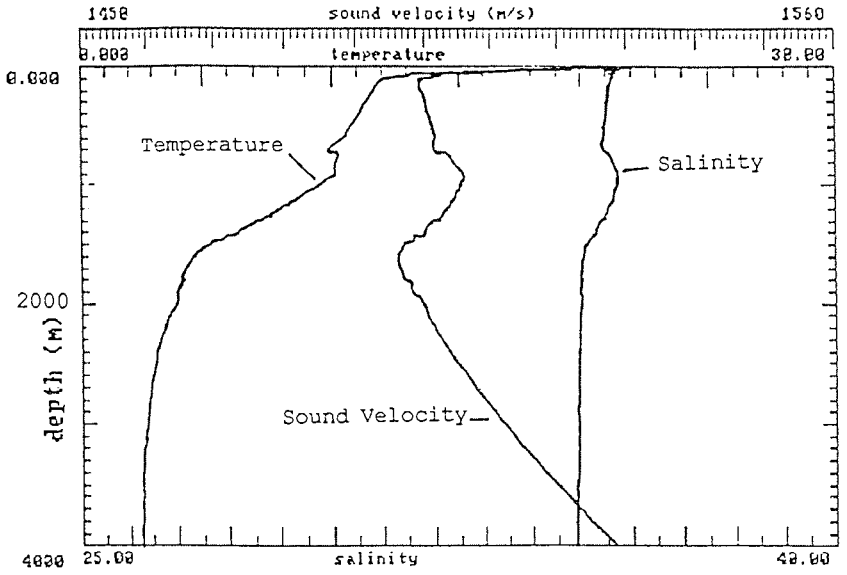

CTD-Messung von Lokation 1 8.8.89
Position : 45:50 N / 6:40 W

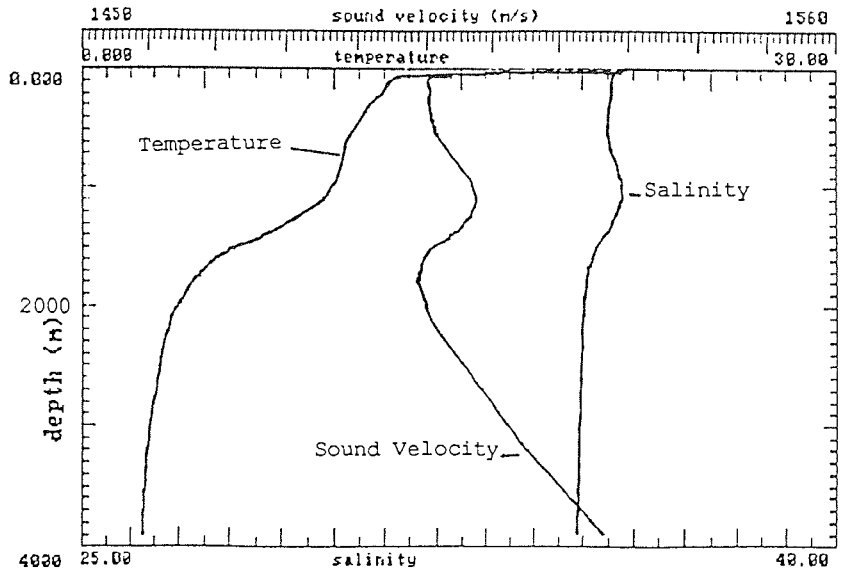

CTD-Messung von Lokation 2B 10.8.89
Position : 45:53 N / 4:40 W

Fig. 14: Results from CTD-measurements at Location 1 (above) and Lokation 2B

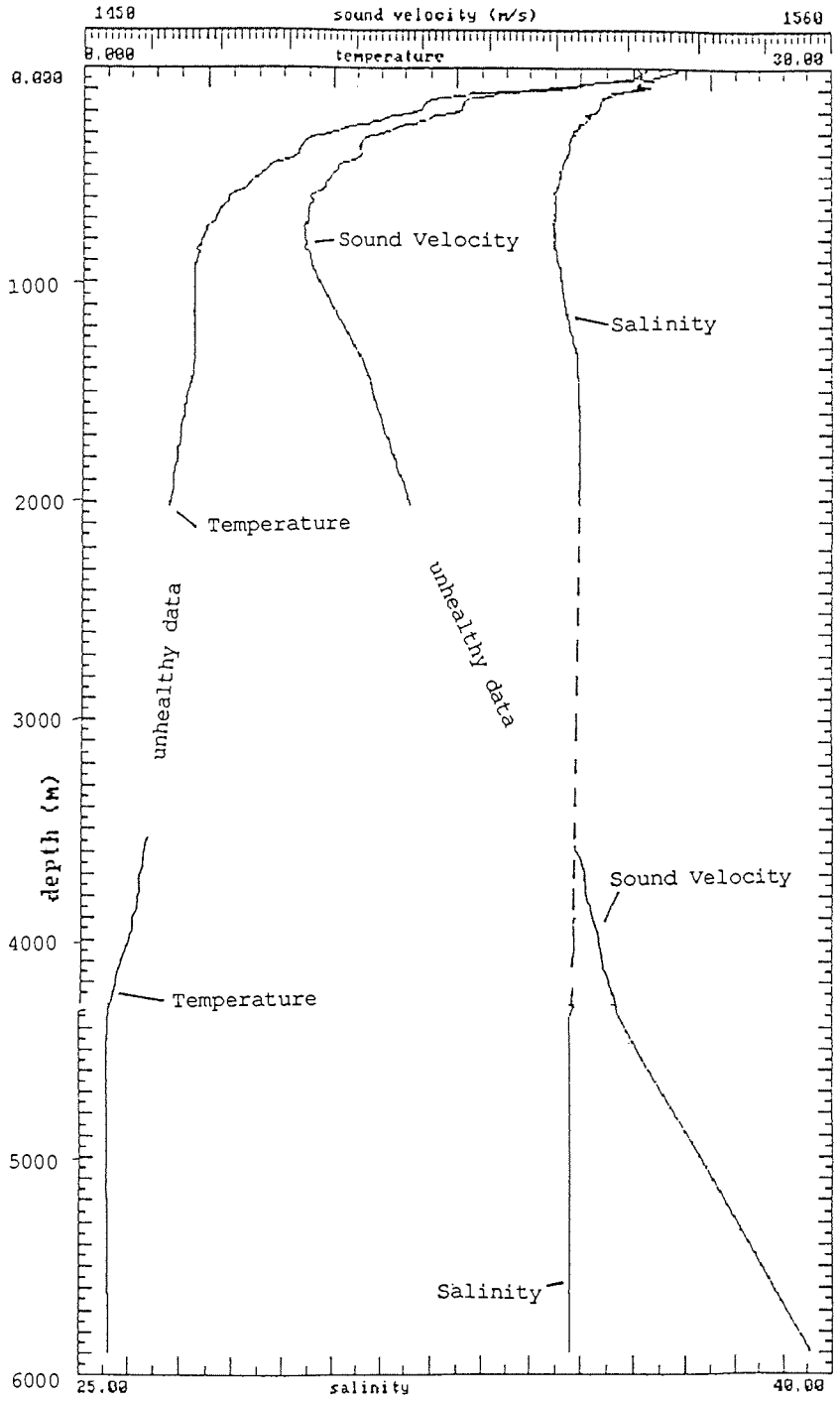

Fig. 15: Result from a CTD profile in the Romanche Fracture Zone

24.8.89

Position : 0:12 S / 18:22 W

The atmospheric concentration of the reactive alkenes were between 100 ppt and below the lower limit of detection of about 10 ppt, e.g. the average ethene concentration south of 20°N was 15 ppt. Average ethene concentrations were significantly lower compared to averages obtained from previous cruises. The concentrations of the longer lived alkanes were comparable with results from previous cruises, e.g. ethane concentrations were between 300 ppt and 600 ppt between 30°N and 30°S.

The CO concentrations south of 40°N were below 100 ppt. In the southern hemisphere, concentrations were close to 40 ppb. These concentrations are on the lower side of the previously reported concentrations of CO.

PAN concentrations showed the highest variability of the measured atmospheric trace gases, as could be expected from the highly temperature-dependent thermal decomposition rate of PAN. North of 40°N, concentrations ranged from 2 ppb down to below 1 ppb. At elevated temperatures between 40°N and 25°S, the PAN concentrations were below the lower limit of detection of 0.5 ppt, except for some episodes with a maximum of 3 ppt. South of 25°S, concentrations of PAN rose again up to 100 ppt at 30°S. These results are in agreement with our findings during the cruise in 1988.

1.1.9 Measurements of Reactive Nitrogen Components in the Atmospheric Boundary Layer over the Atlantic Ocean (IfBG, CRA)

During the *Polarstern* cruise ANT VIII/1, we measured different species of airborne reactive nitrogen components. The measurements have been continued on the following leg ANT VIII/2, so that we have been able to assess a meridional concentration profile of these air constituents over the Atlantic Ocean in the latitudinal range from 50°N to 70°S. We applied a filter pack method, where the investigated gases, ammonia and nitric acid vapor were accumulated on gas absorbing filters after separation of atmospheric aerosol particles with PTFE filters (Fig. 16). In addition to this, we sampled size-fractionated aerosol particles with a casade impactor (Type Sierra).

A steep gradient could be shown between the continentally influenced areas in the northern latitudes and the remote areas over the ocean. The concentrations of nitric acid vapor over the remote oceanic atmosphere were very low (about 10 pptv); differences between remote locations in different latitudes were however small. An increase of ammonia concentrations in equatorial regions indicates nearby ammonia sources. This supports the hypothesis that in tropical regions, the ocean may be a source for atmospheric

Fig 16: Filter Systems for collecting atmospheric trace components in the Atmosphere

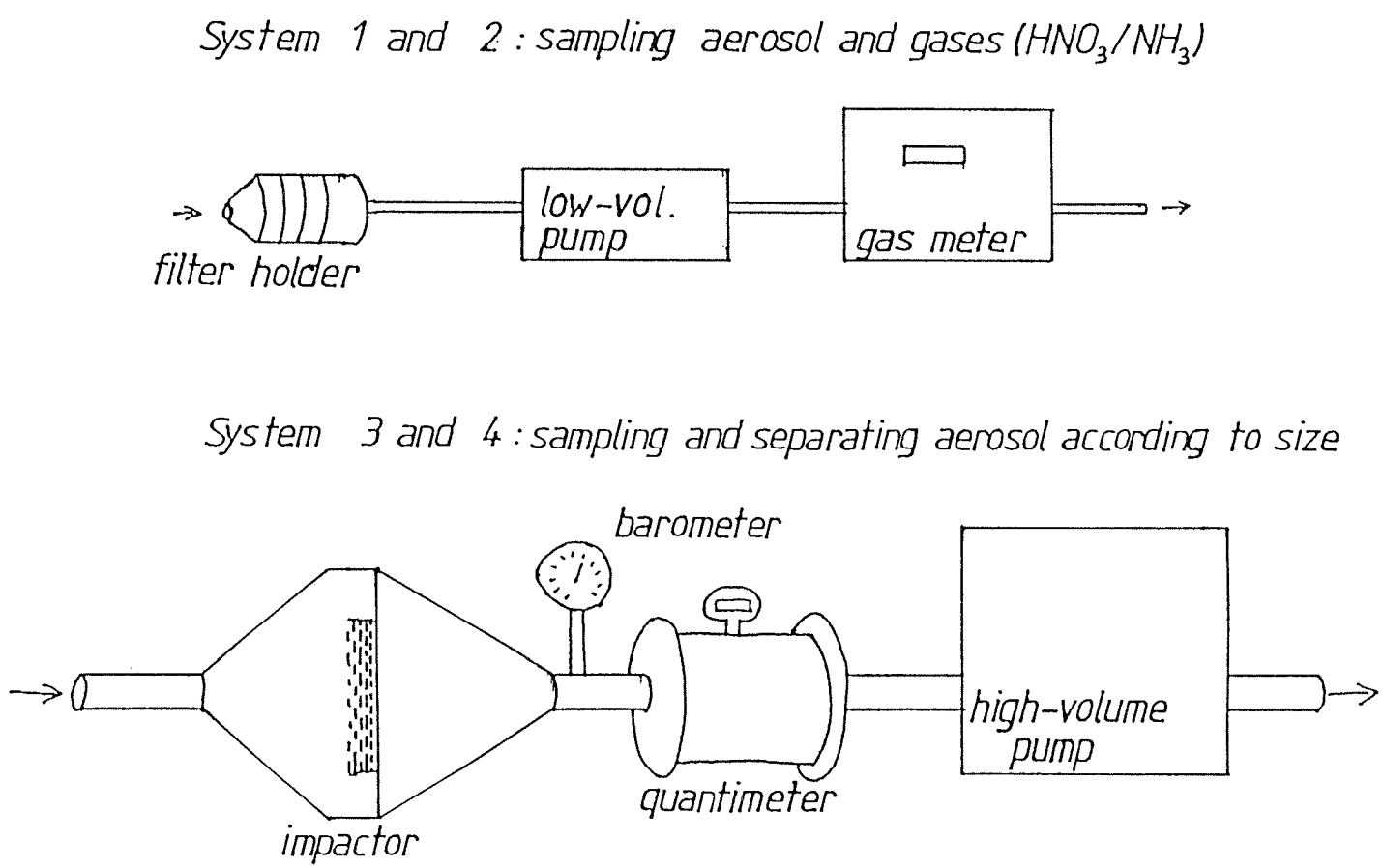

Filter systems for collecting atmospheric trace components

ammonia, as it has been calculated with data of an expedition in the tropical regions of the Pacific Ocean.

The aerosol data show that the excess sulfate and ammonia are concentrated on the small particle size ranges (<1 μm radius), whereas the nitrate is bound to the sea salt size range (>1 μm radius).

1.1.10 Atmospheric Ozone and Turbidity (AARI)

The total content of ozone was measured by the standard Soviet filter ozonoter M-124 as of 6 August 1989. The general aims of these work (as well as measurements of tropospheric ozone) were to verify the performance of the equipment and to solve some technical problems before the main period of the observations in Antarctica. Nevertheless en route from Bremerhaven to Puerto Madryn, some results listed in the Table 2 were obtained. These values should be considered as preliminary ones, because a large part of experimental data is not processed so far. The total ozone content is in general in accordance with values usually measured in this region and season.

Date: August, 89	Point of measurements	Total ozone, Dobson Units	Aerosol optical depth at λ=0.423 microns
6	50 N 0 W	356	NM
7	48 N 5 W	333	NM
8	47 N 6 W	330	NM
9	46 N 7 W	320	NM
11	45 N 4 W	309	NM
12	45 N 3 W	308	NM
14	42 N 9 W	308	NM
15	37 N 11 W	307	NM
16	32 N 13 W	295	0.19
17	25 N 16 W	282	0.36
18	21 N 18 W	281	NM
19	15 N 18 W	282	NM
20	9 N 18 W	230	NP
27	8 S 25 W	NP	0.03
28	13 S 29 W	NP	0.08

Tab. 2:
Daily means of total content of atmospheric ozone according to direct sun observations in the atmosphere and the aerosol part of optical depth (is equal to total optical depth minus Rayleigh scattering). NM means "not measured", NP means "not processed". Preliminary values of aerosol depth are given.

Measurements by means of the Soviet solid state chemiluminescent ozone analyzer began on 7 August 1989. Relatively high values of ozone concentrations in the surface layer were present in the Bay of Biscay region: 40-50 ppb. From 15 to 20 August 1989, concentrations of ozone were lower: from 20 ppb during a night to 30 ppb during a day. Minimal ozone concentrations were observed between 18 and 19 August 1989 close to ITCZ (lower than 20 ppb). From 20 to 22 August 1989 the measurements were interrupted due to technical problems. In the southern hemisphere, ozone concentrations were in the range 20-30 ppb.

Atmospheric turbidity was measured by filter sunphotometer at 6 wavelengths in the range 0.423 - 0.746 microns beginning 16 August 1989 (11 working days). Preliminary analysis of the data (see the Table 2) revealed two regions with different aerosol optical depth: near the African coast (16 and 17 August 1989) and to the south from ITCZ from 27 to 28 August 1989. Sahara dust may be the cause of this increased atmospheric turbidity.

In conclusion it should be noted that the equipment for the ozone studies is working well. The obtained results are in reasonable accordance with the data obtained by other groups participating in the expedition. Detailed comparison may be done after final treatment of obtained data.

1.1.11 Sea Ice Biology, Marine Plankton and Krill (IFB, IFO)

During the first leg of the expedition, the program of the planned field work in Antarctica during the cruise ANT VIII/2 on the investigation of microscopical communities of algae in marine ice, as well as phytoplankton near the ice edge, were studied and examined once more in detail.

Previous studies have shown that methods of modern systematics can be successfully used for eco-morphological investigations of these communities, their taxonomical components, their spatial and temporal distribution, and their different dependence on environmental conditions.

The very small diatoms and siliceous organisms ($<10^{-5}$ m) are an essential part of the winter and spring communities in marine ice. They will be studied during the second leg of the Antarctic expedition. The summarization of literature data, as well as original material, was completed concerning the peculiarities of the seasonal dynamic and spatial composition of Antarctic plankton communities for the Weddell Gyre. The purpose of this work was to determine the best strategy for the collection of plankton samples and for the field examination of samples during the period of *Polarstern* ANT VIII/2,

as well as through the last northward transect of *R/V Academic Fedorov* after the two ships had met.

The scientific library on board the *Polarstern* was of much use for this preparation, because it contains several rather rare books and contributions. We have also used data (published and unpublished) of several German expeditions (*Polarstern, Polarcirkel*), as well as Soviet expeditions (*Akademik Knipovich, Argus, Eurica, Professor Viese*) for the late fall, winter and early spring seasons.

The results of these summarizations confirm, in particular, the need to carry out the plankton collection down to 1000 or 1500 m. It is also imperative to investigate the following subregions of the Weddell Gyre, which are of special interest, in as detailed fashion as possible:

1. The ice-free zones of Drake Passage and the Scotia Sea
2. The waters related to the Bouvet divergence
3. The inshore zone of the Antarctic continent
4. The waters related to the Maud Rise.

In all of these subregions, strong contrasts may be expected with respect to the effect of the seasonal succession on the phases of the massive copepod population development, as well as on the discrepancies in the age-composition of euphausid larvae. Also, a more detailed scale of the maturation stages of the Antarctic krill was prepared, on the basis of the standard scale which is used on USSR expeditions, to make it better adapted to the winter-spring seasons. This increased detail mainly concerns the krill males, which undergo a rapid ripening during these seasons. This scale, while material to krill collecting, will also permit more careful evaluation of the spatial and temporal peculiarities of the winter and early spring processes of the reproductive cycle of krill, which represent one of the key periods for the understanding of krill biology for these seasons.

1.1.12 Zeitplan / Time Table

Departure from Bremerhaven:
5 August 1989

Calibration, Tests and Acceptance of *Hydrosweep* and *Parasound*:
6 to 13 August 1989

Arrival at Vigo, Spain and disembarking of 24 personc:
14 August 1989

Deep sea trials and survey at the Romanche Fracture Zone:
22 to 25 August 1989

Arrival at Puerto Mardryn, Argentina:
5 September 1989

1.1.13 Beteiligte Institute/Participating Institutions

Adresse Address		Teilnehmerzahl Number of Participants
Federal Republic of Germany		
AWI	Alfred-Wegener-Institut für Polar- und Meeresforschung Postfach 120161 D-2850 Bremerhaven	14
DWD	Deutscher Wetterdienst Bernhard-Nocht-Straße 76 D-2000 Hamburg 4	1
GEO	Geophysics Consulting GmbH Büro für Angewandte Geophysik Martastraße 10 D-2300 Kiel 1	2
HALO	Hapag Lloyd Transport & Service GmbH Geo-Plate-Straße D-2850 Bremerhaven-Kaiserhaven	3
IfBG	Georg-August-Universität Forstwissenschaftlicher Fachbereich Institut für Bioklimatologie Büsgenweg 43 D-3400 Göttingen	1
IEH	Institut für Erdmessung der Universität Hannover Nienburger Straße 6 D-3000 Hannover 1	3
IfMG	Institut für Meteorologie und Geophysik der Universität Frankfurt Feldbergstr. 27 D-6000 Frankfurt/Main 1	2
KAE	Krupp Atlas Elektronik GmbH Sebaldsbrücker Heerstraße 235 D-2800 Bremen 44	7
KFA	Kernforschungsanlage Jülich GmbH Institut für Athmosphärische Chemie Postfach 1913 D-5170 Jülich	4

PRAKLA	PRAKLA-SEISMOS AG Buchholzer Straße 100 D-3000 Hannover 51	1
RUB	Ruhr-Universität Bochum Fakultät für Chemie Lehrstuhl für Physikalische Chemie I Universitätsstraße 150 D-4630 Bochum 1	1
ELAC	Honeywell-ELAC Nautik GmbH D-2300 Kiel	1
Canada		
PCT	Pulsearch Consolidated Technology Ltd. Suite 700, 10201 Southport Road S.W. Calgary, Alberta Canada T2W 4X9	1
UoC	The University of Calgary Faculty of Engineering 2500 University Drive N.W. Calgary, Alberta Canada T2N 1N4	1
Republic of China		
CRA	Chinese Research Academy of Environmental Sciences in Peking Beiynan Beijing Peoples Republic of China	2
Union of Socialistic Soviet Republics		
AARI	Arctic and Antarctic Research Institute 38 Berin Street 19226 Leningrad	2
IFB	Institute for Botany Academy of Sciences 2 Popov Street 197022 Leningrad	1
IFO	Institute of Fishery and Oceanography 17a Verkhnyaya Krasnoselskaya 107140 Moskau	1
Unites States of America		
LDGO	Lamont-Doherty Geological Observatory of Columbia University Palisades, N.Y. 10964	1

1.1.14 Fahrtteilnehmer / Participants

Name / Name			Institution
Arps	Erwin	•	ELAC
Beckmann	Hansjürgen	•	HLTS
Block	Peter	*	KAE
Braun	Michael	•	KAE
Briedenhan	Claus	•	HLTS
Brokhoff	Jörg	*	GEO
Bruns	Reinhardt	*	KAE
Castellier	Etienne		AWI
Döscher	Thorsten		AWI
Focke	Jens		AWI
Freking	Benno	*	KAE
Gärtner	Thomas		AWI
Goldan	Hans-Jürgen		IEH
Helmes	Leni		AWI
Hinze	Heinrich		AWI
Höppe	Götz		AWI
Hoppe	Thomas		IEH
Husmann	Claus	*	HLTS
Ibrom	Andreas		IfBG
Jonen	Franz-Joseph		KFA
Kloft	Claus	*	KAE
Knickmeyer	Elfriede	*	UofC
Knickmeyer	Ernst-Heinrich	*	PCT
Koppmann	Ralf	*	KFA
Kuhn	Gerhard	*	AWI
Lyuleev	Maxim		AARI
Makarov	Rodion		IFO
Munsch	Iris		AWI
Niederjasper	Fred		AWI
Nikolaev	Viktor		IFB
Nohr	Guido		KFA
Oesterle-Zell	Alexandra	*	KAE
Ochsenhirt	Wolf-Thilo		DWD
Papenbrock	Thomas		RUB
Plaß	Christian		KFA
Qi	Liwen		CRA
Schacht	Marina		AWI
Schenke	Hans Werner		AWI
Schlonsky	Steffen	*	PRAKLA
Staubes	Regina		IfMG
Steinmetz	Stefan		AWI
Stennett	Joe	*	LDGO
Tietze	Gunnar	*	GEO
Uhrbrock	Jens		KAE
Villinger	Heiner	*	AWI
Weber	Michael	*	AWI
Wolz	Guido		IfMG
Yurganov	Leonid		AARI
Zai	Yi Qi		CRA

• : Bremerhaven - Vigo

1.1.15 Schiffsbesatzung /Chip's Crew

	ANT VIII/1
Kapitän	Jonas
1. Offizier	Gerber
1. Offizier Ladung	Schiel
1. Offizier Nautik	Fahje
Arzt	Dr. Reimers
Ltd. Ingenieur	Dietrich
1. Ingenieur	Schulz
2. Ingenieur	Erreth
2. Ingenieur	Fengler
Elektroniker	Both
Elektroniker	Elvers
Elektroniker	Hoops
Elektroniker	Piskorzynski
Elektriker	Muhle
Funkoffizier	Butz
Funkoffizier	Müller
Koch	Klasen
Kochsmat	Klauck
Kochsmaat	Kröger
1. Steward	Peschke
Krankenschwester/Stewardess	Lieboner
Stewardess	Hopp
Stewardess	Hoppe
Stewardess	Gollmann
2. Steward	Chi-Chun, Chang
2. Steward	Yiu-Sin, Chau
Wäscher	Tzyh-Shyang, Shyu
Bootsmann	Schwarz
Zimmermann	Kassubeck
Matrose	Meiss Torres
Matrose	Garcia Martinez
Matrose	Willbrecht
Matrose	Novo Lovreira
Matrose	Prol Otero
Matrose	Pereira Portela
Matrose	Barth
Lagerhalter	Jordan
Maschinenwart	Fritz
Maschinenwart	Heurich
Maschinenwart	Buchas
Maschinenwart	Reimann
Maschinenwart	

2. ANT VIII/2

(FS Polarstern: E. Augstein
FS Akademik Fedorov: N. Bagriantsev)

2.1. Wissenschaftliche Ziele und Fahrtverlauf

Die *Winter Weddell Gyre Study 1989 (WWGS `89)* war eine Gemeinschaftsunternehmung des *Alfred-Wegener-Instituts für Polar- und Meeresforschung* (AWI), *Bremerhaven* und des *Arktis- und Antarktis-Forschungsinstituts* der UdSSR (AARI), *Leningrad* mit deren Forschungsschiffen *Polarstern* und *Akademik Fedorov*. An den Forschungsarbeiten waren ferner Wissenschaftler aus den *Vereinigten Staaten von Amerika, Großbritannien* und *Kanada* beteiligt. Das Meßprogramm zur Erfassung der Massen-, Wärme-, Salz- und Meereistransporte durch den Weddell-Wirbel und der damit verknüpften Wassermassenveränderungen im südlichen Weddell-Becken bildete den ersten von insgesamt vier Beiträgen ähnlicher Art, die das AWI im Rahmen des *World Ocean Circulation Experiment (WOCE)* unter internationaler Beteiligung bis 1993 vorgesehen hat.

Die ozeanographische Kernstudie wurde durch ausführliche Untersuchungen der Meereisdynamik, der Wechselwirkungen zwischen Luft, Eis und Wasser, der Grundlagen zur Meereis- und Ozeanfernerkundung von Satelliten aus, des Lebens im Meereis und im oberen Bereich der Wassersäule des Weddellmeeres vervollständigt. Die dabei verfolgten Forschungsanliegen unterschiededlicher Fachrichtungen sind zumindest teilweise eng miteinander verzahnt, so daß sie nur in der dieser Expedition zugrundeliegenden interdisziplinären Zusammenarbeit erfolgreich behandelt werden können.

Mit Hilfe der beiden Schiffe konnten im Laufe von sechs Wochen Messungen auf vier Schnitten senkrecht zur Zirkulation des Weddellwirbels durchgeführt werden (Fig.. 2.1). Die beiden Polarstern-Kurse, die von der *Antarktischen Halbinsel* zur *Georg-von-Neumayer-Station* und von dort nordwärts zum *Antarktischen Zirkumpolarstrom* führten, durchquerten jeder die gesamte ozeanische Zyklone. Die beiden Traversen der *Akademik Fedorov* im nordwestlichen Sektor des Weddellmeeres vervollständigten die Beobachtungen im nordostwärts gerichteten Zweig des Strömungssystems. Die Arbeiten auf den beiden Schiffen waren im wesentlichen auf folgende Ziele gerichtet:

- Die Bestimmung des baroklinen Massentransports und der mit ihm verknüpften horizontalen Wärme- und Salzflüsse im Weddell-Wirbel
- Die Abschätzung der Wassermassenumwandlung im inneren Weddellbecken
- Die quantitative empirische Untersuchung mesoskaliger Ozeanstrukturen auf der Leeseite des *Maudrückens*

- Die umfassende Beschreibung der Konzentration, der Dicke, der Bewegung, der physikalischen und chemischen Eigenschaften des Meereises und des darin beheimateten pflanzlichen und tierischen Lebens

- Die Berechnung der atmosphärischen und ozeanischen Einwirkungen auf das Meereis aus Messungen oberhalb und unterhalb der Eisdecke

- Die Beschreibung der regionalen Verteilung des Phyto- und Zooplanktons in der oberen Wassersäule unter dem vorliegenden Nahrungsangebot und den physikalischen und chemischen Umgebungsbedingungen im Spätwinter

- Die Durchführung von Bodenbeobachtungen zur Überprüfung und Verbesserung passiver und aktiver Mikrowellenmessungen von zur Zeit bzw. in Zukunft verfügbaren Satelliten

- Die Erfassung der Ozonkonzentration in der atmosphärischen Säule des antarktischen Polarwirbels im Spätwinter.

An diesen Projekten wirkten 118 Wissenschaftler und Techniker, davon 56 auf *Polarstern* und 62 auf der *Akademik Fedorov* mit, die Forschungs- und Universitätsinstituten der *Bundesrepublik Deutschland*, der *UdSSR*, der *USA*, *Großbritanniens* und *Kanadas* angehören. Die Teilprogramme wurden überwiegend von multinationalen Gruppen geplant und im Feld gemeinsam durchgeführt. Zur ständigen Abstimmung der Arbeiten zwischen den beiden Schiffen dienten tägliche Funkgespräche der wissenschaftlichen Leiter und - soweit notwendig - der für die Teilprojekte verantwortlichen Wissenschaftler. Die enge Zusammenarbiet der Expeditionsteilnehmer soll auch bei der Aufbereitung der Daten und wissenschaftlichen Interpretation der Ergebnisse fortgesetzt werden.

2.1.2 FS Polarstern

Das Forschungsschiff *Polarstern* verließ den argentinischen Hafen *Puerto Madryn* am 6. September 1989 mit 42 Besatzungsmitgliedern und 56 Wissenschaftlern an Bord und hielt Kurs auf die *Bransfield-Straße* nördlich der *Antarktischen Halbinsel*. Das wissenschaftliche Meßprogramm wurde bei 54°S mit täglichen Radiosondenaufstiegen und XBT (Bathythermographen)-Abwürfen in Abständen von 15 sm begonnen. Das erste vollständige hydrographische Vertikalprofil wurde am 10. September auf der Breite 58°S mit der CTD-Sonde und dem Rosettenwasserschöpfer gemessen. Einen Tag später erreichte das Schiff den Meereisrand bei 61°53´S nahe der Insel *King George*. Am selben Tag erfolgte unter mäßigen Sichtbedingungen ein Hubschrauberflug zur chilenischen Station *T. Marsh* auf der *King-George-Insel*, um ein dort deponiertes

Radiometer der NASA-Gruppe abzuholen. Zur Verminderung der Flugstrecke dampfte *Polarstern* bis zur Rückkehr des Hubschraubers in der *Bransfield-Straße* auf die Station zu. Danach kehrte das Schiff zum Rand der kompakten inneren Eisübergangszone zurück, um bei 62°W/57°W ein engmaschiges hydrographisch-biologisches Meßnetz in südöstlicher Richtung über die *Bransfield-Straße* zu beginnen (Fig.. 2.1). Die Beobachtungsprogramme aller Disziplinen wurden am 12. September östlich der Spitze der *Antarktischen Halbinsel* am Startpunkt einer großen zonalen Traverse durch den *Weddell-Wirbel* mit folgenden Messungen aufgenommen:

- Vertikale CTD- und Wasserschöpferprofile (Rosette mit 24 Schöpfern) von der Meeresoberfläche bis zum Meeresboden in horizontalen Abständen von 30 sm. Eine noch engere Maschenweite wurde über den Schelfabhängen - orientiert an vorgegebenen Tiefenlinien - und eine weitere (60 sm) im inneren Bereich der meridionalen Traverse von der *Georg-von-Neumayer-Station* zum *Antarktischen Zirkumpolarstrom* gewählt. Während letzterer wurde der Stationsabstand beim Durchqueren der nördlichen Eisrandzone wieder auf 30 sm verdichtet

- Auslegen von 7 Strommesserverankerungen auf dem Zonalschnitt und Bestimmung des vertikalen Strömungsprofils in den oberen 200 m der Wassersäule mit einem Doppler-Sonar an allen Stationen im Eis als Ergänzung zu den hydrographischen Daten

- Turbulente vertikale Impuls- und Wärmeflüsse in der Luft und im Wasser unter dem Meereis. Die Messungen in der Atmosphäre wurden während aller längeren Stationsaufenthalte diejenigen im Ozean nur während drei mehrtägiger Stationen durchgeführt

- Bestimmung des atmosphärischen Bodendruckfeldes und der Eisbewegungen mit Hilfe zweier Argos-Bojennetze im westlichen und mittleren Weddellmeer. Beide Netzwerke enthielten zwei innere Bojen, die zusätzlich den Windvektor, die Lufttemperatur und über Thermistorketten die vertikale Temperaturverteilung durch das Meereis und in der Wassersäule bis 250 m Tiefe registrierten. Alle Daten des gesamten Bojenfeldes werden voraussichtlich mehrere Monate lang über das Argos-System mit Hilfe von Satelliten automatisch übertragen

- Anlage von Bohrlochprofilen zur Erfassung der Dicke sowie der Morphologie der oberen und unteren Ränder des Meereises und der Schneeauflage. Ferner wurden Eiskerne gewonnen, um die Textur und die physikalischen und chemischen Eigenschaften des Eises zu bestimmen. Die kleinräumige mechanische Beanspruchung der Schollen wurde mit Hilfe von Dehnungsmessungen festgestellt. Schließlich wurden von Hubschraubern aus die Eiskonzentration, das

Schollengrößenspektrum und die Oberflächentopographie durch Photo- und Videoaufnahmen sowie mit einer digitalen Rasterkamera aufgezeichnet

- Aktive und passive Mikrowellenbeobachtungen vom Schiff aus in Verbindung mit in situ-Messungen der bedeutsamen Eis- und Schneeparameter, um die Algorithmen derzeitiger und für die nahe Zukunft vorgesehener Satellitenfernerkundungsdaten zu überprüfen und zu verbessern. Hochauflösende Satellitenbilder (AVHRR) im sichtbaren und infraroten Wellenlängenbereich wurden zur Bewertung der großskaligen Eiskonzentration und -bewegung an Bord regelmäßig aufgenommen

- Ausführliche Analysen der regionalen und vertikalen Verteilung der Meereislebensgemeinschaften in Abhängigkeit von den physikalischen und chemischen Umgebungsbedingungen. Mit besonderer Aufmerksamkeit wurde die Taxonomie der Meereisbewohner vorgenommen

- Bestimmung der Konzentrationen der Nährstoffe sowie des Phyto- und Zooplanktons aus Wasserproben und Fängen mit Multi- und Bongonetzen.

Die genannten Untersuchungen wurden teilweise auf dem Schiff, auf dem Eis oder von Hubschraubern (Typ BO-105) aus durchgeführt. Die Fahrtroute des Schiffes und das Stationsnetz beruhten im wesentlichen auf den Anforderungen der Physikalischen, Chemischen und Biologischen Ozeanographie. Die anderen Disziplinen konnten ihre Meßprogramme ohne wesentliche Einbußen an diese Vorgabe anpassen.

Auf der Route durch das Eis traf *Polarstern* in den verschiedenen geographischen Regionen erwartungsgemäß unterschiedliche Navigationsbedingungen an. Im nordwärts setzenden Oberflächenstrom des westlichen *Weddellbeckens* überwog älteres Eis, das schwer zu brechen war. Dennoch wurde das Fortkommen nicht ungewöhnlich behindert, weil sich bei einer Eisbedeckung von 90% passende Rinnen finden ließen, so daß noch eine mittlere Fahrtgeschwindigkeit von 5 kn erzielt werden konnte. Im Zentrum des Wirbels überwog dann dünneres, einjähriges, dichtgepacktes Eis, in dem häufiger gerammt werden mußte, so daß die zurückgelegten Tagesstrecken etwas schrumpften. Die ungünstigsten Verhältnisse mit einer ausgeprägten Preßeiszone herrschten vor der Ostküste des *Weddellmeeres*. Besonders nachteilig wirkten sich hier gestrandete Eisberge aus, zwischen denen die überwiegend nördlichen Winde das Eis aufgestaut hatten. *Polarstern* geriet dort zweimal in eine Scherungszone des driftenden Eises, aus der sie sich erst in Gebieten mit geringerer Oberflächenkonvergenz befreien konnte. Gleichartige Bedingungen vor der *Atka-Bucht* wurden aufgrund der frischen Erfahrungen bereits mit mehr Geschick leichter überwunden.

Die Eiskonzentration betrug auch auf der meridionalen Traverse von der *Georg-von-Neumayer-Station* nach Norden fast durchgängig über 90%. Besonders große und dicke Schollen lagen südwestlich des *Maudrückens*. Weiter nördlich nahm die Festigkeit des Eises ab und das Manövrieren vereinfachte sich wieder. Besonders erwähnenswert ist die etwa 350 km breite Eisrandzone, die das Schiff erst bei 53°44´S/07°18´E völlig durchquert hatte. Zusammengefaßt ergibt sich nach Abzug der Stationszeiten die unerwartet hohe Durchschnittsgeschwindigkeit von 6.25 kn, die eine Verlängerung der geplanten Arbeitszeiten um 25% und damit die vollständige Befriedigung aller Programmwünsche zuließ.

Die beiden Bojennetze (Fig. 2.2) wurden teils vom Schiff, vor allem aber mit Hilfe der Hubschrauber ausgelegt. Glücklicherweise stellten sich die dafür notwendigen Wetterverhältnisse stets rechtzeitig ein. Zwei der drei längeren Meereisstationen wurden in das Innere der Bojenfelder gelegt, um später die genaueren Informationen über die atmosphärischen und ozeanischen Umgebungsbedingungen bei der Datenanalyse dieser Punktmessungen nutzen zu können. Die dritte längere Meßphase an einem Ort lag im Bereich des östlichen Küstenstroms nördlich der *Atka-Bucht*. Damit konnten die drei Hauptelemente des *Weddellwirbels*, nämlich die westlichen und östlichen Küstenströme und das Zentrum erfaßt werden.

Das Auslegen der sieben Strommesserverankerungen (Fig 2.3) auf dem Zonalschnitt verlief trotz des dicken Eises und des teilweise unangenehmen Wetters problemlos. Hier schlugen die Erfahrungen des eingespielten Bord- und Institutspersonals mit Verankerungen im Eis vorteilhaft zu Buche.

Eine Abwechslung im eingefahrenen Meßbetrieb bot das Ausladen von Fahrzeugen und Containern in der *Atka-Bucht* mit Besuchen der *Georg-von-Neumayer-Station* am 10. und 11. Oktober. In gleichartig guter Stimmung verlief ein Treffen mit der *Akademik Fedorov* am 17. und 18. Oktober westliche des *Maudrückens*. Neben den Vergleichen von Geräten sowie der Probennahme- und Fangmethoden wurde diese Gelegenheit zu Gesprächen mit den Fachkollegen des Partnerschiffes und zu einer gemeinsamen Feier aller auf dem Eis genutzt. Die Zufriedenheit über die reibungslose Zusammenarbeit fand auch in dem übereinstimmenden Wunsch nach der Fortsetzung derartiger gemeinsamer Forschungsunternehmen in der *Antarktis* und in der *Arktis* ihren Niederschlag.

Am 25. Oktober verließ *Polarstern* nach Vollendung zweier hydrographischer Schnitte durch das gesamte Stromsystem des *Weddellwirbels* den Meereisgürtel. Außerdem wurden während der sieben Wochen im winterlichen Meereis der *Antarktis* wertvolle meteorologische, glaziologische und biologische Daten gesammelt und neue Erkenntnisse zur Eisfernerkundung gewonnen. Regelmäßige wissenschaftliche Seminare an Bord dienten sowohl der Aktualisierung des Meßprogramms als auch einer vorläufigen

Bewertung der Ergebnisse. Letztere lassen erwarten, daß die multinationale und interdisziplinäre *Winter Weddell Gyre Study 1989* einen beachtenswerten Beitrag zur Erforschung des südpolaren Ozeans - insbesondere hinsichtlich seiner Beeinflussung des globalen Klimas - geleistet hat. Der Fahrtabschnitt der *Polarstern* endete am 30. Oktober mit dem Einlaufen in den Hafen von Kapstadt.

2.1.3 Akademik Fedorov

Die *Akademik Fedorov* verließ den Hafen von *Montevideo* am 12. September 1989, um der *Polarstern* in das Eis des *Weddellmeeres* zu folgen. Das Schiff wurde von einer 87 Personen starken Besatzung (einschließlich der Hubschraubermannschaft) betrieben und hatte 62 Wissenschaftler und Techniker aus der Sowjetunion, der Bundesrepublik Deutschland und den Vereinigten Staaten an Bord. Letztere bearbeiteten gemeinsam das folgende Meßprogramm:

- CTD- und Wasserschöpferprofile zur quantitativen Erfassung der Zirkulation des Weddellwirbels, insbesondere der winterlichen Wassermassenschichtung und der lateralen Massen-, Wärme-, Salz- und Meereistransporte

- Beobachtung der meso- und kleinskaligen Meereisvariationen in Abhängigkeit vom atmosphärischen Antrieb

- Bestimmung des Energie- und Impulsaustausches zwischen Atmosphäre, Meereis und Ozean im eisbedeckten *Weddellmeer*

- Analyse von Nährstoffen und sonstigen chemischen Spurenstoffen des Meerwassers

- Beobachtung der biologischen Vorgänge in der oberen Wassersäule unter dem winterlichen Meereis

- Messung des Stickoxids und des Ozons in der antarktischen Luftsäule während des Übergangs vom Winter zum Frühling

Die Arbeiten wurden am 15. September etwa 500 km vor dem Eisrand mit einem hydrographischen Vertikalprofil während der Anfahrt aufgenommen und auf Trajektorien durch den Weddellwirbel fortgesetzt (Fig. 2.4). Zunächst wurde die Übergangszone zwischen dem *Antarktischen Zirkumpolarstrom (ACC)* und dem *Weddellwirbel* durchfahren. Der Eisrand wurde etwa im Frontalbereich zwischen den Wassermassen dieser beiden Zirkulationssysteme bei 60°16´S/34°40´W (Fig. 2.4 und 4.1) erreicht. Auf den vornehmlich meridionalen Traversen durch den *Weddellwirbel* betrug der Stationsabstand 60 sm. Er wurde auf dem Wege von 68°S/20°W zum Maudrücken und in dessen Umgebung auf 30 sm verdichtet. Das Stationsnetz wurde außerdem durch Bathythermographenabwürfe verfeinert, um zumindest die Temperaturverteilung in den oberen 800 m der Wassersäule mit höherer Auflösung aufzuzeichnen.

Einen besonderen Schwerpunkt im Programm der *Akademik Fedorov* bildeten die Arbeiten während einer zwölftägigen Drift vom 6. bis 17. Oktober westlich des *Maudrückens*. Durch häufige hydrographische Vertikalprofile sollten relativ kleinräumige und kurzzeitige Variationen der ozeanischen Zustandsgrößen beobachtet werden. Das atmosphärische Feld wurde gleichzeitig durch ein Argosbojendreieck von ca. 150 km Seitenlänge aufgenommen. Informationen über die Wechselwirkungen zwischen dem eisbedeckten Ozean und der Atmosphäre dokumentierten die laufenden Messungen der Strahlungsflüsse und der turbulenten vertikalen Wärme-, Wasserdampf- und Impulstransporte in der Nähe des Schiffes. Die kleinräumige Schollenstruktur und die Eiskonzentration lieferten wiederholte Aufnahmen mit der Rasterkamera vom Hubschrauber aus. Die zweiwöchige Verbindung zu einer bestimmten Eisscholle konnte schließlich auch zur Beobachtung zeitlicher Variationen der Oberflächencharakteristika und der Materialparameter des Meereises genutzt werden.

Nach dem Treffen und den Vergleichsmessungen mit *Polarstern* am 17. Oktober beendete die *Akademik Fedorov* ihre Drift am 18. Oktober und setzte ihre Fahrt mit einem hydrographischen Schnitt zum Eisrand fort. Letzterer wurde am 22. Oktober bei 59°40´S und 12°30´W erreicht. Den Abschluß der Messungen bildete am 23. Oktober eine hydrographische Station im offenen Wasser.

Das Schiff dampfte zunächst zur sowjetischen Station *Bellingshausen* auf der *King-George-Insel*, um dort logistische Aufgaben zu erfüllen und lief dann am 8. November den argentinischen *Hafen Puerto* Madryn an, wo ein Teil des wissenschaftlichen Personals ausgeschifft wurde.

2.2 Summary and Itinerary

The *Winter Weddell Gyre Study 1989 (WWGS´89)* was a joint research project of the German vessel *Polarstern* and the USSR vessel *Akademik Fedorov* to investigate the oceanic circulation of the *Weddell Sea* at the end of the *Austral* winter. This operation was the first of a total of four similar campaigns by which the mass, heat, salt and sea ice transports of the *Weddell Gyre* and the water mass modification in the southerly *Weddell Basin* will be quantitatively determined.

The oceanic core programme is complemented by detailed studies of sea ice dynamics, air- sea ice - water interactions, sea ice remote sensing, sea ice biota as well as the temporal and regional variations of the phyto- and zooplankton development in the *Weddell Gyre* regime.

The recent cruises have supported measurements along four transects perpendicular to the oceanic circulation of the *Weddell Sea* as portrayed in Fig. 2.1. The zonal most southerly and the meridional most easterly track lines provide hydrographic sections across the

entire gyre system while the two others cover the northwesterly part of the eastward branch of the flow. The scientific field work in 1989 was primarily directed towards

- the determination of the baroclinic mass, heat and salt transports by the *Weddell Gyre* circulation
- the estimation of the water mass modification in the inner *Weddell Basin*
- the detection of oceanic mesoscale features caused by orographic forcing of *Maud Rise*
- the quantitative description of the concentration, thickness, physical and chemical properties as well as of the biota of sea ice
- the derivation of the oceanic and atmospheric kinematic and thermodynamic forcing on sea ice
- the analyses of the regional distribution of phyto- and zooplankton under the given availability of nutrients and the observed physical environmental conditions
- ground truth measurements and special microwave studies to improve satellite passive and active microwave remote sensing techniques for sea ice observations
- the detection of the ozone concentration of the atmospheric column within the polar vortex during the transition from winter to spring.

The 118 scientists and technicians paticipating in the cruises of *Polarstern* (56) and *Akademic Fedorov* (62) came from universities and research institutes of the Federal Republic of Germany, the USSR, the USA, Great Britain and Canada. The various subprogrammes on both ships were carried out jointly by multinational groups. A close cooperation between the ships during the campaign was established through daily radio conferences of the chief scientists and representatives of the different research groups.

2.2.1 RV Polarstern

Polarstern departed from the port of *Puerto Madryn, Argentina* , on 6 September 1989 with 42 ship's crew, 56 scientists and technicians on board. The scientific observational programme commenced at latitude 54°S with daily radiosonde launches and XBT casts with 15 nm spacing. The first complete hydrographic vertical profile (CTD and rosette water sampler) was taken at 58°S on 10 September 1989. The ship encountered the ice edge at about 61°53'S latitude near *King George Island* one day later.

During the morning of 11 September a helicopter flight was carried out to the Chilenian Antarctic station *Teniente Marsh* in order to collect a radiometer provided by *NASA* which had to be installed on board the ship. Meanwhile *Polarstern* was steaming towards the *Bransfield Strait* to reduce the flight distance. When the helicopter was on board again the ship moved back to the edge of the inner marginal ice zone at 62°S/57°W to start a detailed hydrographic and biological survey across the *Bransfield Strait* (see Fig 2.1). The full observational programme started on 12 September 1989 with the subsequent work of the various disciplines :

- CTD profiles combined with water sampling (rosette of 24 Niskin bottles) from the sea surface to the ocean bottom on a horizontal grid of 30 nm width.The density of the hydrographic stations was significantly higher only over the continental shelf breaks on the western and eastern boundaries of the *Weddell Basin*. It was coarser (60 nm) on the meridional section from the *Georg-von-Neumayer Station* to the inner side of the marginal ice zone near 5°E. During the passage of the northern ice edge regime the 30 nm distance was chosen again for the CTD network.

- Deployment of seven current meter moorings to complement the hydrographic measurements along the zonal transect and recording of Doppler sonar profiles of the currents in the upper 200 m of the water column at most of the oceanographic stations within the ice belt.

- Measurements of the turbulent vertical momentum and heat fluxes above and below ice floes at 3 extended ice stations, located in the western and eastern coastal current regimes and in the central *Weddell Sea*. The atmospheric fluxes were additionally recorded during most of the ship´s stops at a mast on ice floes and/or at a boom extending the ship´s bow crane. The data of both instruments were generally in good agreement.

- Monitoring of the atmospheric surface pressure field and the movement (deformation) of the sea ice with the aid of two Argos buoy arrays, one in western branch and one in the center of the Weddell Gyre. The western net -work consisted of 8 and the central one of 6 buoys. In both cases the two inner stations were additionally equipped with sensors for air temperature and wind velocity as well as with thermistor strings through the ice and through the water layer down to 250 m depth. The buoy systems are supposed to continue their operations during several months.

- Sea ice work to detect ice thickness, snow cover, bottom and top topography of ice floes along the ship´s track line by drilling holes through the ice. Aditionally ice cores were taken to determine the texture, physical and chemical properties of the sea ice. Strain measurements were executed to study the mechanical forces on the ice. Finally the small scale ice

concentration, floe size distribution and top morphology was obtained by aerial photography, line scan camera data and video observations during helicopter flights.

- Active and passive microwave measurements from the ship together with ground truth data of the relevant snow and ice properties to improve actual and in near future available satellite observations. Visible and infrared AVHRR data of the entire *Weddell Sea* area have been recorded to derive the large scale ice concentration and ice motion.

- The regional and vertical distribution of the sea ice biota in relation to the texture and to the physical and chemical properties of the ice. Special emphasis was put on a detailed taxonomy of the sea ice species.

- Concentrations of nutrients, phyto - and zooplankton from the rosette water samples as well as from multinet and bongonet hauls, respectively

- Ozone concentration and aerosol content of the atmosphere with optical methods.

The above indicated work was carried out either from the ship and from ice floes or with the aid of two helicopters of the type BO- 105. The cruise track and the station grid was primarily based on the requirements of the programmes in physical, chemical and biological oceanography. Nevertheless, all other projects could more or less smoothly adjust to the predetermined itinerary.

On her way through the pack ice *Polarstern* met different navigational conditions. The western side of the *Weddell Sea* was mainly occupied by large ice floes older than one year, as expected. But the concentration was mostly less than 90 % so that the ship could keep the average speed above 5 knots by moving through suitable leads of open water. Ramming was necessary at a few occasions only. In the central and eastern part of the *Weddell Basin* first year ice with concentrations of more than 90 % was predominant and the ships progress was somewhat reduced. The most unfavourable ice conditions were encountered near the east coast where northeasterly winds led to a remarkable compression particularly in the neighbourhood of grounded icebergs. Here *Polarstern* was caught twice in a shear zone of pack ice and she was forced along a distinct shear line which marked the front of the immobile ice trapped by the icebergs. Similar conditions were met

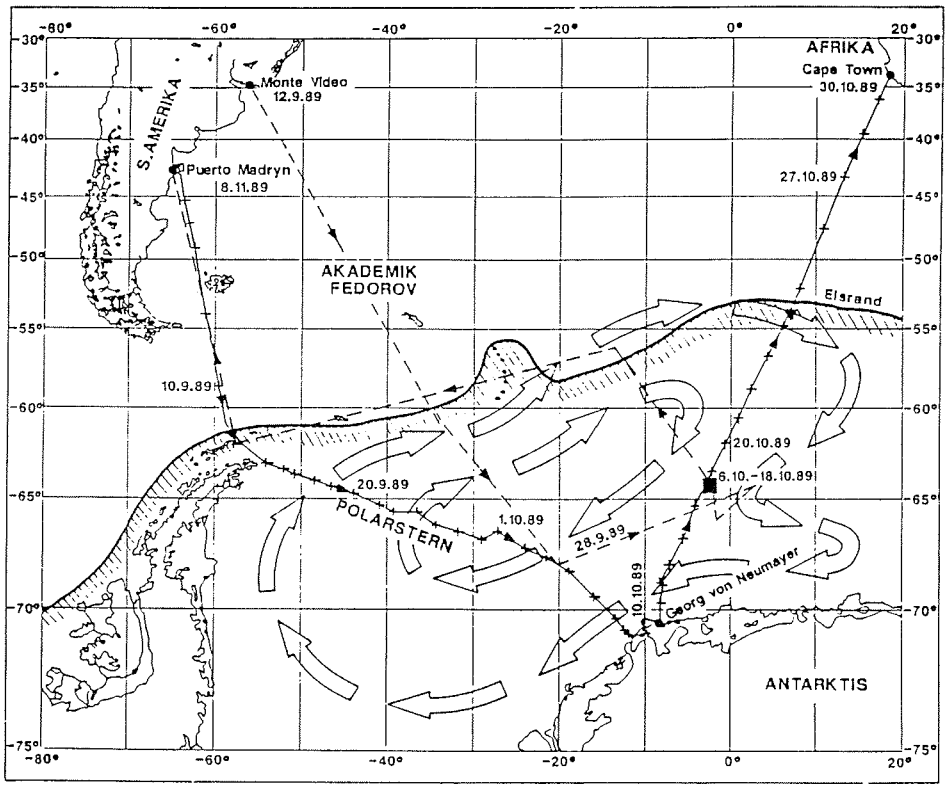

Figure 2.1: Cruise tracks of "Polarstern" (full lines and crosses) and of "Akademik Fedorov" (dashed lines) during WWGS '89

in front of the *Atka Bay* near the German station *Georg-von-Neumayer* (GvN).

On the meridional transect to the north the ice concentration stayed above 90 % from the coast to the transition from the inner to the outer marginal ice zone. The floe sizes and the ice thickness on this leg were largest southwest of *Maud Rise*. The most surprising finding was an extremely wide marginal ice zone covering a latitudinal belt of about 350 km with its most northerly ice band at 53°44´S / 07°18´E .

The total mean speed of *Polarstern* through the ice finally amounts to the relatively high value of 6.25 knots when station time is excluded. Since this result was much better than envisaged the working time at stations could be extended by roughly 25%.

The two surface buoy arrays on Fig. 2.2 were deployed partly by the ship and partly by helicopters. Two of the three longer ice stations (2 to 4 days) were located within each of these buoy networks so that all programmes can later profit from the detailed information on the atmospheric forcing and on the mesoscale ice deformation. The third long ice station was set up in the eastern coastal current north of *GvN*.

The zonal hydrographic cross-section was complemented by 7 current meter bottom moorings (see Fig. 2.3). When these instruments will have been recovered at the end of 1990 the data shall be used for first estimates of the total mass transport within the *Weddell Gyre*.

A short convenient break of the research work occured during a stop of *Polarstern* at *Atka Bay* on 10 and 11 October to unload some equipment for the *GvN Station*. This opportunity was taken by many participants to visit the station and to contact the wintering team. At the end of the unloading procedure the *GvN* crew was invited on the ship for a farewell party.

A second social event took place during the intercomparison meeting with the *Akademik Fedorov* west of *Maud Rise* on 17 and 18 October. The meeting of the personnel of both ships was accompanied by meteorological, oceanographic and biological intercomparisons of instruments and sampling techniques. During a reception on the *Akademik Fedorov* it was agreed among the participants that the successful cooperation in the *Antarctic* should be extended to the *Arctic* in order to support the ongoing international global climate research activities.

When *Polarstern* left the sea ice belt as well as the *Weddell Gyre* at 53°44´S / 07°18´E on 25 October 1989 she had finished two full hydrographic sections across the entire *Weddell Sea* circulation system. Additionally valuable data had been gathered by meteorolo-

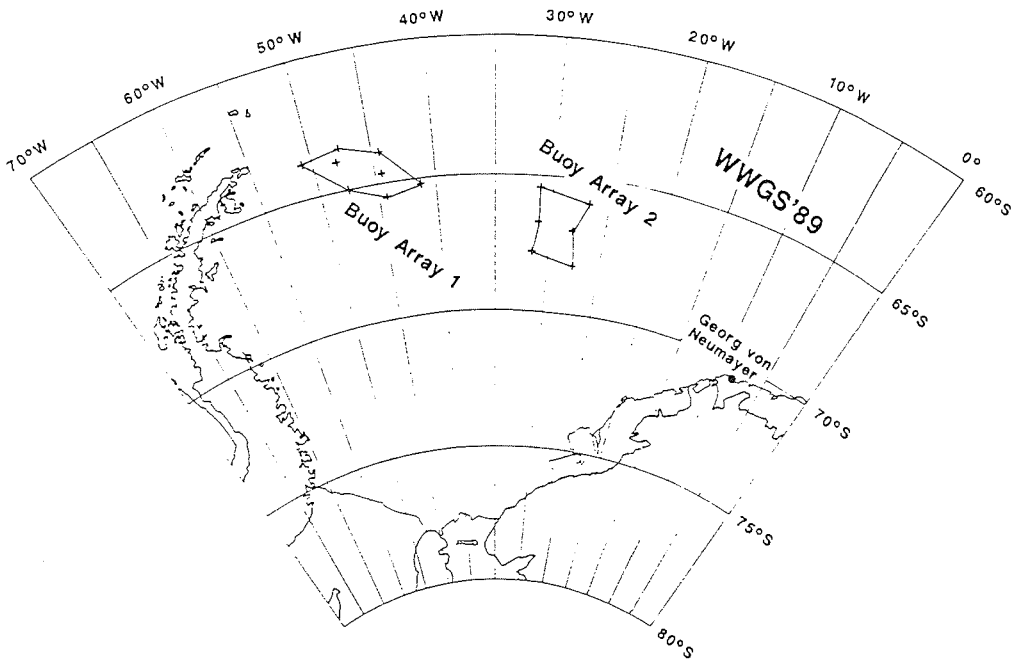

Figure 2.2: Deployment positions of the Argos surface buoy arrays

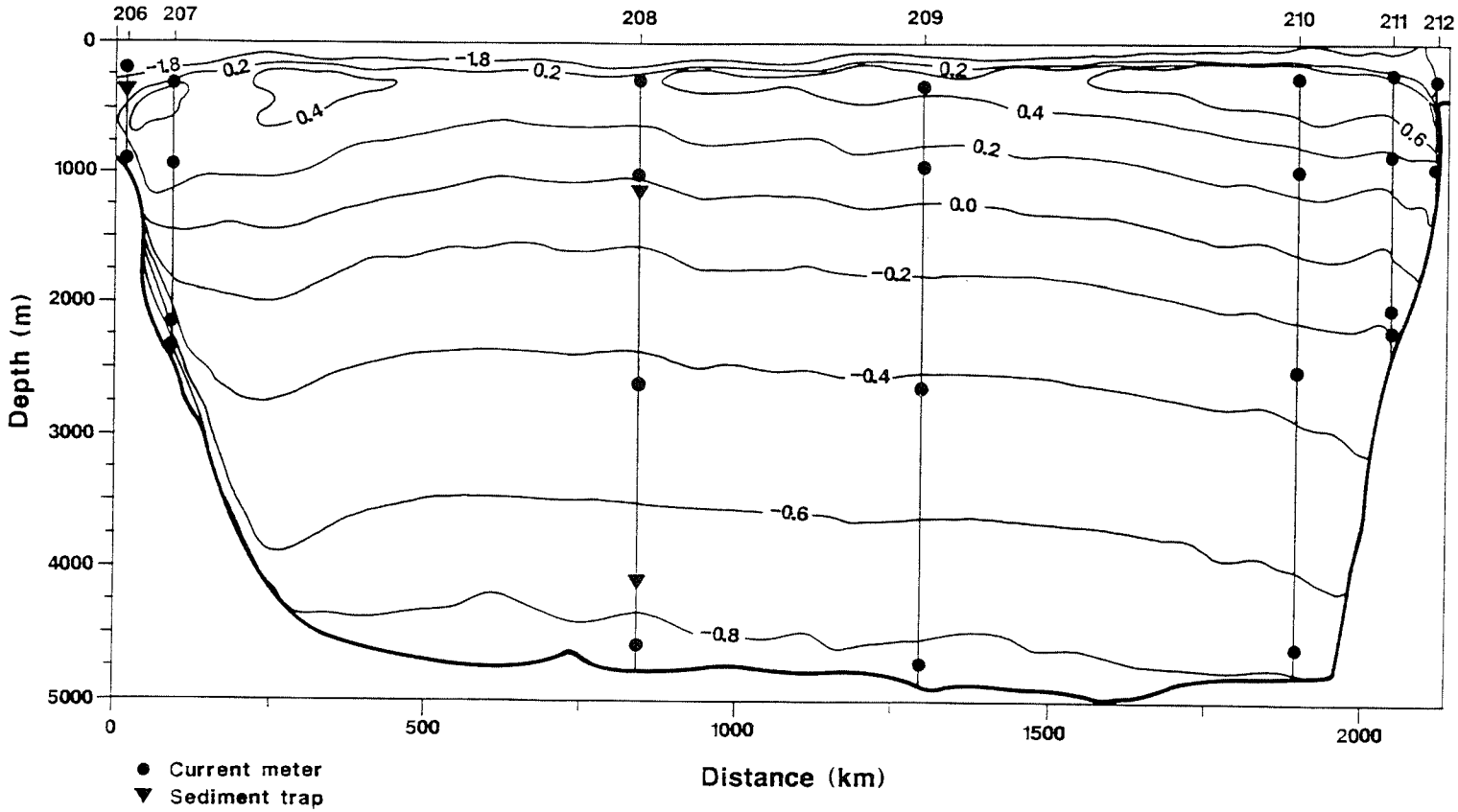

Figure 2.3: Deep sea moorings along the "Polarstern section across the Weddell Gyre

gists, glaciologists, remote sensing specialists and marine biologists during seven weeks of intensive work at sea. Several seminars on board served for discussions of the research topics of the various groups. This cruise leg of *Polarstern's* contribution to a fruitful multinational and multidisciplinary Antarctic marine research programme terminated with a port call to *Cape Town*, South Africa on 30 October 1989.

2.2.2 RV Akademik Fedorov

The RV *Akademik Fedorov* departed from *Montevideo*, Uruguay on 12 September 1989 with 87 crew members and 62 scientists and technicians. The latter belonged to research and university institutes of the USSR, the USA and the FR of Germany. The joint observational programme was mainly directed towards

- a quantitative description of the *Weddell Gyre Circulation* and the associated mass, heat, salt and sea ice transports
- the exploration of the sea ice dynamics and texture in relation to the atmospheric and oceanic forcing
- the detection of the air-sea-ice exchange processes and of the atmospheric and oceanic boundary layer development
- the analysis of nutrients and other chemical tracers of the water column
- the investigation of the biological activity in the upper part of the water column under the sea ice during late winter.
- the assesment of the ozone and NO_2 concentrations in the polar atmosphere during the transition period from winter to spring

The ovservational work started on 15 September with a hydrographic station about 500 km north of the ice edge (Fig. 2.4). Farther southwards the transition zone between the *Antarctic Circumpolar Current* (ACC) and the *Weddell Gyre* was traversed within two days. The ice edge was encountered at the front of the two circulation branches at 60°16´S/34°40´W on 18 September.

The spacing of the hydrographic stations was 60 nm along the more or less meridional legs and 30 nm on the transect from 68°S/20°W to Maud Rise as well as in the environment of *Maud Rise*. A higher resolution was achieved for the temperature distibution in the upper 800 m of the water column with the aid of XBT casts. *Maud Rise* was specially surveyed in order to detect oceanic mesoscale features which are most likely caused by the bottom topography of this region. More efforts to study oceanic mesoscale events were made west of *Maud Rise* during a drift period of 12 days from 6 to 17

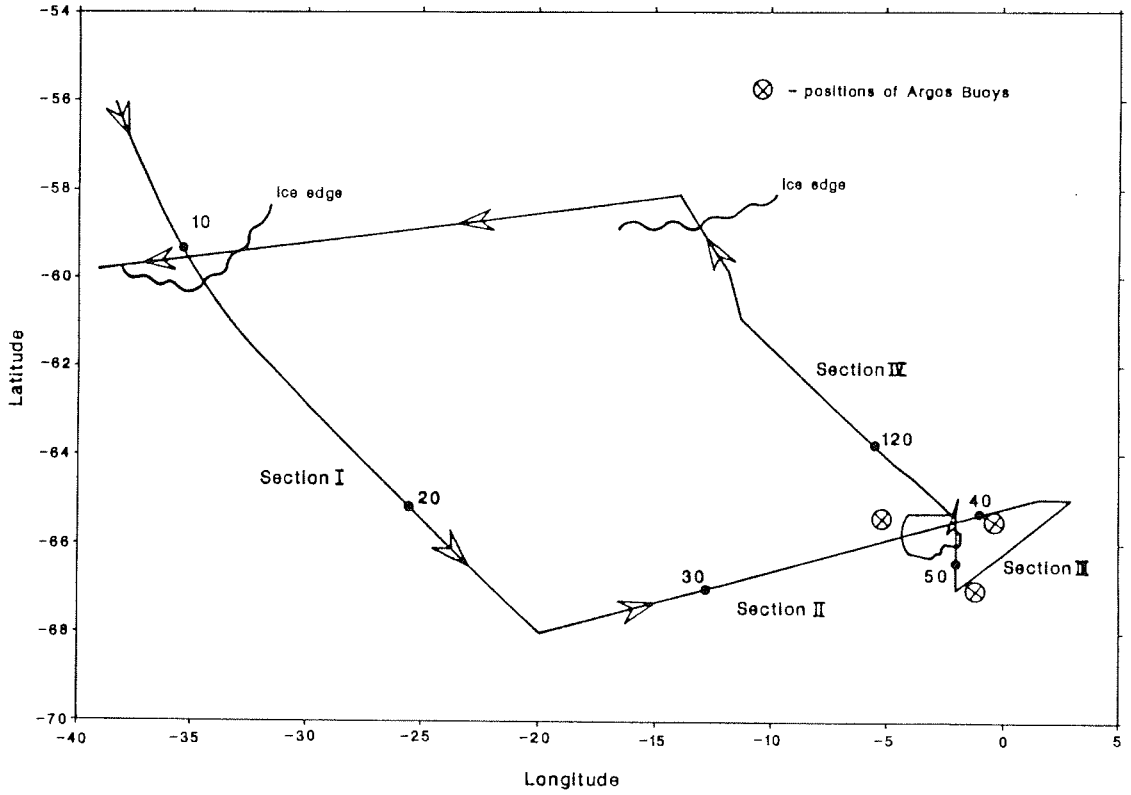

Figure 2.4: The "Akademik Fedorov" track line in the working area, subdivided into 4 sections. Dots with numbers indicate hydrographic stations

October. The extensive hydrographic observations during this phase were complemented by three Argos buoys providing the atmospheric field near the sea surface as well as the ice deformation. Measurements of the radiation fluxes and the vertical turbulent heat, moisture and momentum transports in the atmosphere were taken near *Akademik Fedorov.*

Finally, detailed time series of the texture and the physical properties of the sea ice could be gathered and the ice concentration and floe size distribution was documented with the aid of a line scan camera monitored from a helicopter. The drift programme was terminated at the end of rendezvous with *Polarstern. Akademik Fedorov* started the final hydrographic section on 18 October and reached the ice edge at 59°40´S and 12°30´W on 22 October. The final station occurred on 23 October in the open water. Afterwards the ship sailed to the *Bellingshausen Station* on *King Georg Island* for logistic purposes. *Akademic Fedorov* arrived at the port of *Puerto Madryn, Argentina* on 8 November 1989. Here a part of the scientific crew disembarqued after more than 6 weeks of successfull work in the ice covered *Weddell Gyre* region.

2.3. Research Programmes on RV Polarstern

2.3.1 Physical Oceanography (AWI)*

The physical oceanography programme was primarily concerned with a detailed quantitative description of the *Weddell Gyre* circulation and of the *Atlantic* part of the *Antarctic Circumpolar Current* (ACC). Additionally, measurements were carried out to derive the vertical turbulent fluxes of momentum, heat and salt under the sea ice cover.

Ship-borne measurements were taken with the aid of CTD sondes, expendable bathythermographs (XBTs), a rosette water sampler, an acoustic Doppler current profiler (ADCP) and a thermosalinograph. The flux measurements under the sea ice at three different locations were carried out with a three component acoustic current meter complemented with sensors for temperature and conductivity. Auxilary data were obtained from a profiling instrument of the same kind and from surface moored *Aanderaa* current meters in the depth range from 0.2 to 6 meters. Finally, seven deep sea current meter moorings have been deployed on the track line from the *Antarctic Peninsula* to *Kapp Norwegia.*

A total of 115 CTD-profiles was taken with two *NB Mark IIIb* sondes from *Polarstern.* The instruments have been calibrated at the *Scripps*

* for explanation see list of Participating Institutions

Institution of Oceanography before the cruise, and they will be recalibrated afterwards. Any temporal changes of the temperature sensors during the cruise have been detected by electronic, and mercury reversing thermometers. Due to some nonlinearities in the time variations of the CTD sensors the final accuracy of the data will amount to $5 \cdot 10^{-3}$ K. The calibratrion of the CTD salinity data is achieved on the basis of salinity analyses from 1441 water samples which were measured with a *Guildline Autosal 8400B*. The CTD readings and the bottle values were fitted for each profile individually. The mean deviation of the applied corrections from the bottle data amounts to $1 \cdot 4 \pm 0.5 \cdot 10^{-6}$. The accuracy of the bottle data was determined by a cross-check of 233 multiple samples of the same level resulting in a RMS error of 1.5×10^{-6}. Adding both errors, the corrected salinities will be accurate to $\pm 3 \cdot 10^{-6}$. The obtained CTD-profiles are summarized in the attached station list.

The ADCP was applied when the ship stopped on stations within the pack ice and from the roving ship in open waters. The data quality of these measurements is still uncertain since special evaluation procedures have to be carried out after the cruise.

The thermosalinograph has recorded surface values of water temperature and salinity during 1500 hours. For about 150 hours, i.e. 10 % of the recording period, the sensor was blocked by ice, so that the data are erroneous. The thermosalinograph was continuously calibrated against the CTD -temperatures and the salinities of the water samples. The corrected data are accurate to 0.1 K in temperature and to 0.1 ‰ in salinity.

2.3.1.1 The Large Scale Hydrography of the Weddell Gyre

The aim of the large scale hydrography was to estimate the oceanic transports of mass, heat and salt associated with the *Weddell Gyre* circulation. Of particular interest is the southern part of the gyre, where an extensive water mass transformation is assumed to occur which determines the formation of *Weddell Sea Bottom Water*. The *Polarstern* data set is portrayed by two hydrographic sections (see Fig 2.1) across the *Weddell Gyre*. The first one describes the transect from the tip of the *Antarctic Penisula to Kapp Norwegia* (Fig 3.1). It comprises 46 CTD profiles from the sea surface to the ocean bottom with a station distance of 20 to 60 km. The second one runs from the *Atka Bay* to the *Mid-Ocean Ridge* consisting of 31 stations with spacings from 14 to 125 km. With the exception of the marginal ice zone all profiles reached to the ocean bottom. The meridional temperature cross section is presented in Fig 3.2. The physical data are supplemented by oxygen, nutrient and stable isotope measurements (*Carbon-13 and Oxygen-18*) as well as by samples for *Tritium*, *Helium-3* and *Helium-4* analyses.

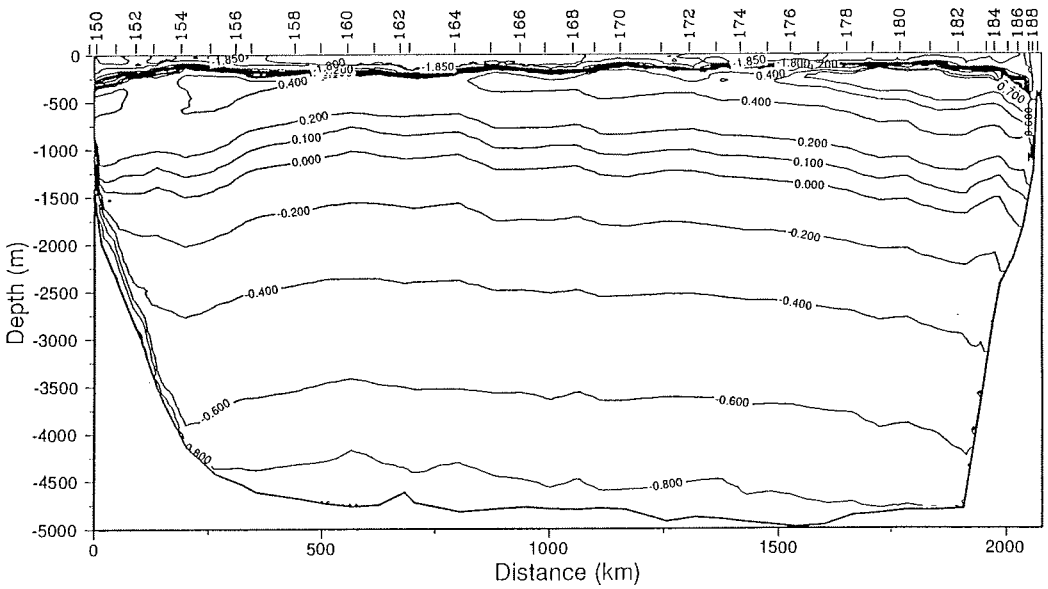

Figure 3.1: Potential temperature distribution on the zonal section of "Polarstern". Numbers on the top line indicate hydrgraphic stations

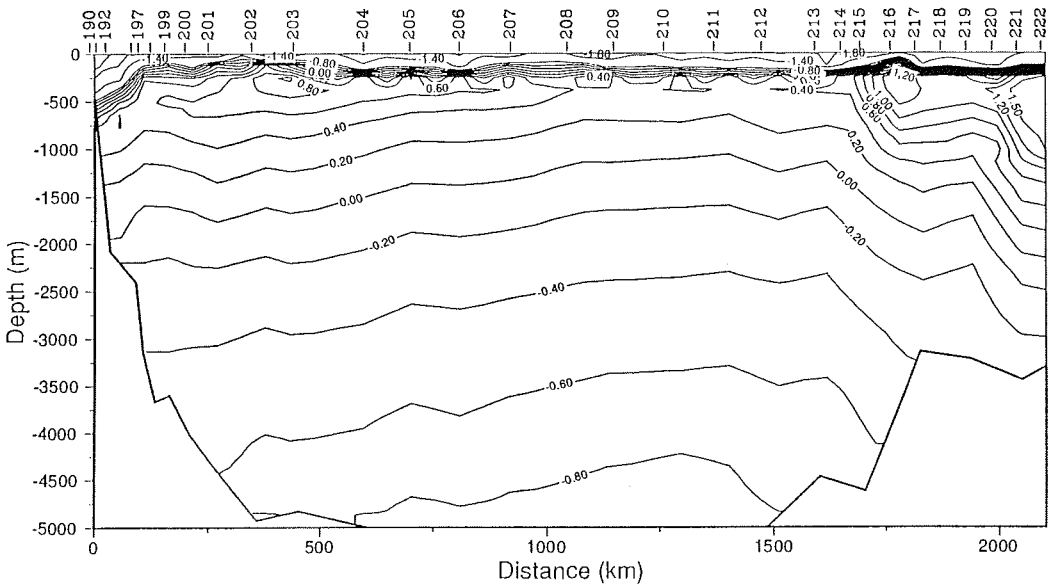

Figure 3.2: Potential temperature distribution on the meridional section of "Polarstern". Numbers on the top line indicate hydrographic stations

2.3.1.2 Current Meter Moorings

Seven current meter moorings were deployed along the more or less zonal section to determine the total current field (Fig 2.3). Two moorings are located each in the western and eastern boundary currents and three were deployed the interior gyre regime. All 24 current meters are *Aanderaa RCM 8* instruments which have been located according to Table 3.1.

Mooring	Longitude Latitude	Date Deployed	Water Depth (m)	Instrument Depth (m)
AWI 206	63°29.6'S 52°07.4'W	13.09.89 11:13	946	AVTP 229 HDWS 349 AVT 876
AWI 207	63°45.8'S 50°54.3'W	14.09.89 10.:39	2503	AVTPC 263 AVTPC 952 AVT 2162 AVT 2410
AWI 208	65°36.3'S 36°29.9'W	24.09.89 18:30	4768	AVTPC 288 AVTP 1037 HDW-S 1090 AVT 2601 HDW-S 4122 AVT 4631
AWI 209	66°36.8'S 27°07.4'W	01.10.89 10:28	4863	AVTPC 293 AVTPC 993 AVT 2659 AVT 4725
AWI 210	69°38.9'S 15°44.5'W	05.10.89 21:11	4751	AVTPC 289 AVTPC 988 AVT 2547 AVT 4617
AWI 211	70°29.5'S 13°07.0'W	06./07.10.89 00:13	2402	AVTPC 247 AVTPC 856 AVT 2066 AVT 2313
AWI 212	70°59.2'S 11°49.4'W	08.10.89	1069	AVTP 309 AVT 999

Table 3.1: Positions and depths of current meter moorings

2.3.1.3 Turbulent and Profile Measurements under the Ice

Three ice stations of two to three days duration were utilized to measure the turbulent fluxes of momentum, heat and to a limited extent salt across the oceanic boundary layer, with a new turbulence system. Additionally, three to five *Aanderaa* current meters were moored under the ice to detect the vertical current profiles between 0.2m and 6m depth. An acoustic current meter and a CTD were also applied to measure vertical profiles of the currents and of the density stratification.

2.3.1.4 The Antarctic Circumpolar Current

Measurements across the *Antarctic Circumpolar Current* (ACC) were taken with the aid of XTB and ADCP profiles. These data will help to better identify mesoscale structures within the ACC which have been observed by satellite altimeter measurements and which also appear in recent eddy resolving model simulations.

2.3.2. Chemical Oceanography (OSU)

The inorganic nutrient and dissolved oxygen determinations were carried out in support of the hydrographic programme. Additionally, water samples were collected for filtration and post-cruise determination of biogenic particulate silica. Nutrient measurements were also made on approximately 300 subsamples from ice cores and brine in support of algal culturing experiments.

The dissolved nutrients (orthophosphate, nitrate, silicic acid, nitrite, and ammonium) were measured in samples from the rosette bottles at all station locations. The nutrient samples were analyzed with the aid of a continuous flow analyser (an *ALPKEM RFA* model 300) using the chemical methods recommended by the manufacturer exept for some modifications in the analyses of ammonium and phosphate. In most cases these analyses were performed immediately after each hydrocast and were completed within 2-3 hours after the cast.

The analysis of dissolved oxygen concentration was made by the familiar *Carpenter-Winkler* method, but the actual titrations were carried out with a radiometer autotitrator. The method used is a dead-stop end-point amperometric titration in which a polarizing potential is applied across the electrodes, and the end-point potential is selected to correspond closely to the visual endpoint. This method was used successfully already during former cruises.

Biogenic particulate silica, the amorphous silica contained in phytoplankton frustules, will be determined in the home laboratory after the cruise. Seawater samples were collected from nearly half of

the CTD casts and filtered through 0.6 micron polycarbonate membrane filters. These filters are subsequently subjected to a hot, basic digestion which dissolves the particulate silica. After neutralization, the resulting solution can be analyzed for silicic acid. A total of nearly 600 such samples was obtained at stations throughout the cruise; about half of which were concentrated in the transits through the ice edge at the beginning and ending of the cruise. It is anticipated that the good spatial resolution in the marginal ice zones will complement similar sections made during other seasons, and provide an improved understanding of the seasonal fluctuations of phytoplankton biomass in the *Weddell Sea*. There were no serious technical problems during the cruise, so that the chemical data set should be of high standard once routine quality control has been completed.

As was the case in *Austral* winter 1986, the surface mixed layer was found to be nearly vertically homogeneous in oxygen and nutrient concentrations. The undersaturation of dissolved oxygen tended to increase southeastwards on the main transect from the *Antarctic Peninsula* to *Kapp Norwegia*. This observation might be related to the amount of entrained *Warm Deep Water* (WDW) and thus to the heat flux from the water to sea ice and to the atmosphere. Both oxygen and silicic acid concentrations in the WDW are inversely correlated with temperature. Because the gradients of phosphate and nitrate across the pycnocline are less strong than those of dissolved oxygen and silicic acid, they are less useful for entrainment calculations. Comparison with *Austral* summer data should alow to determine the increase in mixed layer nutrient concentrations. We expect to extend our earlier estimates of net annual phytoplankton productivity by using the summer/winter differences in mixed layer nutrients.

At the northwestern end of the transect, extremely cold and "fresh" *Weddell Sea Bottom Water* (WSBW) was found with potential temperatures of less than -1.0°C. In this very cold WSBW, the concentration of dissolved oxygen seems to be inversely proportional to the temperature while the unusually low silicid acid concentrations were directly proportional to temperature. Farther along the transect, in the mid-gyre, the variability in the silicic acid content of the WSBW and WDW increased, but the classical *Antarctic Bottom Water* (potential temperature from -0.1 to -0.4°C) did not exhibit this variability. The highest WSBW silicic acid concentrations were found at the southern end of the long transect, were the variability was much less. The data of the northward transect are not yet available.

The analyses of nutrient concentrations in ice core subsamples revealed considerable variability. Ammonium concentrations were usually much higher than in the underlying surface waters, and often higher than any normal seawater ammonium levels. Phosphate also exhibited greater variability than did the other nutrients, perhaps because it is microbially remineralized directly as phosphate, while

the nitrogen species undergo a series of oxidations before ending up in nitrate. The nutrient concentrations were obviously not correlated with the structure or texture of the ice.

During the rendezvous of *Polarstern* and *Akademic Fedorov*, samples were exchanged between the ships for analyses. The preliminary results of those determinations show an encouraging agreement. Oxygen and phosphate values were very similar. Only in the deep water silicic acid measurements was a significant disagreement. The *Fedorov* values were about 4-5 micromole per liter higher than the measurements onboard *Polarstern*. By prior arrangement, duplicate samples from six hydrographic stations had been collected and frozen during the *Fedorov's* cruise. These samples were analyzed onboard *Polarstern* after the two ships met for further comparison of the data in order to resolve any descrepancies.

2.3.3 Atmospheric Physics and Chemistry (IfBG, IMH, MPIfM, AARI)

2.3.3.1 The Atmospheric Boundary Layer and Air-Sea Exchanges

The meteorological work concentrated on the heat and momentum exchanges between ocean and atmosphere and on the determination of the sea ice motion. For this purose micrometeorological and turbulence measurements were carried out both at the ship's boom and on ice floes in the vicinity of *Polarstern*. Additionally, aerological soundings were performed, and helicopter flights with a laser altimeter provided data on the surface topography.

Atmospheric and oceanic surface values as well as the drift velocity of sea ice were determined with the aid of two arrays of Argos buoys. The first array was centered at 64.4°S, 45.7°W, the second at 66.7°S, 29.4°W. Both of them consisted of two highly instrumented central buoys separated (at the beginning) by approximately 130 km and of six (first array) or four (second array) simpler ones surrounding the centre stations. The distance between the outer and the central buoys was between 80 and 140 km. The peripheral buoys provided air pressure and position only. The central buoys measured additionally the air temperature in two heights, the wind velocity and the vertical temperature profiles through the ice and in the oceanic upper layer down to 250 m depth. The drift of the first buoy array from 25.9. to 22.10.89 is displayed on Fig. 3.3. The starting point is indicated by the buoy number at the western end of the tracks. All buoys move eastward with slight undulations caused by the passages of low pressure systems.

The vertical turbulent fluxes of heat and momentum were derived from wind and temperature fluctuations, measured with sonic

devices at the ship's boom and at a 5 m high mast on ice floes during station periods. A comparison of the fluxes measured at the two locations showed no significant differences when the wind direction was $\pm 60°$ from the bow (Fig. 3.4). Two 3-day ice stations in the centers of the buoy arrays will be used to compare the bulk aerodynamic flux method with the sonic eddy correlation technique to provide information on the reliability of the heat and momentum fluxes derived from the drifting buoy measurements. Since the turbulent fluxes of heat and momentum are supposed to vary with floe size distribution and surface roughness, helicopter flights with a laser altimeter have been performed to collect information on the surface topography. In addition to the turbulent transports, the downward shortwave and longwave radiation fluxes as well as the radiation surface temperature have been recorded to complement the surface information on the energy balance.

Upper air soundings were performed routinely 4 times per day. One sounding per day was transmitted into the GTS, in order to improve the input data of numerical models and of objective analysis products. Intensified measurements have been carried out at *Polarstern*, *Akademik Fedorov* and the *Georg von Neumayer Station* from 20 September to 4 October when the three stations formed a reasonable triangle for special analyses of large scale advection. Examples of the *Polarstern* measurements are shown in the Figs 3.5 to 3.7.

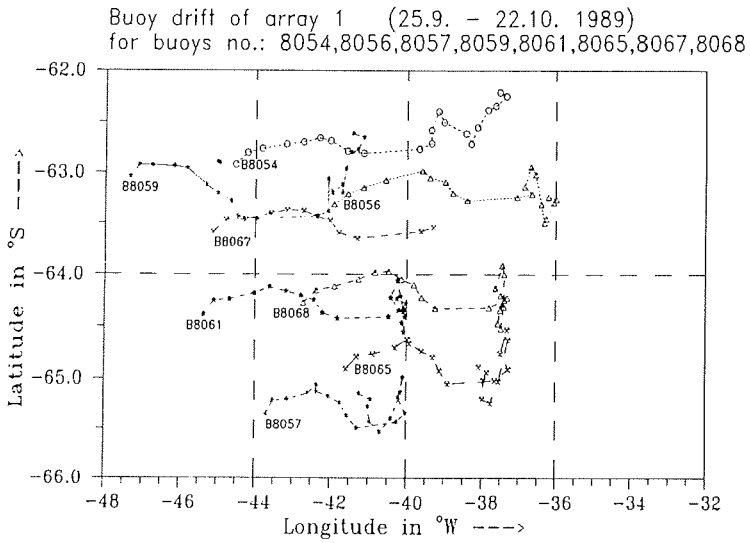

Figure 3.3: Drift of Argos surface buoys from 25 September to 22 October 1989

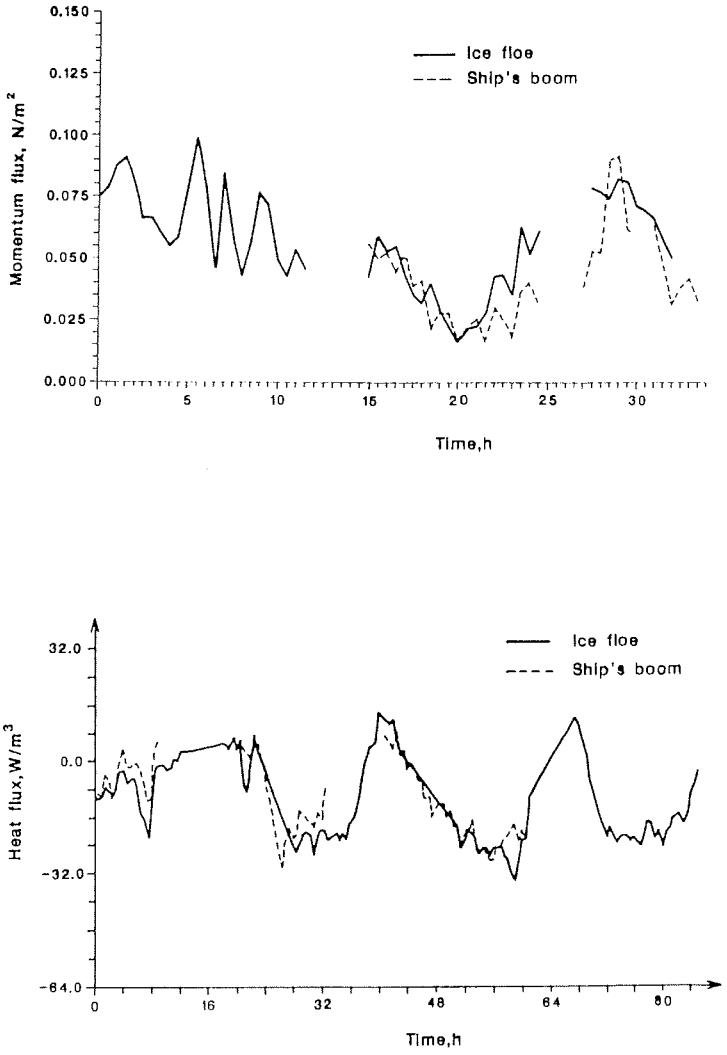

Figure 3.4: Turbulent fluxes of momentum (a) and of sensible heat (b) measured at the ship's boom (dashed line) and at a mast on an ice flow (full line)

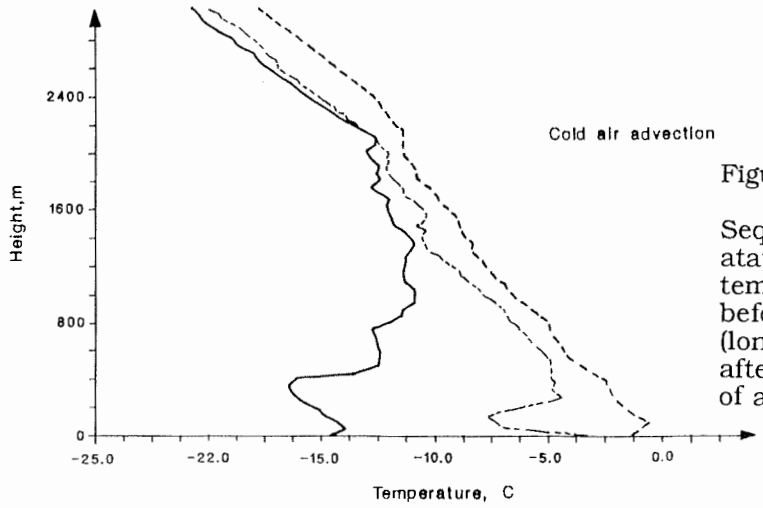

Figure 3.5:

Sequence of atmospheri atatmospheric temperature soundings before (dashed), during (long-short dashed) and after (full) the passage of a cold front

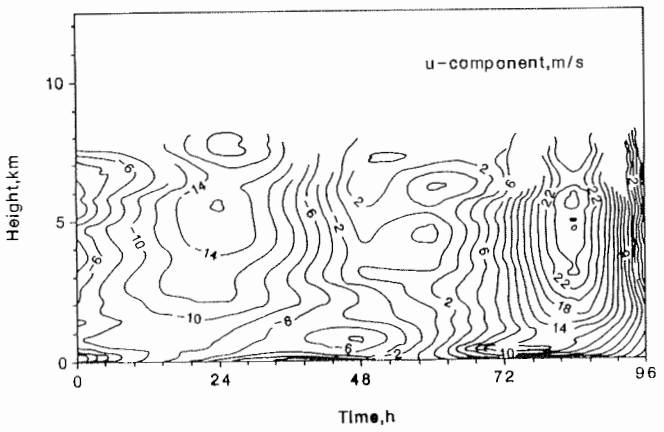

Figure 3.6:

Vertical distribution of the zonal wind component during a 4 days period

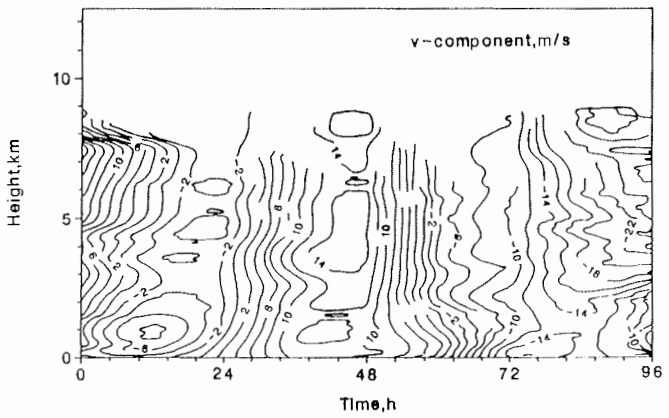

Figure 3.7:

Vertical distribution of the meridional wind compoentnt during a four days period

2.3.3.2 Atmospheric Ozone and Air Turbidity

Measurements of the total content of ozone in the atmospheric column, concentrations of ozone in surface layer and turbidity of the whole atmosphere at different wavelengths of the visible spectral range have been carried out to study the spring decrease of atmospheric ozone in *Antarctica* and its influence on physical quantities of the lower atmosphere. A similar set of data was obtained simultaneously on board the *Akademik Fedorov.*

The total ozone has been determined with the aid of a filter ozone photometer M-124. Concentrations of tropospheric ozone have been measured by a solid state chemiluminescent analyser. Atmospheric spectral turbidity has been observed with a sunphotometer. The performance of the instruments was tested on the transect of the ship from *Bremerhaven* to *Puerto Madryn.* The measurements of total ozone started on 8 September 1989, at 49 °S latitude. In this latitudinal regional increased ozone levels were previously observed, especially during the period of depleted ozone in the central *Antarctic.* In consistancy with these results an abrupt decrease of ozone was obvious on the passage from 49°S to 59°S (see Table 3.2).

During the remaining observational period (11 September to 16 October) large fluctuations of the total ozone concentration (from 166 DU to 320 DU) were detected . These fluctuations appear to be closely correlated with the temperature of the stratosphere. Reduced ozone is coupled with the cold air of the circumpolar stratospheric vortex. Comparing our values with measurements of the two preceding years at the Soviet station *Novolazarevskaya* we find that the conditions 1989 are rather similar to those of 1987 when the lowest values of total ozone were found over *Antarctica.* The ozone of the surface layer was measured during the entire expedition. Unfortunately a standard ozone generator, used for calibration did not work satisfactorily so that our data are of qualitative nature only. According to these measurements one can determine a few different levels of ozone which more or less characterize different air masses. In moderate latitudes ozone concentrations are higher than 30 ppb with small variations. In the subpolar latitudinal belt (south of 64°S), the variations of tropospheric ozone became larger reflecting the transition zone of air masses.

The measurements of spectral atmospheric transparency have been carried out during sunny days. Preliminary results show that the aerosol optical thickness varied around typical values for late winter in the *Antarctic.* For the final analyses the data of both ships and of coastal stations from the *Weddell Sea* area will be combined in order to delineate the late winter ozone variations of the year 1989.

Date (1989)	Latitude	Longitude	Total ozone DU	N		Observational conditions
September						
08	49.41 S	62.14 W	340	17	2	10
59.30 S	59.14 W	204	26	3	11	
62.06 S	56.43 W	220	23	2,3	12	
63.20 S	52.59 W	284	27	3	13	
63.29 S	51.43 W	290	34	1,3	14	
63.45 S	50.45 W	253	56	1,2	15	
64.07 S	47.58 W	238	19	3	16	
64.37 S	44.13 W	296	48	1,2	17	
64.36 S	44.15 W	320	09	2	18	
64.41 S	44.00 W	308	10	2	19	
64.44 S	43.46 W	274	07	3	20	
64.36 S	43.35 W	237	07	1,2	22	
65.25 S	40.36 W	223	11	2,3	23	
65.40 S	38.46 W	196	03	2,3	24	
65.36 S	36.30 W	166	25	1,2	26	
66.36 S	31.34 W	220	35	1,2	27	
66.53 S	29.13 W	220	13	3	28	
66.51 S	27.39 W	269	33	1,2	30	
66.44 S	27.17 W	231	36	1,2		
October						
01	66.37 S	27.08 W	243	32	1,2	
02	67.17 S	24.31 W	213	31	1,2	
03	67.47 S	21.15 W	210	29	3	
04	68.35 S	18.12 W	194	04	3	
05	69.38 S	15.43 W	208	20	3	
06	70.21 S	13.25 W	173	04	3	
09	70.39 S	10.11 W	185	04	3	
10	70.20 S	10.07 W	196	11	2	
11	70.30 S	08.09 W	183	24	1,2	
12	69.45 S	08.08 W	178	08	3	
13	68.58 S	07.57 W	206	18	3	
14	68.55 S	08.12 W	168	17	1,2	

Table 3.2: Daily averages of the ozone concentration in the atmospheric column.

Observational Conditions: 1 - direct sun, 2 -clear zenith, 3 - cloudy zenith. N - number of individual measurements, DU = Dobson Units

2.3.3.3 Reactive Nitrogen Compounds in the Boundary Layer over Water and Sea Ice

The gaseous atmospheric nitrogen compounds HNO_3 and NH_3 as well as atmospheric aerosols were sampled in order to determine their concentrations close to the sea and ice surfaces. Samples of precipitation and surface snow on ice floes were also collected to undergo chemical analyses for major ionic constituents. These measurements will provide a first orientation for the investigation of Nitrogen dynamics of the boundary layer over the open water and ice in the *Southern Ocean* and the *Weddel Sea*. Gaseous HNO_3 and NH_3 were adsorbed and enriched on filters, which will be analyzed by ion chromatography.

The filter systems for air sampling were installed on the obvservation deck of *Polarstern* (24 m above sea level). Filterpacks were attached to a boom of 2 m length fixed horizontally to the rail and pointing towards the bow of the ship. Air samples were taken by two air pumps which were controlled by a vane-switch allowing only air from $\pm$ 45° relative to the bow of the ship to be filtered in order to minimize contamination.

HNO_3 and NH_3 were absorbed and enriched by two filter systems, each of which consisted of a PTFE-filter (0.45 um pore size) followed by three gas absorption filters. This arrangement allows for separation of aerosol and gas phases of the sampled air and to control the absorption quality. HNO_3 was absorbed by nylon filters, while NH_3 was collected on cellulose filters impregnated with 0.05 NH_3PO_4.

According to the very low concentrations which can be expected in the *Antarctic* atmosphere, high volumes had to be filtered by sampling periods of at least 24 hours. 168 filter samples during 21 sampling episodes (most of them on the *Weddell Sea* transect) were obtained. Additionally, nine samples of precipitation and 83 surface snow samples from ice floes were collected. Chemical analyses will be carried out in the home laboratory. The results will be interpreted in the context of surface water chemistry and meteorological data.

2.3.4. Sea Ice Studies (AWI, SPRI, CRREL)

2.3.4.1 Sea Ice Physics

The sea ice subprogramm comprises the following elements:

- Continuous ice observations including icebergs
- In situ measurements at ice stations
- Analyses of ice cores
- Air-borne video and still photography.

The ice observations log of hourly entries provides a description of ice conditions along the ship's track with a total of 28 ice stations during which :

- ice core drilling and in situ measurements
- brine sampling
- snow and ice thickness profiling
- heave-tilt measuremments
- surface snow and ice characterizations

were carried out.

2.3.4.1.1 Snow and Ice Thickness Distributions

The thickness of the snow and sea ice covers strongly influence the energy transfer between ocean and atmopshere. Surface and bottom roughnesses of the ice determine the drag coefficients for air and water and thus control the momentum transfer between atmosphere and ice and ocean and ice, respectively. The snow depth modifies the surface brightness temperature, the free board of the floes and the heat transfer between the ice and the atmosphere.

Snow and ice thicknesses were detected on all daily ice stations by thermally or mechanically drilled holes. The hole distances were 1m along two more or less perpendicular lines of 100 m length to assess the major characteristics of the floe, i.e., the individual line patterns were chosen at rafted and rigded parts as well as at flat areas. In a few instances, a number of shorter profiles were drilled through extended ridges, in order to obtain details on their structure. The data were subsequently stored in a computer for statistical analyses.

Fig 3.8 displays the mean values of ice thickness as a function of longitude and latitude for the west-east and the south-north transects respectively. The ice thickness decreases from west to east (Fig. 3.8 a), but no simple function is found versus latitude. This is mainly due to the frequent occurence of heavily rigded floes along

the meridional transect, which amounted to larger mean values in comparison to neighbouring flat stations.

Fig 3.9 portrays the overall probability density functions (PD´s) for the entire data set. The maximum for ice thickness lies at 0.6-0.7 m, with a long trailing stretch >0.9m, mainly indicating rigded portions of the sampled floes. The mean ice thickness for all data amounts to 0.97 ± 0.73m.

Upon closed inspection we define four floe thickness classes (I - IV), each of which represents a different stage of sea ice formation. Class I identifies deformed first year ice, classes II and III indicate undeformed first and second year ice and class IV contains deformed second or possibly multi-year ice. Table 3.3 provides some statistics of each class as well as of the entire data set.

The spatial distribution of the floe classes is given in Fig 3.10. Classes III and IV are concentrated in the region west of 45°W but no such clear regional limit is foud for class I and II floes.

Table 3.3: Basic parameters of floe thickness classes (z_{ice}, z_{snow} z_{tot}, z_d=ice, snow, total thickness and ice draft), respectively

Class	Points	z_{ice}, m	z_{snow}, m	z_{tot}, m	z_d, m	mean/st. dev.
I	2195	1.03	0.23	1.26	1.00	mean
		0.60	0.17	0.64	0.55	st. dev.
II	2034	0.60	0.16	0.76	0.60	mean
		0.21	0.10	0.24	0.20	st. dev.
III	349	1.17	0.63	1.80	1.25	mean
		0.35	0.18	0.45	0.36	st. dev.
IV	282	2.51	0.79	3.30	2.48	mean
		1.08	0.22	1.09	1.04	st. dev.

Figure 3.8 a:

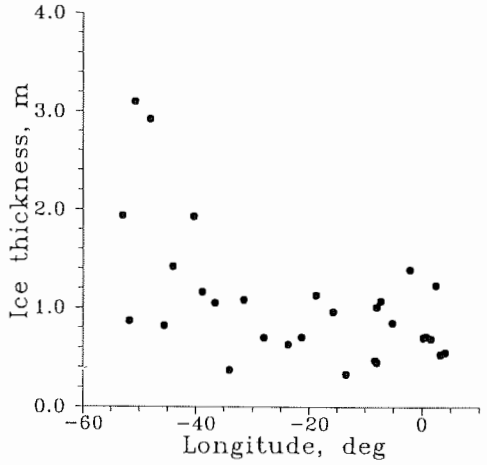

Figure 3.8 b:

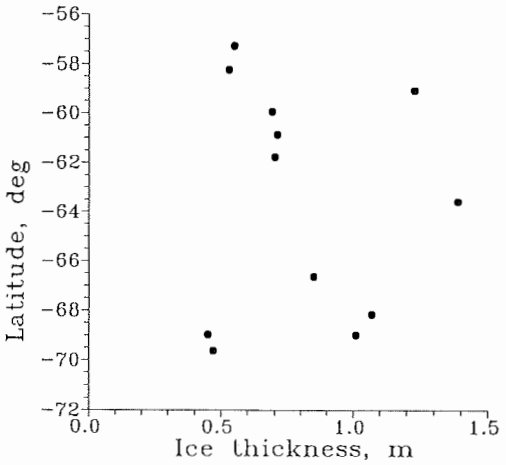

Figure 3.8: The zonal (a) and meridional (b) ice thickness distribution, measured at "Polarstern"

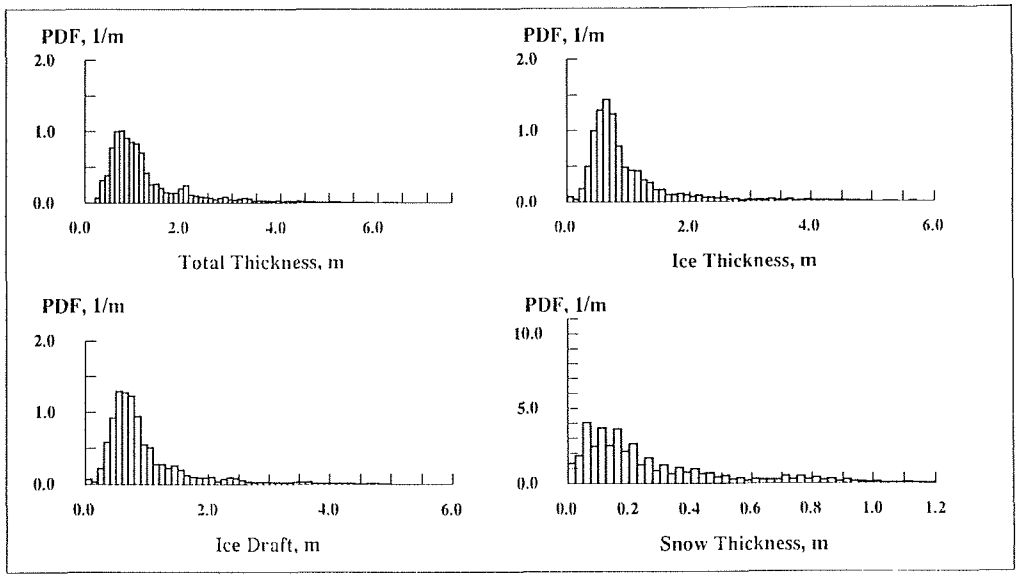

Figure 3.9: Propability density distribution for several ice and snow quantities, obtained on "Polarstern"

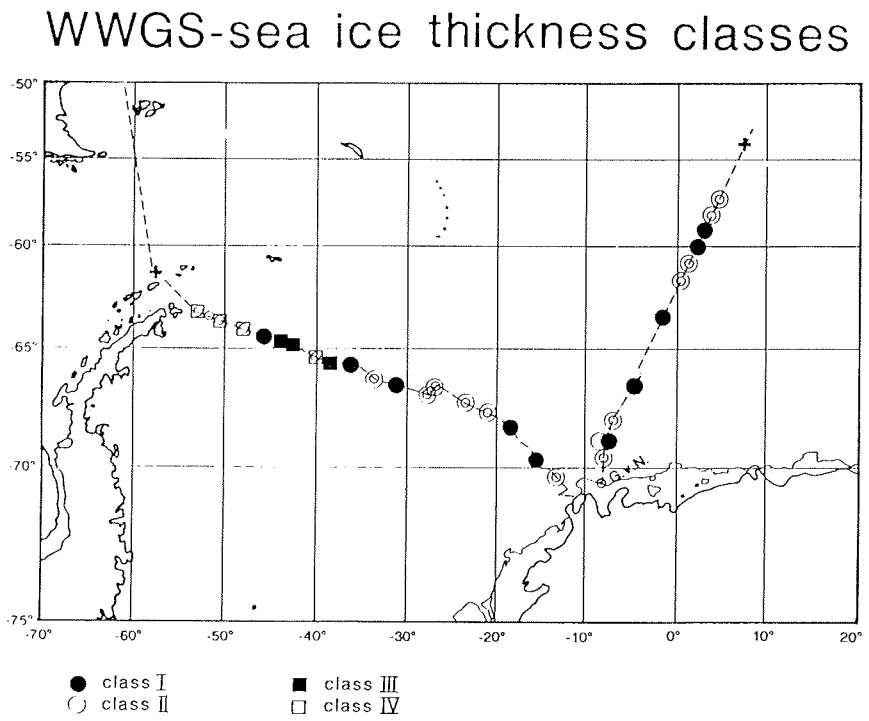

Figure 3.10: Ice thickness classes (increasing thickness from I to IV) along the "Polarstern" cruise track

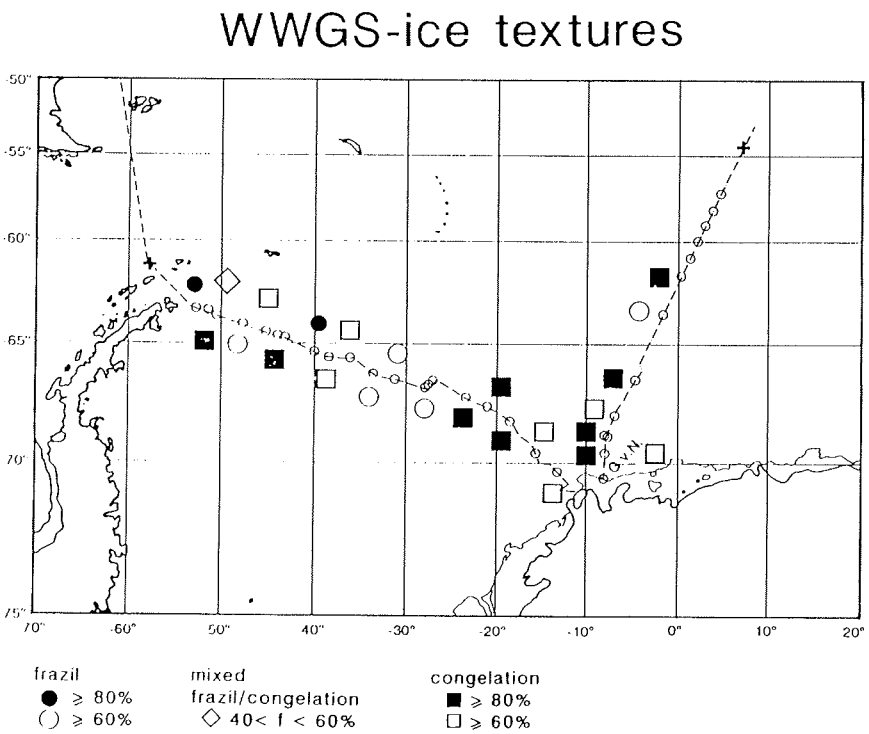

Figure 3.11: Sea ice textures along the "Polarstern" cruise track

2.3.4.1.2 Texture, Chemical and Physical Properties

Ice cores were obtained at 52 sites (37 ship or helicopter stations). A number of parameters were recorded inmediately at each station including a temperature profile and light intensities within and under the ice. Detailed analyses were performed in a glaciological cold lab at -25°C on the ship The stratigraphy of cores was determined with the aid of thick sections cut vertically across the whole core. Various quantities like salinity, concentrations of nutrients and hydrogen peroxide as well as the chlorophyll a concentration have been measured as well.

Fig 3.11 shows the distribution of genetic ice classes along the ship's track as determined through textural analysis. Five classes may be recognized according to the ratio of ice resulting from frazil or congelation growths. The former mostly takes place in the upper meters of the water column whereas the latter occurs at the advancing ice-water interface. From Fig 3.11 a zonation into at least three different regions is evident. Zone 1 extends from the *Antarctic Peninsula* to about 30°W, with a slight prevalence of frazil growth. In zone 2, i.e. the coastal polynya region 60% congelation growth is dominant. Near the ice edge (zone 3) frazil growth is predominant at least in some of the samples. Table 3.4 indicates the relative proportions of the different textural classes. The ratio between congelation and frazil ice amounts to 58:42, which is slightly higher than found on previous cruises in the *Weddell Sea*.

As examples of first- and second-year cores, texture, salinity, and concentrations of chlorophyll a and hydrogen peroxide of samples 257 and 268 are shown in Figs 3.12 and 3.13. The salinity distribution with maxima at the bottom and the top seems to be due to gravity drainage and to expulsion of brine onto the ice surface and into the snow. The distribution of chlorophyll a reflects the most recent bottom growth occurring on a large fraction of first-year floes. Hydrogen peroxide seems to be uncorrelated to any of the other parameters.

Fig 3.13 shows a second-year floe. The complex texture is a result of both, dynamic hydrographic growth as well as deformation events. The salinity profile exhibits rather low values at the top as a consequence of retexturing and desalination during the previous summer melt season. The lower portions follow the trend outlined for first-year ice. Chlorophyll a is highly concentrated in two bands in the interior, most likely as a result of growth during the previous summer. Both chlorophyll a maxima correspond to peaks in ammonia and phosphate concentrations, presumably due to heterotrophic activity within this older community. It is interesting to note that H_2O_2 is heavily enriched within the brine (roughly 20 times as large

as the concentration in the water column). This enrichment may be due to biological production.

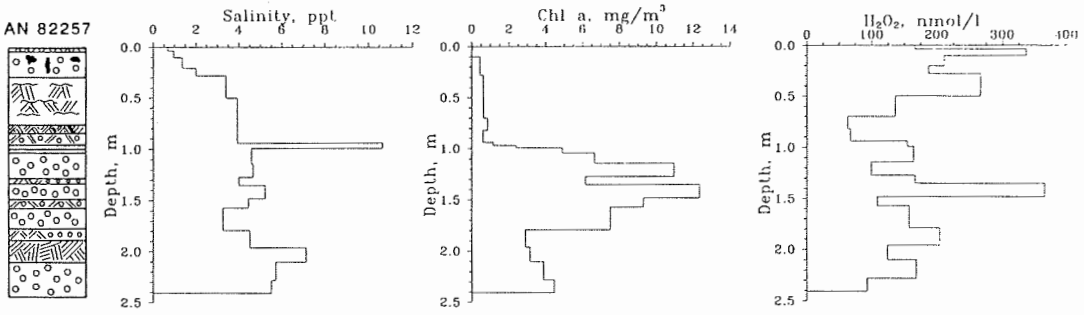

Figure 3.12: Vertical distribution of salinita, chlorophyll a and H2O2 in a first year ice floe

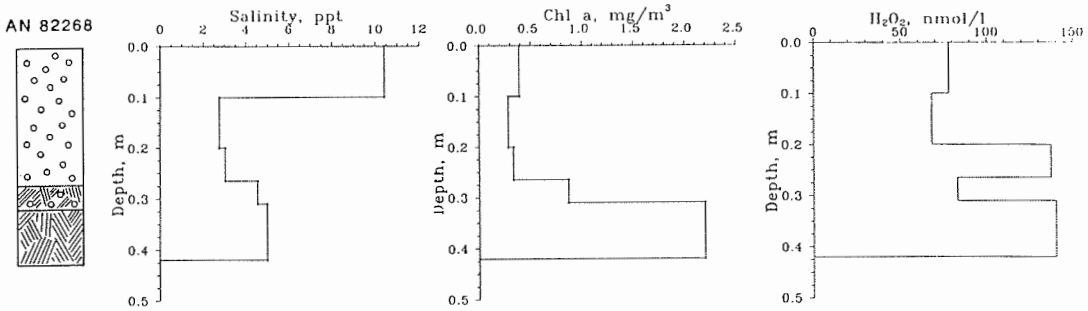

Figure 3.13: Same as Figure 3.12 in a second year ice floe

Textural class	Frequency of occurrence
1. Polygonal granular	3%
2. Orbicular granular	35%
3. Mixed c/g	10%
4. Intermediate c/g	3%
5. Columnar	48%
6. Platelet	1%

Table 3.4: The textural composition of the Antarctic sea ice

2.3.4.1.3 Ice Deformation

During the ice drilling programme special attention was paid to pressure ridges and rafted structures. Block sizes and thicknesses in the protruding parts of the ridges were measured, and the under-ice parts of some ridges could be viewed by a video camera deployed through a hole in the ice.

It is apparent that the ice deformation mechanism in the *Antarctic* is quite different from the *Arctic*, where pressure ridges are formed through crushing of young refrozen leads by thick floes. In the *Antarctic* the ridging occurs either by simple rafting or the buckling failure of two floes which are pushed together. The blocks from the parent floes are pushed upwards and downwards to create the ridge. The resulting ridge is only loosely packed and all ridges were less than 6 m in depth (Arctic depths can be as large 20-30 m). Ridge frequencies were also quite low. More information on the ridging will be obtained from the analysis of aerial photography and video data, especially on days when surveys were carried out at a low sun angle. The linkage of ridging, and the extent of rafting, per unit area of ice surface, will give a correction factor to the overall distribution functions of ice thickness estimated from the drilling.

Attempts were made to tow a sidescan sonar behind the ship to measure the underside profiles of ridges on passage, but the towfish was severely affected by ice blocks carried under the vessel and re-emerging at the stern.

2.3.4.1.4 Propagation of Waves through Ice

The purpose of this programme was to measure the wave propagation through the ice-covered *Weddell Sea*, and to determine the source areas and mechanisms of generation of the waves observed. Waves in icefields are important because near the ice edge they determine the ice morphology through breaking up the ice into floes, or maintaining it in the form of pancakes in the case of an advancing ice edge. Within the interior of the pack the occasional deep penetration of wave energy from an intense storm can cause break-up and reworking of the entire ice cover, while waves are also believed to be a contributing factor in the calving of icebergs.

At each of the 28 ice stations an array of wave-measuring instruments was deployed on the ice, comprising

- a vertical accelerometer
- two tiltmeters at right angles
- three strainmeters in a 120 degree configuration (not in every case).

These instruments measured the directional spectrum of the flexural-gravity waves propagating through the ice. The vertical accelerometer and two tiltmeters act in the same way as a directional wave recorder at sea, while the strainmeter array provides an independent directional wave measurement by recording the linear strain associated with the curvature of the ice surface over a gauge length of 30 cm. At most of the stations two arrays were deployed to enable cross-correlations between the two sets of recordings for the computation of the phase velocity of the waves to be measured.

Table 3.5 lists the 40 experiments that were carried out, and the combinations of instruments used. Recording periods of 1-3 hours were employed, and the data were recorded on a digital data logger. A parallel and independent programme was carried out aboard *Akademik Fedorov* so that measurements exist at two widely separated points in the icefield at different distances from the ice edge.

An associated programme was the measurement of ambient noise levels under the ice at depths of 1 m and 10 m below the ice surface. It was necessary to fly more than 30 nm from the ship by helicopter to achieve sufficiently quiet conditions. The hydrophone at a depth of 1 m recorded mainly high-pitched pulses caused by microcracks forming in the ice. The lower hydrophone recorded an overall background spectrum together with a series of creaking sounds caused by the flexure of the ice. From previous observations we

expect waves in icefields to have four principal source mechanisms, reflected in four dominant ranges of periods:

Fig 3.14 shows a typical swell-like tilt record (experiment 13) with a dominant period of about 18 s.Full analysis of the data has not yet been carried out, but we have examined some one-dimensional power spectra generated from one axis of tilt on some of the experiments. Fig 3.15 shows a typical spectrum. The dominant spectral peaks were identified and correlated with the average wind speed during the ice station.

Fig 3.16 shows all results which support the above interpretation. At low wind speeds the spectrum is dominated by swell of 16-33 s period and by very short period waves. At 11-12 m/s wind speed waves of period 6-10 s become dominant, representing local wave generation by the wind. It will be most interesting to compare these results with measurements of oceanic turbulence just under the ice obtained during the long ice stations, since we expect to see some of these spectral peaks in the velocity data.

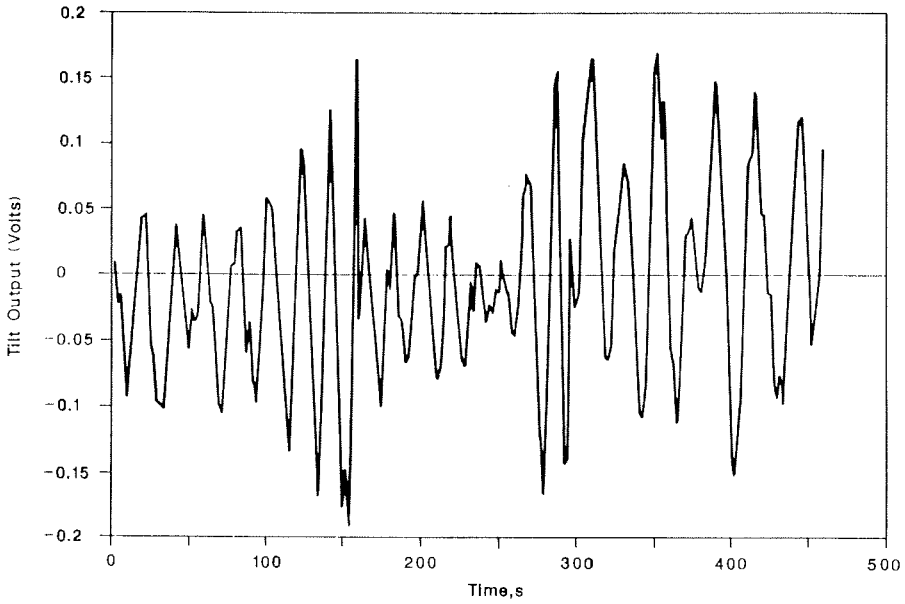

Figure 3.14: Tilt variations of an ice floe

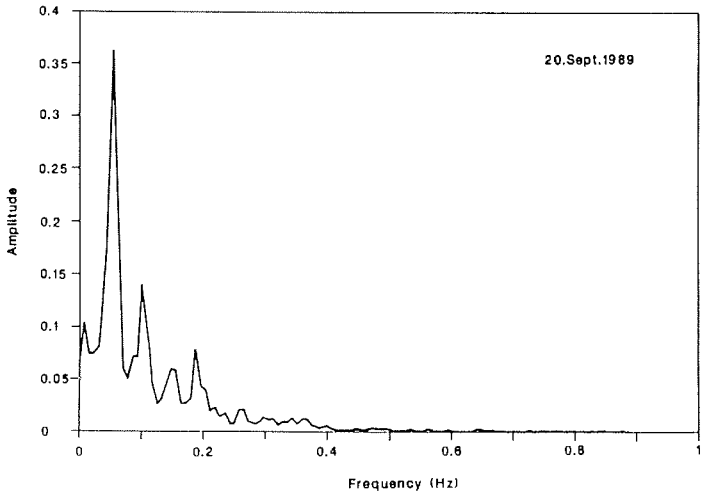

Figure 3.15: Power spectrum of tilt motions

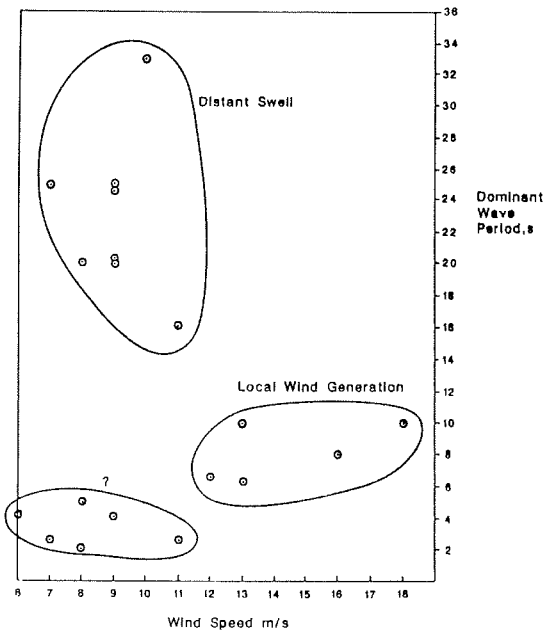

Figure 3.16: Wave periods versus local wind speed

Experiment no.	Date	No. of arrays	Spacing m	Instruments in each array Acceleration	Tilt	Strain
1	12 Sept	1		1	2	3
2	13	1		1	2	3
3	14	1		1	2	3
4	15	1		1	2	3
5	16	1		1	2	3
6	17	1		1	2	3
7	17	2	50	1	2	3
8	18	2	50	1	2	3
9	18	1		1	2	3
10	18	2	50	1	2	3
11	19	2	50	1	2	3
12	20	2	50	1	2	
13	20	2	50	1	2	
14	21	2	50	1	2	
15	22	1		1	2	3
16	23	1		1	2	
17	24	1		1	2	
18	25	1		1	2	
19	26	1		2	2	
20	28	2	300	2	2	
21	29	2	300	1	2	
22	30	2	300	1	2	
23	3 Oct	2	40	1	2	
24	4	2	40	1	2	
25	5	2	37	1	2	
26	6	1			2	
27	11	1		1	2	
28	12	2	43	1	2	
29	14	2	43	1	2	
30	14	2	43	1	2	
31	15	1		1	2	
32	16	2	43	1	2	
33	17	1		1	2	
34	19	2	39	1	2	
35	20	2	64	1	2	
36	21	1		1	2	
37	21	2	61	1	2	
38	22	1		1	2	
39	22	1		1	2	
40	23	2	64	1	2	

Table 3.5: Wave experiments

2.3.4.1.5 The Distribution of Icebergs

Iceberg observations were made throughout the voyage, mainly using the ship's radar in order to determine the geographical distribution of icebergs within the *Weddell Sea* and the *Southern Ocean*, and to relate this to the oceanic and atmospheric surface circulations. We also sought to measure the size distribution of icebergs, in order to determine decay rates and mechanisms and estimate mass fluxes. Finally, the entire data set was used as a way of determining the radar detectability of icebergs.

At 10-20 nm intervals while on passage, and at every station, the X-band radar screen was scanned for icebergs. The range and angular bearing of each berg were measured. Where possible, the radar observations were calibrated by visual measurements of the angular diameter of each berg. About 20 bergs were also photographed vertically using a 70 mm aerial survey camera mounted in the helicopter.

A total of 3500 individual iceberg measurements were made to give a preliminary picture of iceberg distributions. Fig 3.17 shows iceberg numbers averaged over 1 degree longitude bins for the crossing of the Weddell Sea. No bergs were seen until the southern end of *Drake Passage*. *Bransfield Strait* was rich in icebergs, although many of these must have been grounded. A large array of grounded bergs was seen near *Danger Rocks* on the NE tip of the *Antarctic Peninsula*. Within the *Weddell Sea* there is a broad peak of berg densities in the longitude range 36-47°W. This corresponds to the northward flow of ice and water on the western side of the *Weddell Gyre*. Berg numbers are low in the eastern *Weddell Sea* until grounded bergs are once again observed off *Kapp Norwegia*.

Fig. 3.18 shows the iceberg densities on the northward transect across *Maud Rise* up to 60°S, averaged in 0.5 deg latitude bins. The large numbers of grounded bergs in *Atka Bay* are omitted. An extraordinary effect is apparent. Berg densities rise steadily with northward distance until 63.5°S is reached, when the numbers suddenly drop to near zero. No explanation is yet available for this phenomenon.

A second interesting effect occurs near the ice edge. Fig. 3.19 is a schematic diagram of changes in sea ice and iceberg characteristics as the ice edge was approached. The final ice stations, from 60 to 57°S, were carried out in an "interior zone" with typical characteristics of vast, snow-covered first-year floes separated by narrow leads 1-3 km apart. Icebergs continued to be very scarce. At 57°S the effect of ocean swell penetration became apparent; swell

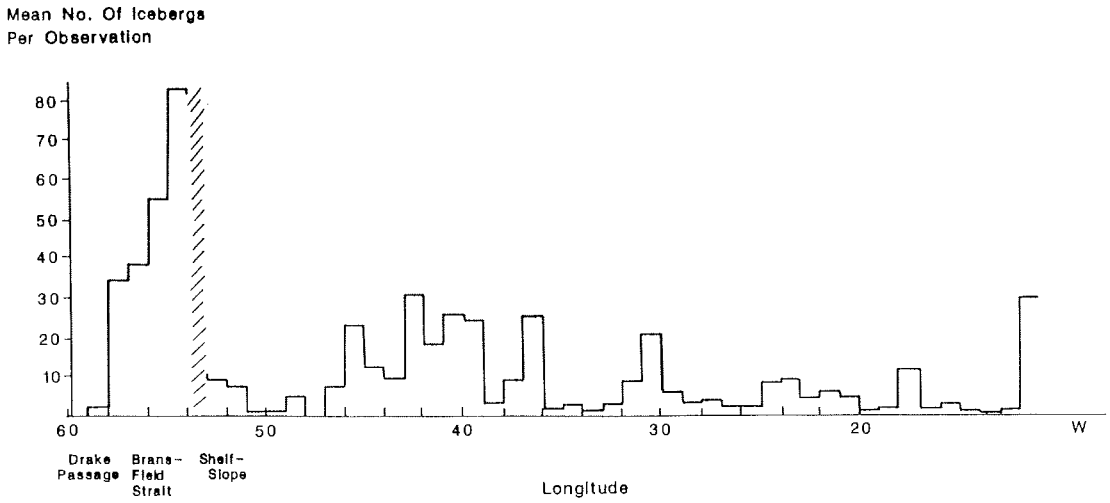

Figure 3.17: Number of observed ice bergs on "Polarstern's" zonal transect

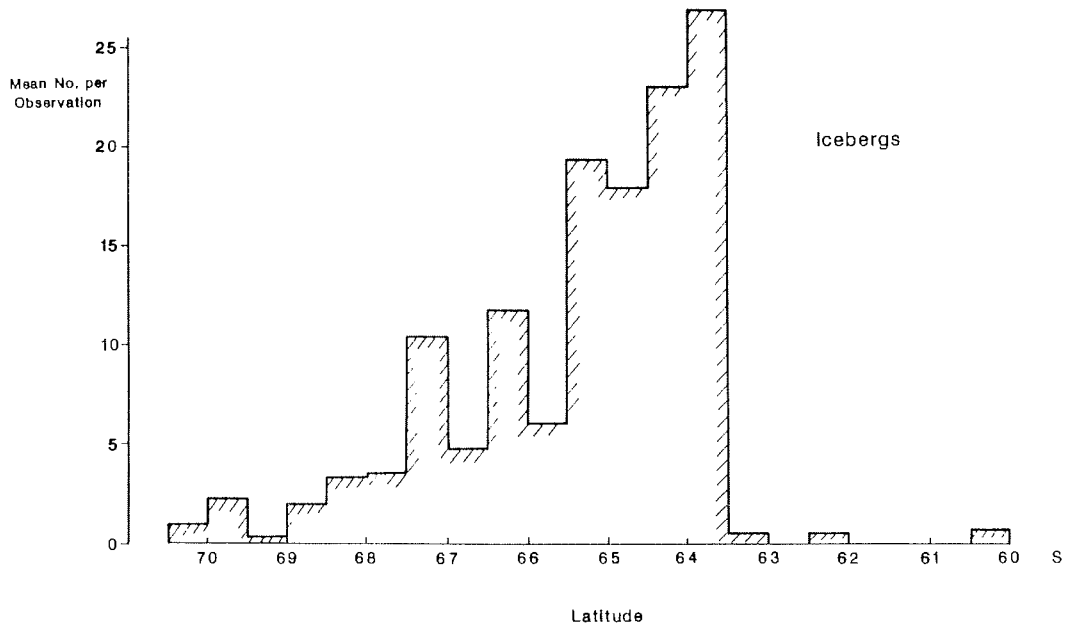

Figure 3.18: Number of observed icebergs on "Polarstern's" meridional transect

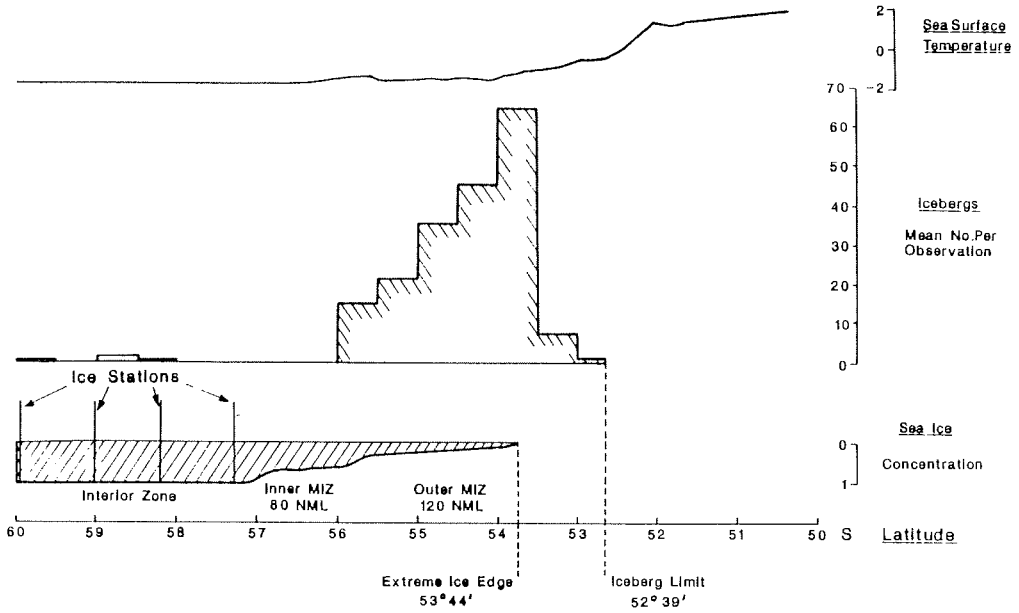

Figure 3.19: Sea surface temperature (top), number of icebergs (middle) and sea ice concentration (bottom) across the marginal ice zone

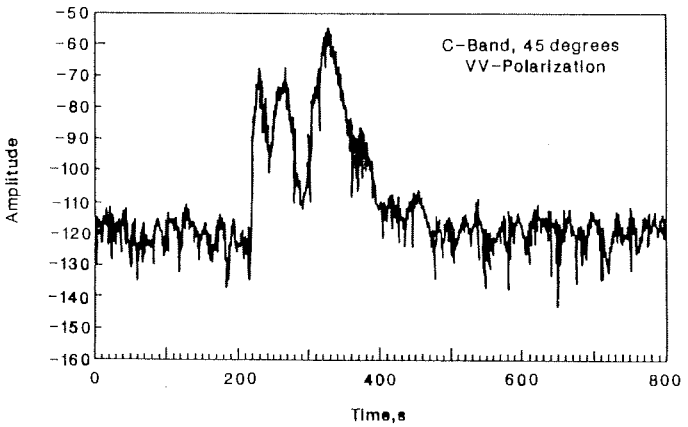

Figure 3.20: Time series of radar signals back scattered by sea ice and snow

was visible, and the ice was broken up into individual floes of diameters from a few tens of metres to about 100 metres. However, the pack as a whole remained quite compact; this can be described as an "inner marginal ice zone", resembling that observed during the EPOS-cruise of *Polarstern*. About 80 nm further north, the pack began to open up under a westerly wind, which organised the floes into distinct bands, each a few km across and with stretches of open water between them which became increasingly wide with northward distance. This more open "outer marginal ice zone", again resembling that of the *EPOS*-cruise or of the *Bering Sea* findings, where bands due to off-ice winds are common, lasted for 120 nm until the extreme ice edge (a final narrow strip of small pieces of brash) was reached. Throughout the outer MIZ increasing numbers of icebergs were seen, rising to a high peak near the extreme ice edge. Some of these were growlers and bergy bits, arising from the decay of larger icebergs, but many were large substantial bergs. Once the ice edge was crossed, the sea surface temperature began to rise rapidly, and iceberg numbers fell rapidly. The last iceberg was observed some 65 nm north of the ice edge, floating in water of surface temperature just below 0°C.

Again there is no obvious explanation of the large numbers of bergs seen near the ice edge after such a dearth further south. There is the possibility that bergs are carried embedded in the pack and are then released when the pack opens up or is broken up by wave action. Visual observation from the helicopter suggested that this was the case.

2.3.5. Sea Ice Remote Sensing (AWI, AES, CRREL, UNIM)

2.3.5.1 Passive Microwave Remote Sensing of Antarctic Sea Ice

The primary objectives of the project are:

- to explore the physics of the passive microwave radiometric characteristics of *Antarctic* sea ice
- to determine which types of ice surfaces can be uniquely identified by passive microwave radiometers
- to improve on the current interpretation of satellite SMM/I data
- to define the growth and decay characteristics of sea ice cover as revealed by time series of satellite and in situ data.

To achieve these goals, passive microwave emissivities were measured at 3 frequencies (6 GHz, 33 GHz, and 85 GHz) and at horizontal and vertical polarizations from on board the ship.In particular, angular measurements were made during ice stations when the ship was stopped and measurements at a fixed beam position were carried out when the ship was moving through ice and

leads. During ice stations, the emissivities were recorded at different incident angles from 20° to 80°. The physical properties of the ice floe at or in the vicinity of the footprint of the sensors were obtained in taking profiles (with depth) of temperature, wetness, density, salinity, granularity, and structure of both snow and ice. The sampling interval was 1 meter over three lines, each about 20 m long and intersecting each other at about equal angles and at the approximate center of the radiometer observation area. The real and imaginary parts of the dielectric constant of sea ice and snow were detected with a dielectric probe at 10 GHz and 18 GHz. Additionally, extensive observations of the cover were made visually, by still photography, and video.

The brightness temperature profiles at different frequencies were displayed on a color monitor while the ship was moving between stations. A PRT-5 infrared radiometer provided concurrent surface physical temperature measurements. The multifrequency response to different surfaces was visually observed and surfaces which tend to cluster at about the same point were identified. For example, water, gray nilas, white nilas, and young ice form four different clusters of data points in a scatter plot using 10 GHz and 85 GHz brightness temperatures. Also ice of various roughnesses, and snow cover thicknesses, is uniquely represented in the same diagramm as a cigar shaped cluster. The latter is elongated at 85 GHz indicating that much of the variability is due to snow cover variations, which affect the brigthness temperatures at 85 GHz considerably more then at 10 GHz. The ability to categorize the ice in this way supports our expectation to achieve similar results with satellite microwave sensors. However, the footprints of the satellite systems (about 30 km) are quite large and the clustering satellite data points may be difficult to match with those on the high resolution ship measurements. Nevertheless, the latter allow to judge how well inversion techniques for satellite multichannel brightness temperature data reflect reality.

Unique to this project was the ability to evaluate the application of the 85 GHz SSM/I channel to characterize the *Antarctic* sea ice cover. Detection of multiyear ice in the *Antarctic* region has not been possible with previous passive microwave satellite sensors because its brightness temperatures appeared to be similar to those of first year ice. Our measurements of the emissivity of thick multiyear ice at 85 GHz indicate constantly low values compared with those of first year ice. Preliminary results show that the observed low emissivity is caused by a thick snow cover (part of which is old snow and granular) mainly associated with *Antarctic* multiyear ice. Thus, the potential in detecting multiyear ice is not in probing the opacity (and internal scattering characteristics) of the ice as is usually done in the *Arctic*, but in identifying ice floes with a thick snow cover. Although, it may be difficult to doubtlessly identify the type of particular ice floes with

this technique, it would provide useful information about statistical distributions of *Antarctic* multiyear ice. The potential of the 85 GHz channel in detecting new and young ice was also found to be strong. Because of the short wavelength, the brightness temperature saturates when the ice is still relatively thin. In conjunction with a low frequency channel, the brightness temperatures of new ice seem to be uniquely identifiable. The measurements of variation in emissivity with angle is expected to provide insight into the wetness and structure condition of the ice floe. The data are also expected to provide information necessary to better understand variations in emissivity due to roughness.

Three long ice stations (with the ship anchored to the ice floe) provided a good opportunity to study the variability of the brightness temperatures of some ice floes with time. During some of the usual 3 to 4 day periods, drastic changes in weather conditions occurred, enabling measurements to be made of the same ice floe during extreme differences of wetness and physical temperature conditions. Preliminary results show a strong sensitivity to changes in the physical temperature of the surface. Comprehensive measurements of several parameters, however, were made at a few hours interval, and further correlation studies will be undertaken.

Overall, about 28 ice floes were studied in detail, and brightness temperatures of more than 500 km of *Antarctic* sea ice cover were measured by the radiometers while a the ship was in transit. The signatures of different types of surfaces were identified and documented with simultaneous visual, video and some still photography coverage. Such signatures will be compared with near simultaneous satellite data to improve interpretation of the latter. Further work and analysis of the data is obviously necessary, but the data will definitely be useful in establishing the real merit of satellite observations in the *Antarctic* region.

2.3.5.2 Radar Measurements

Radar backscatter measurements were carried out at C-band (5.3 GHz) and Ku-band (13.9 GHz) frequencies. The objective of this experiment was to collect surface information to improve the interpretation of satellite acquired radar altimeter and SAR data in terms of polar geophysical parameters. Both instruments were step frequency radars with a 500 MHz bandwidth. Measurements were performed at each station, as well as in transit and during selected CTD stations. Multi-year ice, first-year ice, nilas, ridges, and pancake ice were measured.

The C-band radar was mounted on the port side of the ship, near the bow about 8 meters above the ice surface. The measurements in

transit were primarily at VV polarization and 45 degree incidence angle. At ice stations all four polarizations were measured (VV,VH, HV and HH) at angles from 30 to 75 degrees. Additionally, at most ice stations the ship was moved slowly along the edge of the floe on which physical property measurements were collected. Concurrent radar observations were made at all four polarizations for estimating variance of the backscattered signal. These data will be used in preparatory studies related to ERS-1-SAR imaging of the *Weddell Sea.*

The Ku-band radar was mounted on the bow crane of the ship. Measurements were taken at ice stations by moving the crane to 10 different spots over the ice and measuring the backscatter at angles from 0 to 30 degrees at VV polarization. Up to 1100 measurements were also taken at normal incidence as the crane was slowly moved across the ice. These will be used to estimate the statistical distribution of radar echo amplitudes over different ice types. Measurements were also taken while the ship was in transit, but because of the vibrations from the ship only thinner ice could effectively be detected. These measurements will be used to correlate the GEOSAT altimeter waveforms with ice type and concentration.

For each mesurement the real and imaginary part of either 401 (C-band) or 801 (Ku-band) frequencies were applied over the 500 MHz bandwidth. A *Fourier* transform can be done to abtain a time domain representation of the data. An observational example after this transform for the C-Band data is shown in Fig. 3.20. This will be time gated to eliminate the system response so that the total backscattered power from the snow and ice can be calculated. Half-power points as well as the scattering width will also be calculated to determine any correlation with ice type. Approximately 300 Megabytes of raw data have been gathered.

2.3.5.3 Ice Thickness Determination with an UHF-Radiometer

A UHF (611 MHz) radiometer was installed on broad the ship to test the instrument's operation and stability in polar regions and to determine the feasibility of measuring sea ice thickness remotely. The radiometer operated continuously from Sept 16 to Oct 25, though periodically suffering from radio frequency interference. Four sources were identified, but one remains at large. The bulk of the data was taken while in transit, in conjunction with video coverage of the footprint. These will be correlated to study the UHF response to varying thickness as well as effects due to ridges, snow drift, and sun glint. Angular scans were made at ice stations to determine depth of penetration which will be compared to drilled thickness measurements. Finally, calibration data were collected in leads as

often as possible. Preliminary analysis indicates that the maximum ice penetration depth was roughly 40 cm (49 cm slant depth at 35 deg incidence), but the final verification must be left open until the full data analysis has been done.

2.3.5.4 SSM/I Satellite Passive Microwave Ice Maps

Data from the passive microwave sensor of the US DMSP-satellite were received at the *Institute for Space and Terrestrial Science* in Toronto, Canada. Here ice maps giving total ice and old ice concentrations were produced and faxed to the *Polarstern* about 3 hours after the overpass of the satellite. Both, 19 GHz and 37 GHz channels were used for deriving the above mentioned products. The algorithm applied was developed for the Arctic and is accurate for cold periods. Once the snow warms up, associated with the free water content in the snow, the analysis becomes meaningless. Earlier experiments on *Polarstern* in the *Arctic* have led to a good understanding of microwave signatures at 37 GHz for snow covered sea ice.

Since the ice in the *Antarctic* is relatively thin and melts mainly from the bottom, first year (FY) ice has a similar vertical salinity profile as second year (SY) ice except at the snow/ice interface. It is the upper surface of the ice that is important when classifying ice by type using the SSM/I frequencies. However, the flooding at the snow/ice interface makes the snow cover an important, if not main, contributor to the emission from the ice during the *Antarctic* spring. When comparing the numerous surface measurements from the ice stations and ice observations to the SSM/I derived ice maps an understanding of the microwave signatures emerged.

In the western *Weddell Sea* we found mainly SY ice covered with about 1 m of snow which caused a negative freeboard of the ice floes and thus flooding at the snow/ice interface. Therefore the microwave emission originated from the snow cover and slush and not from the ice which is typical for old ice (OI) signatures.

The snow cover on FY ice, found predominantly in the eastern *Weddell Sea*, was much thinner ranging from about 3 cm to 20 cm as compared to the SY. Thus, most of the emission was from the saline ice surface causing a higher emissivity than for the SY ice. However, annother situation that yields OI microwave signatures is rafted FY ice with snow thicknesses greater than about 50 cm and again slush (16 cm) at the snow/ice interface. *RV Polarstern* went through this type of ice at ice station 28, when the SSM/I OI map shows 20 % concentration of this "diffferent" ice type. The large amount of snow and slush decreases the emission from the ice surface.

A further task was to see how accurate the total ice concentration maps were especially near the ice edge. A preliminary analysis, using ice observations from the bridge and helicopter ice reconnaissances, indicated that in general, the ice concentrations are overestimated by 10-20 %. This results from the fact that the algorithm contains constants for *Arctic* ice. It appears that these constants have to be different for the *Weddell Sea* area and must be changed by using information gained from the shipborne ice observations and the radiometric data.

According to our present assumptions open water would have to be about 10 % of the sensors field of view (2.5 x 2.5 km for SSM/I) to be detected by satellites. It will be interesting to compare the *Advanced Very High Resolution Radiometer* (AVHRR) of NOAA satellites with the SSM/I microwave data in the areas for polynyas and leads. The AVHRR data could get a better answer on the size and probably the shape of the polynya that changes the calculation of the total ice cover in the footprint (field of view) of the SSM/I. A global set of constants or one for each hemisphere will be determined using the similar data sets collected in the *Arctic* and *Antarctic*. These constants are expected to be a function of season due to the variable snow cover.

Passive microwave signatures from floating ice can be influenced significantly by the snow cover especially in spring, summer and fall. This is quite well understood for nearly all the SSMI channels (19 and 37 GHz). The 85 GHz channel is more sensitive to snow due to the smaller wavelength. Therefore the electrical and physical properties of the snow cover were measured during the 28 ice stations in conjunction with radiometric data. A total of 191 snow pits were surveyed totalling 324 measurements of the electrical and physical properties at different snow depths. 45 of these snow pits were from 45 different ice floes which were reached by helicopter on October 13, 14, and 21. This provided a good average of the snow characteristics for a footprint of the satellite.

When the ship stopped beside an ice floe, first the emission as a function of incidence angle was measured for each of 10 GHz, 33 GHz and 85 GHz frequencies. The following measurements of the snow were made at different depths: vertical temperature profile, grain sizes, permittivity, density and free water content in the snow by volume. All of these quantities influence the passive microwave signatures from snow covered sea ice.

During this cruise, there were opportunities to get time series of 3 different ice floes from 2-4 days. The snow was characterized in conjunction with radiometric measurements about every 3 hours from 10.00 to 23.00 local time. Luckily, the air temperature changed significantly during the first time series, yielding a good data set.

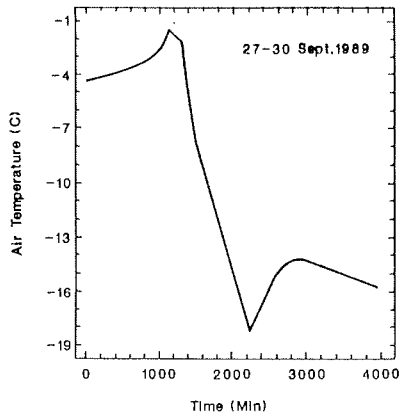

Figure 3.21:

Air temperature changes from 27 to 30 September 1989

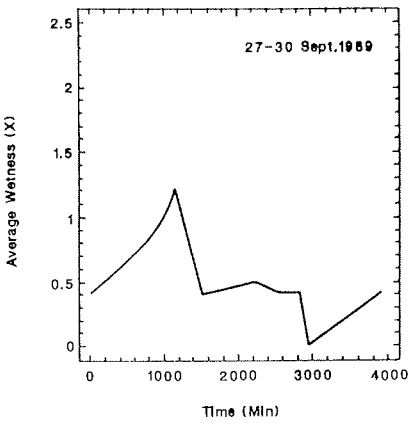

Figure 3.22

Free water concent in snow in percent

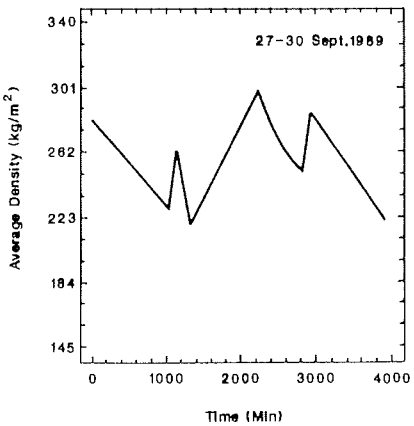

Figure 3.23:

Density of snow on ice floes

For example, Fig. 3.21 shows the decrease in air temperature from about -2°C to -18°C from September 27 to 29. This caused a change in the average free water content from 1.2 % to 0.4 % in the snow as shown in Fig. 3.22. This change in snow wetness caused a significant increase in the emission at 85 GHz from the ice.

The average density of the snow cover changed with time (Fig. 3.23). Correlation of density, as well as the other parameters, to each of the measurements made at the different frequencies will help to understand the 85 GHz ice signatures. The effect of the following snow conditions on passive microwave signatures will be investigated

- wetness
- refreezing
- thick fine grained snow
- thick coarse grained snow.

The snow thickness for a homogeneous snow cover shows a decrease in the emission at 85 GHz. This is due to the scattering of energy within the snow cover. Refreezing, thus forming a surface crust and/or different layers (stratification) in the snow also causes a decrease in the emission as well as an increase in polarization. (Polarization is the difference between horizontal and vertical channels at one frequency. It is another parameter that helps the understanding of emission from snow). Granularity of a snow cover is hard to quantify. It is an important factor and the grain size will have different effects at different frequencies. More effort will be put into this area.

It may be possible, based on preliminary analysis, to obtain useful information of a snow cover from satellite passive microwave measurements such as: snow thickness, free water equivalent of the snow and granularity. This will be useful information since the amount of snow will influence the freezing rate, the snow wetness indicates how much melt is occuring and the granularity is associated with albedo.

The snow cover in the *Weddell Sea* is less complicated than on *Arctic* ice. The snow structure as well as the amount of snow on SY and FY ice are clearly different in the *Weddell Sea* as compared to the *Arctic* where there can be a lot of structure on all ice types. It is for this reason, that the *Weddell Sea* is a good area to further the understanding of microwave signatures from snow covered sea ice.

2.3.5.5 Passive Visible and Infrared Satellite Remote Sensing

The data of the *Advanced Very High Resolution Radiometer* (AVHRR) were received onboard the ship for three purposes. First, changes of ice concentration, sizes and orientation of leads have been documented for various atmospheric forcing conditions. Second, the sea ice drift velocity has been determined from floe displacements in time. The so found spatial distribution of the sea ice drift extends the information obtained from the buoy arrays. Third, the AVHRR results were tested by local observations compared with the lower resolution SSM/I data as well as with the higher resolution *LineScan Camera* observations.

The *High Resolution Picture Transmission* (HRPT) data from the AVHRR onboard the polar orbiting satellites NOAA-10 and NOAA-11 were received by a shipborne station. In the period from 9 September to 25 Oktober 94 digital data sets were gathered, 58 of which were stored for detailed analysis. The area from about 70°W to 40°E longitude and from about 78°S to 50°S latitude was generally observed. The limiting factor in selecting useful data sets for ice analyis was the cloud coverage.

The opening of a large polynia at the Eastcoast of the *Antarctic Peninsula* between 63°S and 73°S and the development of mesoscale lead systems in the eastern and southeastern part of the *Weddell Gyre* could be observed in detail (Fig. 3.24). A preliminary drift analysis could be done for the period from 27.September to 1 October. For this purpose the data were transferred into independent geographical projections. The drift was calculated by invariant feature tracking. The resulting floe motions for the area of the second long ice station are displayed in Fig. 3.25.

Measurements of atmospheric extinction, which had started already during *Polarstern's* first leg from *Bremerhaven* to *Puerto Madryn*, have been continued. During cloudless conditions, direct solar radiation in different narrow spectral bands has been measured by a sunphotometer in order to determine the atmospheric aerosol extinction. Together with the atmospheric water vapour content, obtained from the radiosondes, these measurements will be applied to improve the atmospheric correction algorithms of the AVHRR data.

The antenna, the computer and the image processing system worked without major problems. During periods of extreme low temperatures the motor units and the gearboxes had to be heated to guarantee an undisturbed reception of the data. The sampled data set represents a comprehensive information on the early spring ice conditions in the *Weddell Sea*.

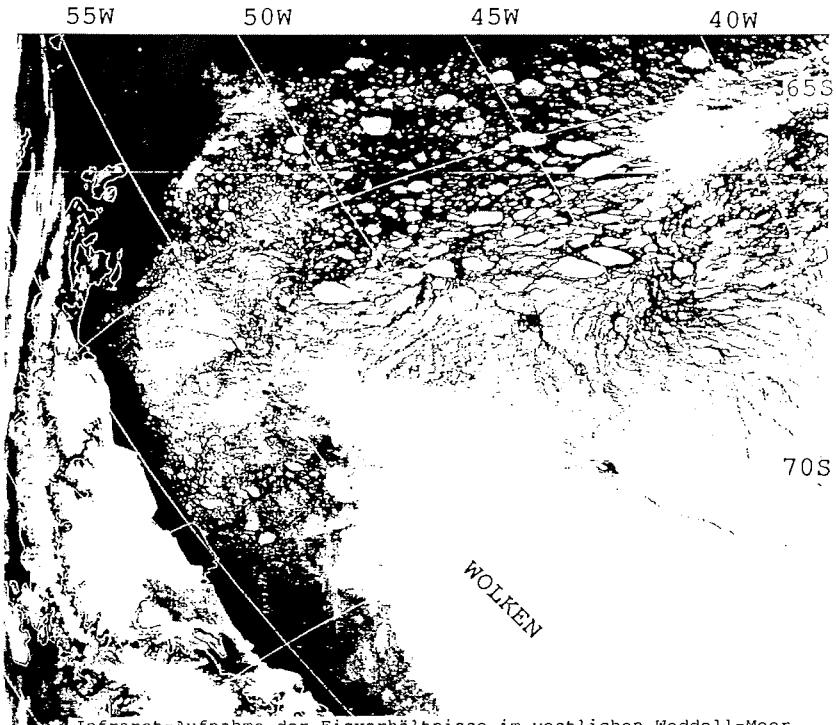

Infrarot-Aufnahme der Eisverhältnisse im westlichen Weddell-Meer vom 30.9.1989 09:03 UTC. Die Daten wurden vom polarumlaufenden US-Wettersatelliten NOAA-10 gemessen und direkt zur POLARSTERN gesendet. Helle Flächen entsprechen niedrigen Temperaturen, dunkle Flächen entsprechen hohen Temperaturen. Am linken Bildrand ist die Antarktische Halbinsel zu erkennen.

Figure 3.24: Infrared satellite picture of the western Weddell Sea on 30 September 1989

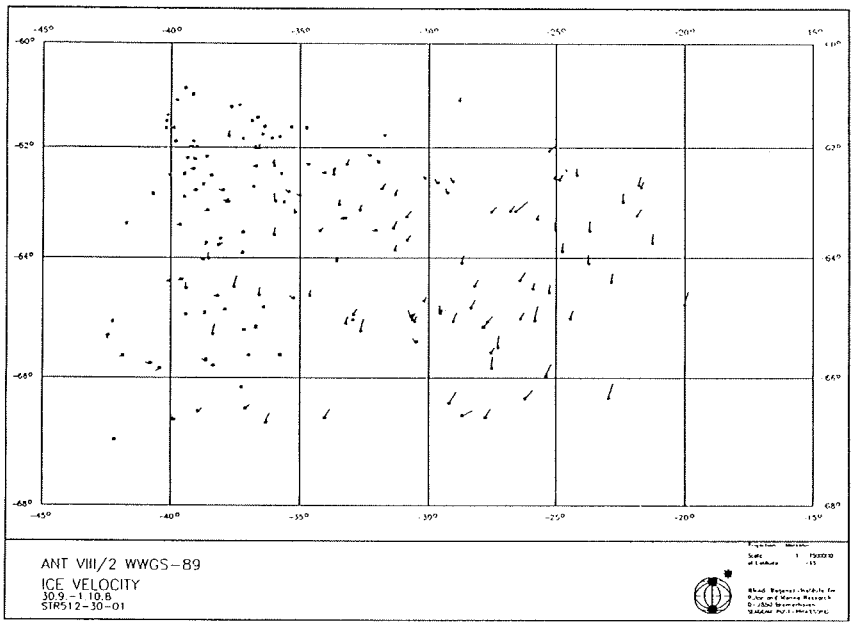

Figure 3.25: Ice motion as derived from satellite images

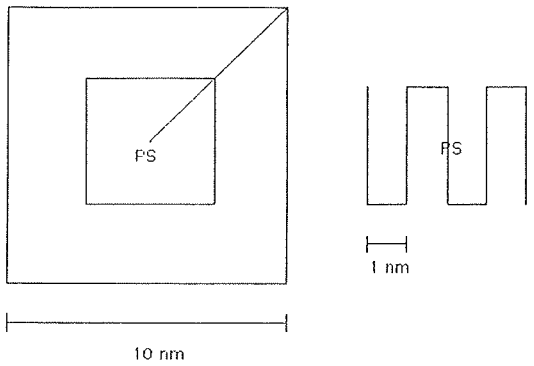

Figure 3.26: Helicopter flight patterns for line scan camera observations. Standard pattern (left), high resolution pattern (right)

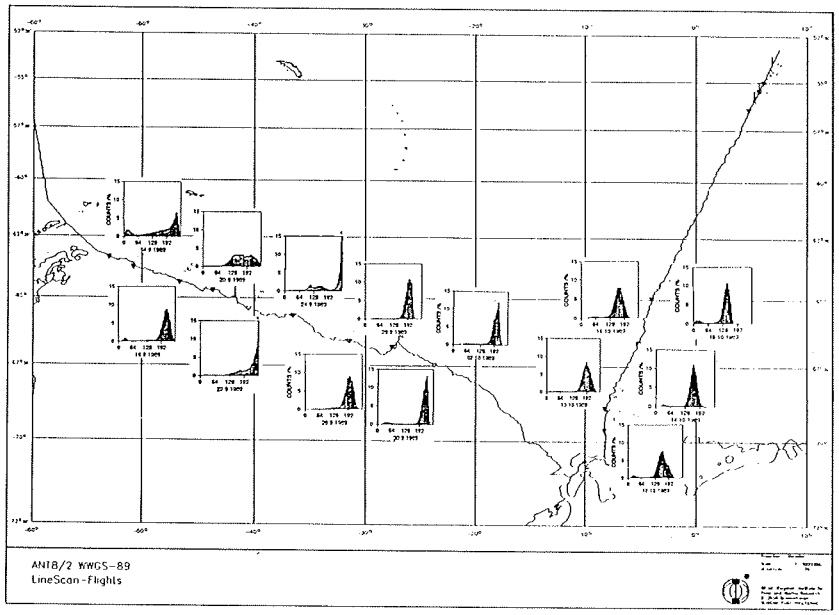

Figure 3.27: Line scan camera measurements of the grey scales (brightness is increasing from left to right) along "Polarstern's" cruise track

2.3.5.6 LineScan Camera Survey

High resolution digital data of the ice coverage were sampled by a *LineScan Camera* system from helicopters. Between 12 September and 23 October 21 successful flights could be executed. The chosen flight patterns are shown in Fig. 3.26. The location of the flight areas and the resulting distribution of the brightness values are indicated in Fig. 3.27. All data are corrected for scan-angle distortions and spikes. Mean brightness value distributions for areas of about 1 x 1 km are calculated. This corresponds to the geometric resolution of the AVHRR pixels. Using an interactive dynamic threshold method three different classes of ice/water coverage are obtained. The mean concentrations for these three classes have been calculated. The camera data will later be compared with the concentrations derived from the AVHRR and LANDSAT data as well as with the video measurements taken simultaneously during the helicopter flights.

2.3.6 Marine Biologie (AWI, AARI, IFB, IFO, UNIB)

2.3.6.1 General Remarks

The biological programme focused on four major topics, namely

- studies of the sea ice biocoenosis (ice algae, bacteria, micro- and macroheterotrophs) within icecores to resolve variations on the horizontal (along the northwest- southeast transect) and the vertical scales (according to vertical ice core texture) and the taxonomy of ice diatoms of the infiltration layer,

- determination of the composition and abundances of phyto-, protozoo- and mesozooplankton species at the marginal ice zone and across the *Weddell Gyre* as well as of the biochemical composition within the water column and directly under the ice,

- the registration of vertical pelagic particle flux to characterize the different biological areas within the *Weddell Gyre* according to the material loss associated to those systems,

- experiments of simulated biological spring (potential primary production at different light levels) and winter conditions (survival in total darkness, description of loss processes) of the various algal communities to examine the potential growth capacities of the different biota.

The ice core samples were analysed with respect to autotrophic and heterotrophic species by means of epifluorescence and light microscopy. Taxonomy of ice diatoms was done for the infiltration layer and for distinct ice core sections. Foraminifera and metazoa were sorted to species level, counted and measured for numerous ice cores. Samples for particulate organic carbon, nitrogen and silica of defined ice layers will be analysed in the home laboratory. The vertical distribution of chl a was determined in relation to ice texture. Primary production measurements under the ice layer were carried out *in situ* six times. Brine was sampled *in situ* and by the means of gravity filtration on board to derive salinity, pH and chl a values. Light intensity was measured within and directly under ice floes. The morphology of the bottom of ice floes was recorded on video-tape at several ice stations.

In the water column light was measured by means of a 2 sensor lithgt detector and a Secci disc. Water samples have been taken to analyse chl a, seston, particulate organic carbon (POC), nitrogen (PON) and silica (PSi), phyto- and protozooplankton species composition and abundances. The biochemical parameters were recorded to a depth of 3.000 m whenever possible. The composition of surface phytoplankton species was obtained by means of a 20 µm net and taped with a video sytem attached to the inverted microscope. Makrozooplankton was sampled by means of a "mulit-net" and a "bongo-net" and analysed on board with respect to three main copepod species. Subsamples have been separated for carbon and nitrogen determination of the main zooplankton species and trace metals will be investigated from special samples. Three sediment traps were attached to current meter moorings to record the pelagic vertical particle flux during a 16 months period.

Algae from 150 m, 10 m depths and from water directly under the ice as well as algae from upper, middle and bottom parts of ice cores were incubated on board under *in situ* temperatures for two light regimes. Simultaneously, feeding of the main copepod species on these cultures was investigated. Measurements on the relation between carbon assimilation and irradiance (P versus J-curves) were performed both, for open water samples and for samples during experiments on the growth potential of phytoplankton. In addition, experiments were carried out to simulate the dark winter situation and dark respiration, during which the cellular carbohydrate content and the extracellular release of dissolved organic carbon was monitored. Long terme solution experiments of amorphous biogenic silicia were started as well.

2.3.6.2 Ice Biology

In the ice cores 61 species of diatoms, 3 different siliceous cysts and three species of other algae than diatoms were found by means of an inverted microscope. 32 species of diatoms and two siliceous cysts were dominant or at least very abundant in the ice samples.Three different community types could be distinguished. The top community was found in the upper 10-20 cm of the ice cores at the interface between snow and ice, mostly at floes with negative freeboard. Therefore this community had its most pronounced occurrence in the western and middle part of the Weddell Sea with a thick snow cover on the floes. Dinoflagellates and diatoms *(Nitzschia cylindrus, Nitzschia closterium, Tropidonies glacialis)* were the main primary producers of this stratum. These algae live in an extreme environment and must be capable to stand a wide range of temperature and salinity values. The diatoms of this layer reached with $1.9 \cdot 10^5$ cells/ml the highest densities of all analysed samples.

Internal populations of ice algae were found only in the western part of the *Weddell Sea*. They were observed on varying depths of probably second year ice floes. The great density of resting stages of dinoflagellates and other cysts indicate that these layers represent the overwintering residuals of the last year's ice algal blooms.

The third type of populations of ice organisms, the bottom community was found in the lower 10-20 cm of the ice floes. It was mainly restricted to the lower 1-2 cm of the floe. In this horizon metazoa showed their abundance maximum. A wide range of taxonomic groups could be observed (e.g. ctenophores, copepods, gastropodes, polychaetes, turbellaria) in varying densities.

Along the west-east transect, three regions can be distinguished (Fig. 3.28). Only in the western part (I) of the *Weddell Sea* internal communities were observed, mostly in second year ice floes of 125 to 152 cm thickness. The bottom community was dominated by pennate diatoms of the genus *Nitzschia* (*Fragillariopsis*). The central area of the *Weddell Sea* (II) accommodates both top and bottom communities which are characterized by high densities of the centric diatom *Corethron criophilum* and the prymnesiophyte *Phaeocystis*. These findings suggest that water from the north must have been mixed into this area of the *Weddell Gyre*. In the eastern part of the Weddell Sea only bottom communities were found consisting mainly of *Nitzschia* and autotrophic athecate dinoflagellates (*Gymnodinium*).

The preliminary conclusion is that the ice in the *Weddell Sea* is an unique habitat, dominated by diatoms, dinoflagellates and bacteria. Thus, intensive interactions between algae and bacteria seem to be rather likely. Furthermore, an ice floe of 1 m thickness contains

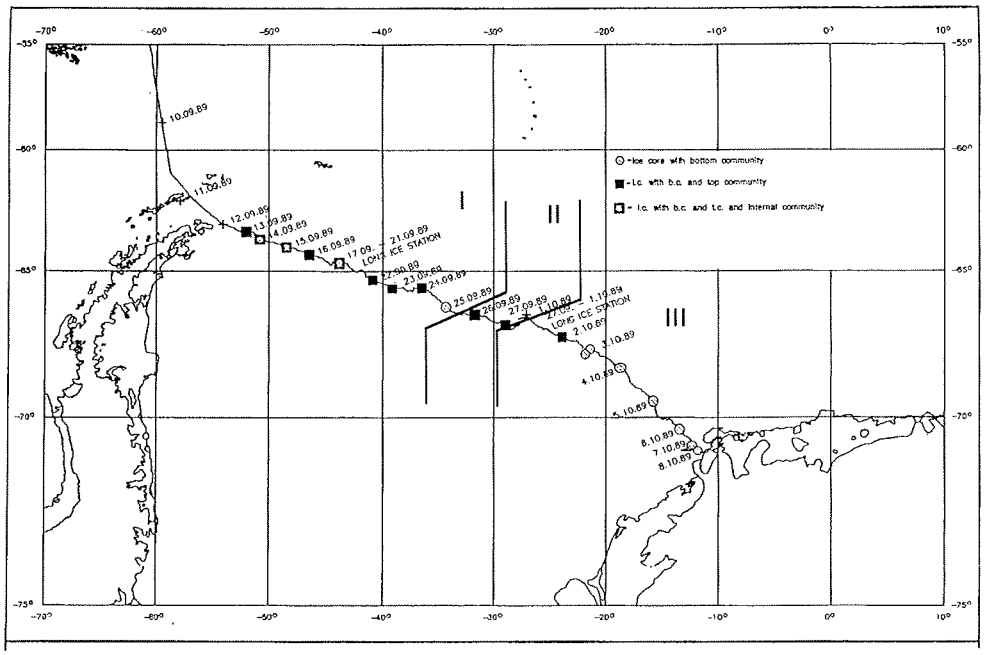

Figure 3.28: Classification of the biological population in sea ice on "Polarstern's" zonal transect

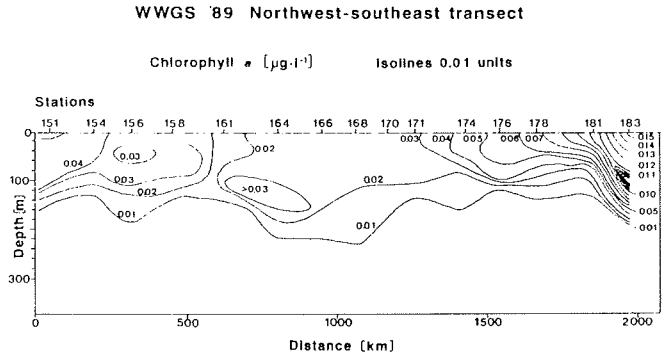

Figure 3.29: Chlorophyll a distribution along the northeast southwest transect across the Weddell Gyre

nearly the same amount of biomass as the upper 200 m of the water column. The presence of different larval stages (polychaetes, copepods, gastropods) indicate a direct coupling between the pelagial and the ice due to adapted life cycles of several metazoa.

2.3.6.3 Light Measurements

Measurements of radiation available for photosynthesis (PAR) in the ice, under the ice and in the open water were performed to detect the depth of the 1% surface irradiation. This is thought to be the depth were loss processes (respiration, extracelluar release) and production should be equal. In the water column this mean compensation depth was 90 m ($\pm$ 25 m).

PAR in the open water and under ice cover was used for *in situ* measurements of primary production in order to extrapolate the *in situ* carbon assimilation from the incubation time of usually less than 8 hours to daily values.

2.3.6.4 Pelagic Biology

2.3.6.4.1 Chlorophyll a and Phytoplankton

The biological properties along the west-east transect of *Polarstern* clearly showed the influence of shelf waters in both costal regimes. The center of the *Weddell Gyre* at about 30 °W was marked by changes in the phytoplankton species composition and chlorophyll a concentrations.

In the *Drake Passage* the net phytoplankton composition within the upper 10 m of the water column showed rather high cell abundances. Besides various diatoms, many heterotrophic protozoan species were observed. Species diversity and chl a concentrations decreased to the south. While the chl a concentrations ranged between 0.2 and 0.4 $\mu g\ l^{-1}$ in the upper 100m of the water column north of the tip of the *Antarctic Peninsula* they first decreased to 0.1 μgl^{-1} and finally to 0.03 $\mu g\ l^{-1}$ at the shelf slope further to the east. A change in species composition was observed at the northern boundary of *Bransfield Strait*. Here, so far not documented species (such as *Porosira pseudodenticulata*, *Stellarima microtrias* and *Rhizosolenia truncata*) were found. At all stations in the western shelf area high amounts of anorganic minerals and resuspendend organic matter were also observed.

In the heavy pack ice zone of the central Weddell Sea, where species abundance was low, chl a values decreased to about 0.02 µg l^{-1}. The most common forms were *Distephanus speculum, Coscinodiscus spp., Asteromphalus* spp., *Actinocyclus actinochulus, Rhizosolenia truncata* and some *Chaetoceros spp.* Only few ice algae were found in the upper water column but no ciliates, tintinnids and dinoflagellates; the most prominent protozoans were radiolaria. The chl a concentrations increased continuously from the center of the *Weddell Gyre* towards the western and eastern shelf regions. In the diatom compositions *Chaetoceros dichaeta, Nitzschia sp.* and *Nitzschia kerguelensis* were more abundant in the samples near the eastern coast of the *Weddell Sea.*

At the shelf break off *Kap Norwegia,* on the eastern side of the *Weddell Sea* a chl a patch with concentrations higher than 0.14 µg l^{-1} appeared at the hydrographic shelf front (Fig.3.29). The diversity of diatom species was also maximal at this front while the number of ice algae increased and the variety of species decreased near the ice shelf front.

Along the south-north transect, only slight changes of the phytoplankton community were observed in the inner ice belt. Further to the north the marginal ice zone was investigated with stations on a 30 nm grid. Near the ice edge at the transition zone to the *Antarctic Circumpolar Current* (ACC) the biomass increased to more than 0.55 µg l^{-1} and a distinct shift in phytoplankton and zooplankton species composition became obvious. *Corethron criophilum,* a diatom species and *Salpa* spp. a pelagic tunicate both typical for the *Antarctic Circumpolar Current,* became the dominant species.

2.3.6.4.2 Zooplankton

The winter state of the dominant phytophagous copepods of the *Antarctic* plankton (*Calanoides acutus, Calanus propinquus* and *Rhincalanus gigas*) was investigated for the first time in the *Weddell Gyre* during this curise. The results described below are based on 15 "multinet" hauls (five levels for each tow; 0,25 m^2, 100 µm). Maximal depths were 1000, 2000 or 3000 m, but results presented below refer to the upper 1000 m of the water column only. The investigations were carried out along a west-east transect.

Calanoides acutus showed the most regular distribution (Fig. 3.30) with average quantities about $1\text{-}2 \cdot 10^3$ Ind./1000 m^3. Maximum abundance was $5 \cdot 10^3$ Ind./1000 m^3. The population consisted of copepodit stages III-VI, but stage III was represented rather rarely (Fig. 3.30). The maximal density of this copepod species was

restricted to the 500-1000 m layer. In the deeper regime the densities decreased and copepodits IV were dominant.

Calanus propinquus was most abundant at the middle part of the transect (Fig. 3.30) with a maximum of 4,4·10 ^{3} Ind./1000 m^3. Its abundances decreased to the north and to the south. The population consisted of copepodit stages II -VI, with copepodit stage III clearly dominant. In general, maximal density of the species was observed in the oceanic mixed layer with rather low water temperatures (<1.85°C) (Fig. 3.31B). Copepodits III were also dominant in the deep layers (1000-2000 m and 2000-3000 m).

The numbers of *Rhincalanus gigas* were one order of magnitude smaller than of other species with typical concentrations of 100-150 Ind./1000 m^3 (Fig. 3.30C). Their maxima occured in the eastern part of the transect (340 and 384 Ind./1000 m^3). The population consisted mainly of copepodit stages IV-VI, but copepodits II and III were present also in low numbers mainly at the south-eastern part of the transect. This species was restricted to the layer between 250 and 500 (1000) m (Fig. 3.31C). The most frequent species along the west-east transect were *Calanus acutus* and *Calanus propinquus* (Fig. 3.32).

A new feature is the high concentration of *Calanus propinquus* in the surface water during winter since these species inhabit deep layers during the cold season in the ACC. It seems reasonable that marine species at high latitudes may prefer to live near the sea surface. In this respect, *Calanus propinquus* behaves similar to *Euphausia superba*, which are found also near the surface during late winter. We suppose a trophical adaptation of these two species to the algal flora of the bottom layers of ice floes, which grow rich at the end of winter. It is still open whether the high population under the ice results from their ascent in the late winter or their permanent presence in the upper water column. No other species were observed in the cold oceanic mixed layer but in the underlying *Warm Deep Water*.

The observed age composition was as expected only for *Calanus acutus*. *Calanus propinuquus* were surprisingly young (stage III). The presence of young copepodit stages of *Rhincalanus gigas* in small numbers makes us believe that they represent the "rest" of late summer spawning events.

The species distribution along the transect is related to different water masses. *Calanus propinquus* is characteristic for the *Weddell Gyre*. They are rare in other parts of the Antarctic. The increased numbers of *Rhincalanus gigas* at the north-western and south-eastern parts of the transect indicate its preference for warmer water in accordance with its most usual habitat, namely the ACC.

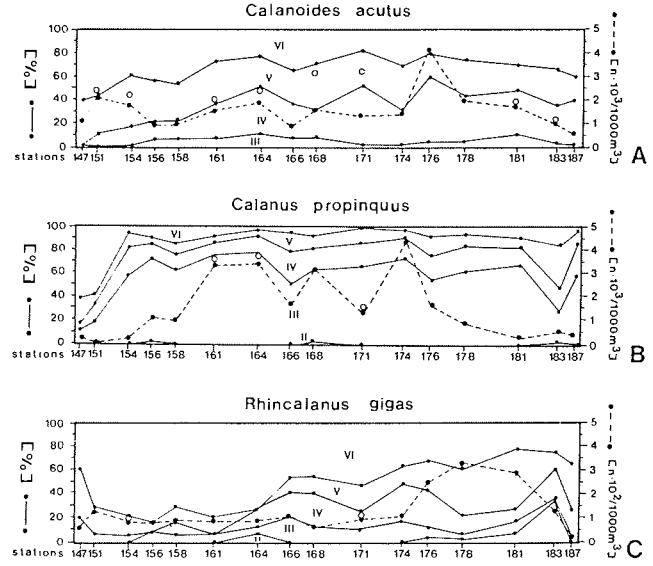

Figure 3.30:

Age composition (copepodit stages II to VI). Calanus propingus gigas (C) between O and 1.000 m along the northwest-south-east transect (13.9-8.10.89). Additional points correspond to total individuals per station

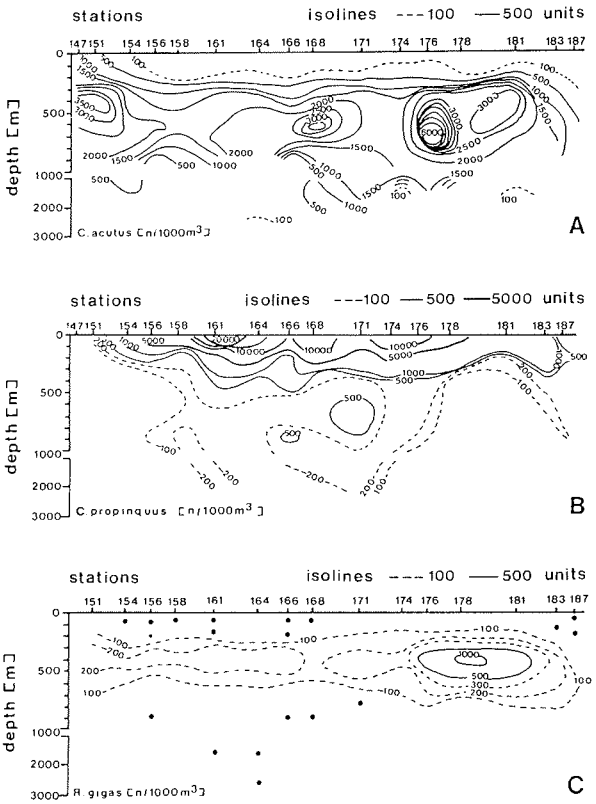

Figure 3.31:

Vertical distribution (ind. 1.000 m-3) of Calanoides actus (A), Calanus Propingus (B) and Rhincalanus gigas (C) along the northwest-southeast transect (13.9.-8.10.1989)

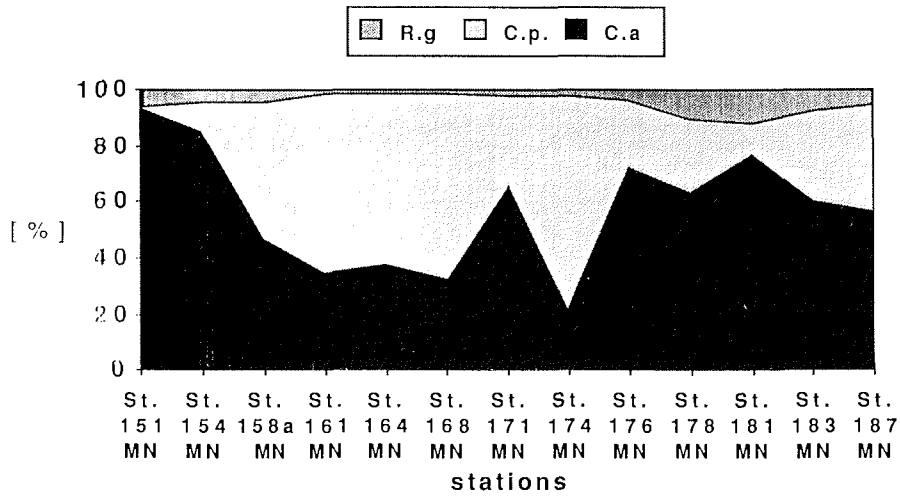

Figure 3.32: Relative abundance of Calanoides acutus (C.a.), Calanus propingus (C.p.) and Rhincalanus gigas (R.g.) along the northwest-southeast transect (13.9.-8.10.1989)

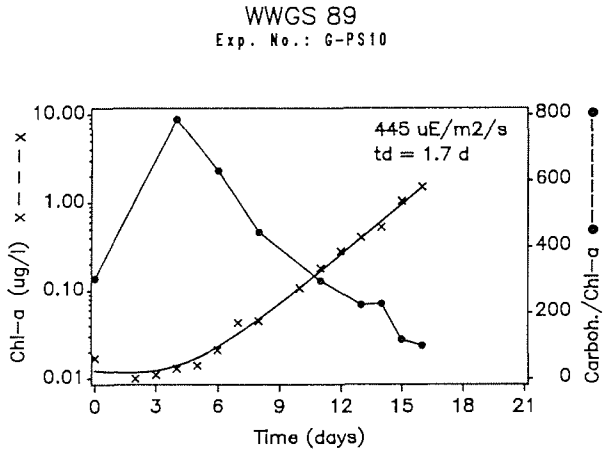

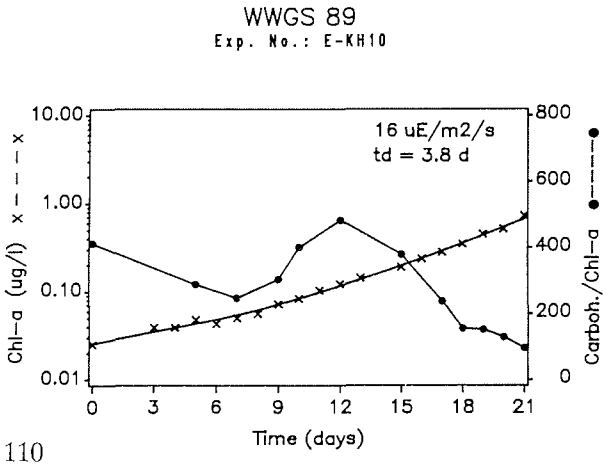

Figure 3.33:

Increase (In-plot) of chl.a concentrations (left scale versus time in relation to light intensity

a) 445µE m $^{-2}$s^{-1}

Right scale refers to quotient of carbohydrate to chl.a. Biomass dobbling (td) indicated in days

2.3.6.4.3 Under-ice Pelagic Biology

The water layer under the ice (0- to about 2.5m depth) was studied with by means of an L-shaped instrument (L'se). First the light was measured in the atmosphere then the instrument was lowered to a depth of 2.5 m to detect the light there again. An underwater camera was mounted to scan the bottom of the ice floes. Water (10 l) was pumped by means of a vacuum pump through perforations of a silicon tube at the end of the arm of L´se (at 3 - 5 depth intervals) to analyse the same parameters (salinity, nutrients, chl a, particulate organic carbon and nitrogen, species composition) as in the entire water column.

Light under the ice ranged between 0,01 and 1 % (0,02 - 9,6 $\mu E\ m^{-2}\ s^{-1}$) of the incoming light (198 - 1021 $\mu E\ m^{-2}\ s^{-1}$ measured with a 2 π sensor). In most cases the bottom of the ice was relatively smooth and no remarkable concentrations of algae or zooplankton could be observed. No small scale variations in nutrients as well as in biomass could be detected within the first two meters under the ice. The values were similar to those of the uppermost water bottle of the rosette sampler.

2.3.6.5 Experimental Biology

2.3.6.5.1 Growth Experiments

Growth experiments with planktonic algae and ice algae were carried out in 10 l glas bottles by incubation at two different light levels. The experiment set up was as follows:

Bottle	Source
L1/D1	water from 150m depth
L2/D2	water from 10m depth
L3/D3	water from 10 cm under the ice
L4/D4	water plus bottom part of ice core (110-120 cm)
L5/D5	water plus middle part of ice core (40-50 cm)
L6/D6	water plus upper part of ice core (0-10 cm)
D5-Cop1	water as for D5 but with 18 *Calanus propinquus*
D5-Cop2	water as for D5 but with 19 *Calanoides acutus*

L= 50 $\mu E\ m^{-2}\ s^{-1}$, D= 5 $\mu E\ m^{-2}\ s^{-1}$

Samples for growth rates and species composition (chl a and microscopical counting) were taken in two or three day intervalls (for copepod experiments every day). Nutrient concentrations were determined occasionally at the beginning of the experiments and regularly at chl a levels above 15 mg l^{-1}.

The first significant increase of biomass (exponential growth) was encountered in the light bottles (L4 to L6) containing the melted sea ice, followed by the three bottles (D4 to D6) which were kept under lower light conditions. In the various bottles different species became dominant, e.g. in L4 /D4 *Nitzschia cylindrus* (small form) together with some centric diatoms, in L5 /D5 *Nitzschia cylindrus* (long form) and in L6 /D6 *Phaeocystis*.

The growth rates in the six other bottles (L1-L3, D1-D3) were significantly lower and the exponential growth phases started much later. The D-bottles did not reach maximum chl a concentrations until the end of the cruise. *Nitzschia cylindrus* (small form as in L4 and D4) was the dominant diatom in the light bottles and was accompagnied again by some centric diatoms. The abundances of bacteria, auto- and heterotrophic flagellates will be analysed at home to investigate the coupling between autotrophic production and bacterial activity in different growth phases of the algae.

Both zooplankton species did feed well on algae so that no exponential increase of the algal population could be established. The feeding of *Calanus propinquus* was more pronounced than that of *Calanus acutus*. Individuals of the first ones produced an order of magnitude more faecal pellets than the latter. The experiments showed that ice algae are able to grow as fast as pelagic forms when they are released into sea water. Therefore, they should be regarded as an important contribution to the primary production, particularly in spring. Copepod feeding may reduce bloom development if their numbers are already high prior to the algal growth.

2.3.6.5.2 Survival of Phytoplankton under Winter Conditions

During the *Antarctic* winter, phytoplankton has to overcome some darkness until growth conditions become more favourable again in spring. We tried to simulate winter (no light at all) and spring (some light) conditions.

The changes in biochemical parameters (chl a, carbohydrates), photosynthetic potential (by measuring the relationship between carbon assimilation and irradiance at seven light levels), dark losses (due to respiration) and extracellular release of dissolved organic carbon (EOC) were recorded. Because of the low biomasses, the

radiotracer ^{14}C was used in the experiments which will be analysed in the home laboratory later.

2.3.6.5.2.1 Survival in Darkness

In the marginal ice zone water from 10 m and 80 m depths was sampled, filled into 4 polycarbonate-containers (20 l) and kept in total darkness at the ambient temperature (-1°C). In daily intervalls the following measurements were conducted: chl a and phaeopigments (all containers), carbohydrates and photosynthetic potential under saturating irradiances (380 µE m^{-2} s^{-1}) (two containers). A complete photosynthesis-irradiance measurement was done every week. Species composition was counted repeatedly.

Chlorophyll content remained constant for about 1 to 2 days, then it decreased within 5 days to half of its initial value. After three weeks the chl a had decreased to 1/3 of the initial value.

To study short term changes (^{14}C) water samples from 10 and 80m depths at a photosynthesis saturating light level (560 µE m^{-2} s^{-1}) were incubated for at least 12h (in one case the incubation lasted for 2.25 full photoperiods of 12h light and dark each). Then the assays were transferred into total darkness and samples taken every 12 to 24 hours. The following parameters were measured:

- particulate organic carbon after filtering on membrane filters. The expected decrease in radioactive carbon in the dark is a measure of dark losses,

- dissolved organic carbon. Due to extracellular release a certain amount of radioactive carbon is transferred into dissolved organic substances in the filtrate of the samples; losses of particulate organic carbon which cannot be attributed to extracellular release provide a measure of dark respiration.

These experiments were conducted 5 times either directly or preincubated for several days under high or low irradiances (445 µE m^{-2} s^{-1} and 16 µE m^{-2} s^{-1}, respectively) in order to obtain higher biomasses and to check the influence of light to shade adaptation on loss processes.

2.3.6.5.2.2 Growth potential

Simulation of *Antarctic* spring conditions was achieved with water samples from 10m and 80m depths (corresponding to a light depth of 50% and 1% surface irradiance) to be stored at -1°C and illuminated by fluorescent tubes (spectral composition similar to daylight) for 12h followed by 12 darkness. The containers were either aeriated with sterile-filtered air or shaken every day. The following parameters were measured:

- chl a in daily intervalls
- carbohydrates every two days
- photosynthesis-irradiance relationships at 7 light levels every two days,
- species composition every 2 to 3 days.

Under the experimental conditions algal growth started after a lag-phase of about 2-5 days. Chl a as well as cellular carbohydrates increased exponentially with rather high growth rates ranging from 0.3 to 0.7 per day, corresponding to a doubling time of about 2 to 1 days. This exponential growth persisted for about 10 days until a decrease in growth rate -probably due to nutrient limitation- was observed (Fig. 3.33a).

When algal communities were exposed to low light levels of about 16 $\mu E\ m^{-2}\ s^{-1}$ they started to grow exponentially with a considerable longer time lag of about 6 to 8 days. The maximal growth rates were also distinctly lower, ranging from 0.19 to 0.15 per day corresponding to a doubling time of about 4.5 to 3.6 days. The end of this exponential growth period could not be reached within the experimental time of 21 days.

Carbohydrate: chl a ratios in cultures changed with high and low quantum fluxes rather similarly. Samples directly taken from the open water showed values of the ratio carbohydrate chl a from 300 to 500. Until the beginning of exponential growth these values increased to about 1000 and decreased again at the end of exponential growth phase to low values of about 100 (Fig. 3.33b).

2.4. Research programme on RV Akademik Fedorov

The subprogramme on *Akademik Fedorov* were rather similar to those on Polarstern which have been described in the previous chapter. Therefore, the first ones will only be briefly portrayed here in order to demonstrate their supplementary capacity.

2.4.1 Physical Oceanography (AARI, LDGO, INIDEP)

The investigations are based on hydrocasts with a Neil Brown Mark III CTD and a rosette water sampler as well as on XBT launches. The main aim of this subprogramme was to establish hydrographic sections across the northern part of the *Weddell Gyre* and to extend *Polarstern's* zonal transect from 68°S/20°W to Maud Rise (see Fig. 2.4). Furthermore, a detailed survey of the *Maud Rise* area and the region west of *Maud Rise* has been carried out. The latter high resolution CTD mapping during the ship's drift was omplemented by helicopter supported VTD casts in a mesoscale polygon.

Examples of preliminary vertical temperature sections along the transects I, II and III of Figure 2.4 are desplayed on Figures 4.1, 4.2 and 4.3. The first section clearly portrays the frontal structure which separates the ACC on the left side from the *Weddell Gyre* on the right side of figure 4.1. The relatively dolc core of the latter is well marked between stations 13 and 20 in the pressure regime from 200 to 700 db. At the mmost southerly side of the section the reverse flow of warmer circumpolar water in the gyre circulation becomes already abvious. This feature is more distinct further to the east on Figure 4.2. The warm layer is most pronounced on the leeward side of *Maud Rise* between stations 36 and 41. The extension of this water body to the south is documented on Figure 4.3. Here the colder water over *Maud Rise* becomes apparent at stations 43, 44 and 45.

The nearly 12 day drift station was located west of Maud Rise in the area with the maximum Warm Deep Water on Figure 4.2. During this time intervall the ship drifted with the sea ice along the track line shown on Figure 4.4 which marks more or less a free drift path forced by the local winds. The hydrocasts along the track were complemented by current meter measurements at 40 m (mixed layer), 70 m (pycnocline) and 200 m (T-maximum layer) depth to derive the vertical shear flow in relation to the thermal structure.

2.4.2 Atmospheric Physics (AARI, AWI)

The meteorological measurements on the *Akademik Fecorov* were primarily concerned with the determination of the surface inergy budget. For this purpose the upward and downward radiative fluxes wered recorded parthly on board the vessel and parthly on the sea ice. The turbulent vertical heat and momentum fluxes were obtained by the eddy correlation technique with the aid of a sonic instrument and the turbulent latent heat transports have been derived from slightly advance bulk formulae. Through various instrumental cross checks it is beliebed that the full data set provides valid information on the surface heat budget as e.g. documented by the mean values for the entire drift phase on Figure 4.5. More detailed values are expected from the final data set. The latter includes also the radiosonde ascents, information on the sea ice concentration from helicopter flights with a line scan camera and further atmospheric and sea ice data from three Argos surface buoys.

2.4.3 Sea Ice Physics (AARI, CRREL, LSU)

The sea ice investigations were consisted of routine observations from the ship, helicopter flights with a line scan camera and an infrared radiometer, in situ measurements on ice cores and ice thickness determinations through drilling. Additionally, data of the *Meteor* and NOAA satellites will be processed for large scale sea ice characteristis. The routine visual ice observations include also detailed iceberg statistics. Finally, strain measurements were carried out to study the mechanical behaviour of sea ice under given environmental conditions. In particular elastic and gravity waves induced by local wind forcing and sea swell were recorded.

2.4.4 Marine and Sea Ice Biology (IFB, IFO, CRREL)

Zooplanktion was investigated with the aid of 47 Bongo and Juday net hauls down to 1000 m depth. The population and the composition of copepods of the cold central region of the *Weddell Gyre* differed distinctly from the warmer outer regions. In principle the findings of the *Akademik Fedorov* agreed with the results of *Polarstern.*

The biology sea ice work concentrated on the study of the diatoms throughout the entire ice layer. Certain activities of phytoplankton were observed in the middle and lower parts of the ice floes.

2.4.5 Air Chemistry (CAD, IAP, UNIB)

Surface Air samples were analysed for Radon, Radium 226 and 228. Additionally, the CO_2 and the ozone concentrations were recorded routinely.

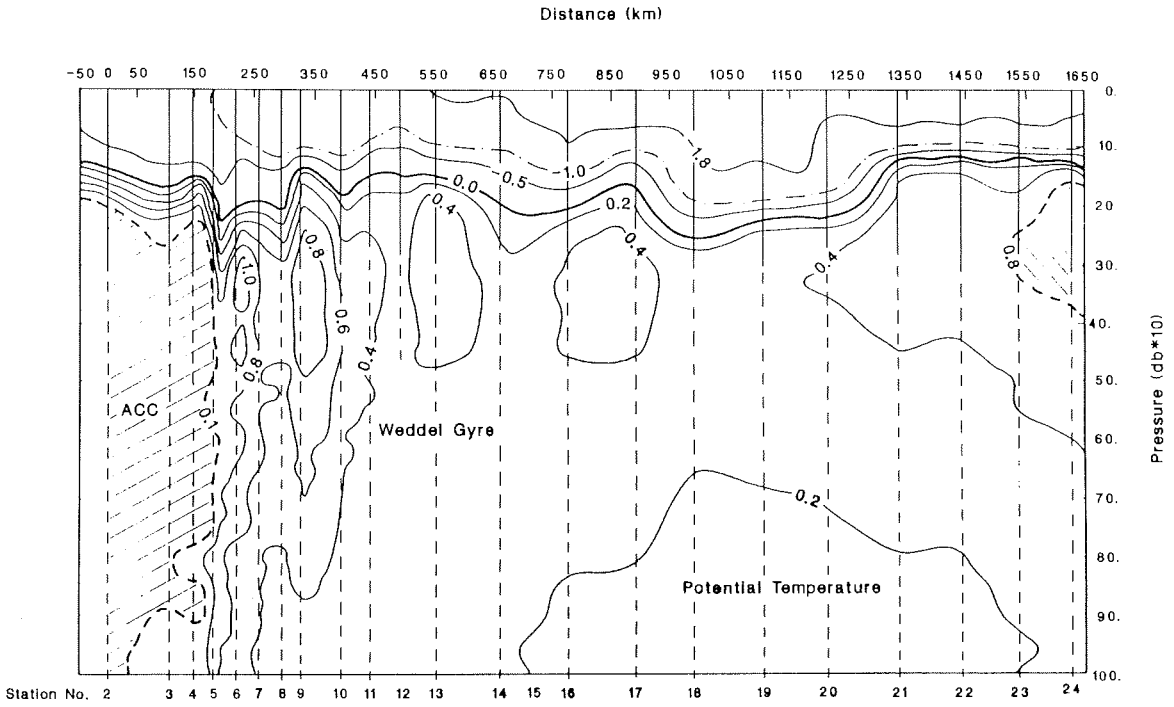

Figure 4.1: The vertical distribution of potential temperature on the southward leg of "Akademik Fedorov" (Section I)

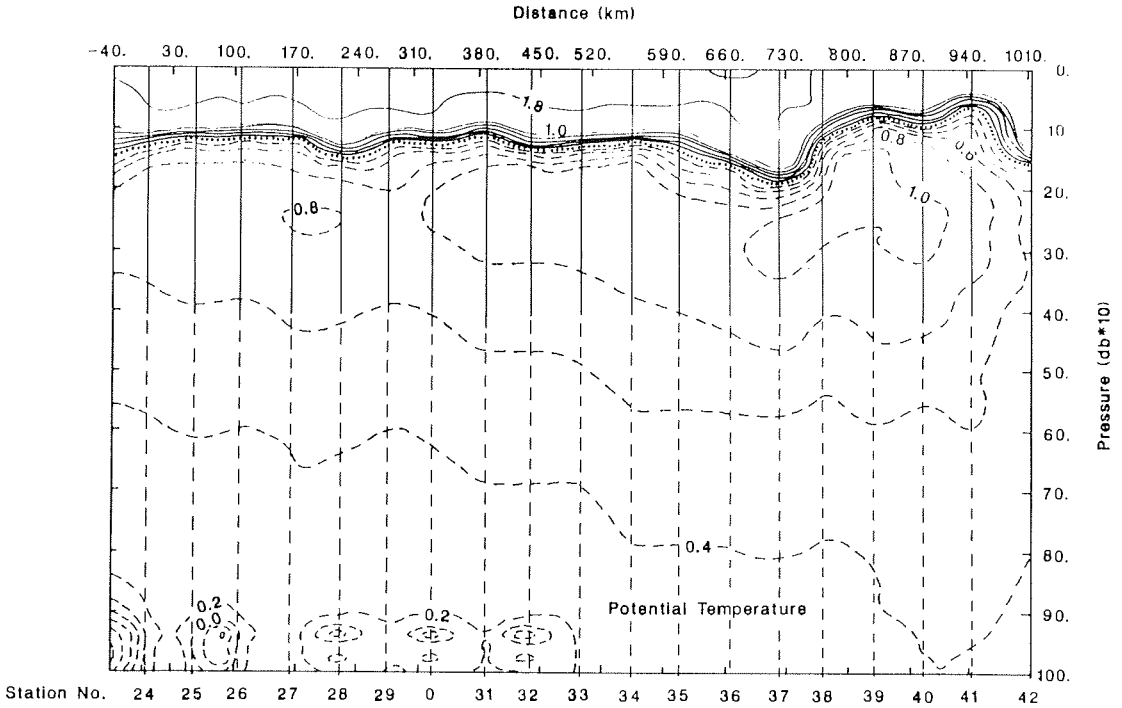

Figure 4.2: The vertical distribution of potential temperature on the southern zonal leg of "Akademik Fedorov" (Section II)

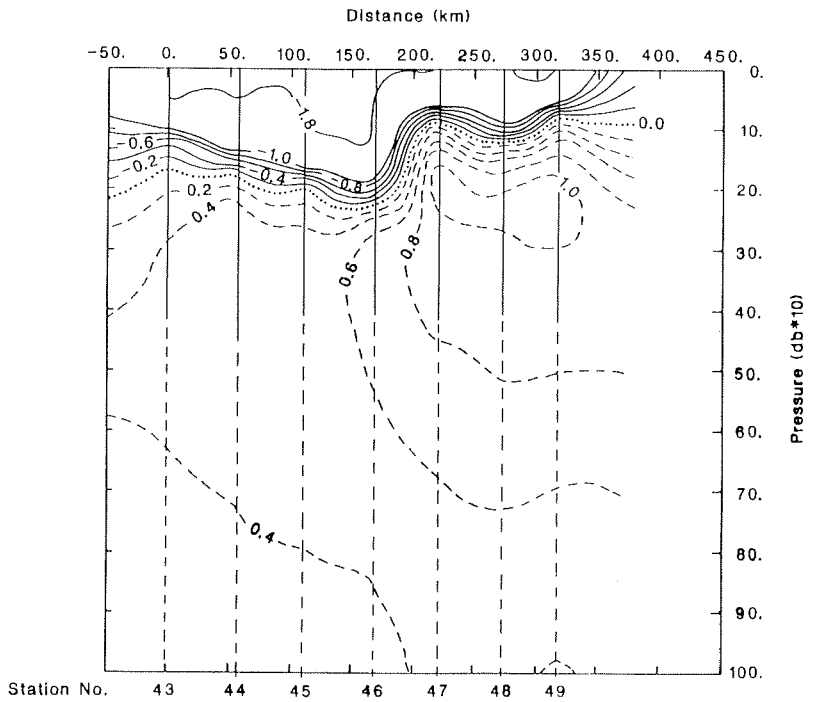

Figure 4.3: The vertical distribution of potential temperature on Section III of the "Akademik Fedorov" cruise

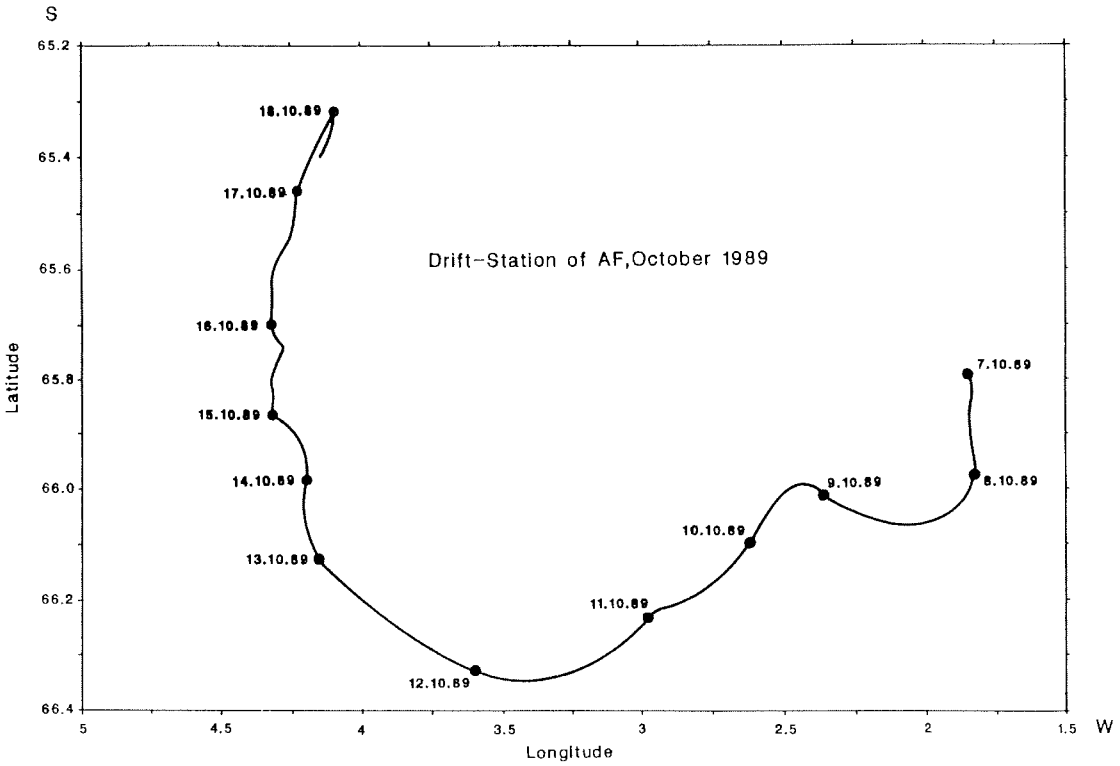

Figure 4.4: The course of "Akademik Fedorov's" drift west of Maud Rise

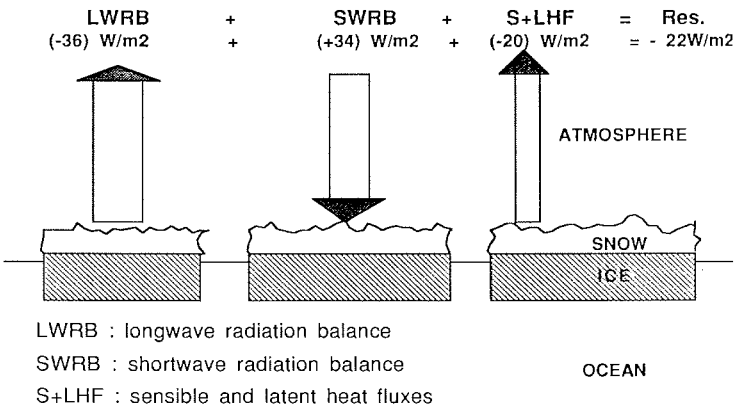

LWRB : longwave radiation balance
SWRB : shortwave radiation balance
S+LHF : sensible and latent heat fluxes

Figure 4.5: The surface radiation and heat balance estimated from measurements on "Akademik Fedorov"

2.5. Stationsliste ANT VIII/2
Station List ANT VIII/2

Station No.	Date	Start Time (GMT)	Start Position	Depth (m)	Work
16/103	09.09.89	12:03	54°00,0'S 61°01,2'W	126	XBT
16/104	09.09.89	13:08	54°11,6'S 60°57,1'W	126	XBT
16/105	09.09.89	14:42	54°29,8'S 60°51,0'W	50	XBT
16/106	09.09.89	15:50	54°44,0'S 60°46,0'W	138	XBT
16/107	09.09.89	17:20	54°59,7'S 60°42,2'W	1557	XBT
16/108	09.09.89	18:40	55°18,8'S 60°34,8'W	3820	XBT
16/109	09.09.89	19:30	55°30,0'S 60°28,4'W	4197	XBT
16/110	09.09.89	20:46	55°46,0'S 60°24,6'W	4112	XBT
16/111	09.09.89	21:58	56°00,6'S 60°22,8'W	4325	XBT
16/112	09.09.89	23:13	56°15,9'S 60°17,1'W	4702	XBT
16/113	10.09.89	00:20	56°30,8'S 60°14,7'W	3903	XBT
16/114	10.09.89	01:26	56°45,6'S 60°10,0'W	3768	XBT
16/115	10.09.89	02:40	57°02,3'S 60°04,9'W	3737	XBT
16/116	10.09.89	03:38	57°15,6'S 59°59,9'W	4279	XBT
16/117	10.09.89	04:42	57°30,1'S 59°54,1'W	4140	XBT
16/118	10.09.89	05:50	57°44,6'S 59°49,2'W	2496	XBT
16/119	10.09.89	07:17	58°01,1'S 59°45,2'W	4326	CTD
16/120	10.09.89	09:06	58°06,8'S 59°41,9'W	3887	XBT
16/121	10.09.89	09:47	58°15,5'S 59°38,0'W	3473	XBT
16/122	10.09.89	10:55	58°30,1'S 59°33,4'W	3698	XBT
16/123	10.09.89	12:08	58°45,9'S 59°27,2'W	4119	XBT
16/124	10.09.89	13:20	59°00,0'S 59°25,2'W	4078	CTD, SED
16/125	10.09.89	15:33	59°15,9'S 59°19,4'W	3831	XBT
16/126	10.09.89	16:48	59°30,0'S 59°14,1'W	4292	CTD
16/127	10.09.89	17:21	59°30,0'S 59°13,7'W	4314	LS
16/128	10.09.89	17:58	59°30,5'S 59°14,3'W	4155	XBT
16/129	10.09.89	20:27	59°59,8'S 59°00,4'W	3396	CTD
16/130	10.09.89	21:34	60°00,5'S 58°59,3'W	3530	XBT
16/131	10.09.89	22:41	60°17,2'S 58°56,0'W	3671	XBT
16/132	10.09.89	23:36	60°29,6'S 58°53,1'W	4086	XBT
16/133	11.09.89	00:50	60°46,2'S 58°46,7'W	4365	XBT
16/134	11.09.89	01:57	61°00,0'S 58°42,0'W	5204	CTD
16/135	11.09.89	04:28	61°15,5'S 58°14,7'W	2784	XBT
16/136	11.09.89	07:31	61°47,0'S 57°20,4'W	2200	XBT
16/137	11.09.89	16:04	62°00,6'S 56°59,8'W	687	CTD,APN,LS
16/138	11.09.89	19:39	62°10,0'S 56°32,3'W	1148	CTD,SED,MN
16/139	11.09.89	22:23	62°20,2'S 56°10,6'W	439	CTD
16/140	12.09.89	00:51	62°30,0'S 55°45,7'W	185	CTD
16/141	12.09.89	03:08	62°40,2'S 55°21,6'W	190	CTD
16/142	12.09.89	05:38	62°50,5'S 54°54,5'W	189	CTD
16/143	12.09.89	08:18	63°00,3'S 54°30,8'W	311	CTD,APN,SSS
16/144	12.09.89	11:11	63°11,0'S 54°05,3'W	234	CTD,SED,LS,
16/145	12.09.89	18:20	63°20,6'S 53°02,0'W	461	CTD,SED,
16/146	12.09.89	23:55	63°26,0'S 52°35,1'W	506	CTD

16/147	13.09.89	04:45	63°30,5'S 52°03,6'W	1019	CTD,BO
16/148	13.09.89	08:57	63°30,1'S 52°09,9'W	911	AWI-206,
16/149	13.09.89	15:25	63°29,4'S 51°42,7'W	1496	ICE WORK,CTD,
16/150	13.09.89	20:53	63°29,1'S 51°23,6'W	2019	CTD
16/151	14.09.89	03:08	63°46,6'S 50°53,8'W	2503	ICE WORK,
16/152	14.09.89	21:21	63°52,9'S 49°57,3'W	3004	CTD
16/153	15.09.89	02:08	63°57,1'S 49°09,5'W	3525	CTD
16/154	15.09.89	15:57	64°07,0'S 48°02,9'W	4066	ICE WORK,CTD DEPL .K6, O1
16/155	16.09.89	07:17	64°16,8'S 46°42,6'W	4378	CTD
16/156	16.09.89	16:35	64°28,7'S 45°35,4'W	4488	ICE WORK, CTD MN,SED,BO,APN DEPL. K3, K5 ,LS
16/157	17.09.89	12:50	64°45,7'S 44°31,0'W	4562	CTD
16/158	17.09.89	06:10	64°37,5'S 44°15,7'W	4582	ICE STATION CTD,MN,LS
16/159	21.09.89	21:32	64°57,1'S 42°32,9'W	4682	CTD
16/160	22.09.89	04:52	65°13,6'S 41°31,6'W	4709	CTD, DEPL. K4
16/161	22.09.89	14:50	65°24,8'S 40°19,0'W	4698	ICE WORK,CTD, MN,LS,BO,SED, APN
16/162	23.09.89	08:31	65°38,9'S 39°13,6'W	4667	CTD
16/163	23.09.89	15:00	65°40,1'S 38°46,3'W	4668	ICE WORK,CTD, SED,APN,LS
16/164	24.09.89	08:38	65°40,2'S 36°32,2'W	4761	ICE WORK, CTD,SED,APN, MN,AWI-208
16/165	25.09.89	03:55	66°02,4'S 35°04,6'W	4730	CTD
16/166	25.09.89	14:45	66°25,2'S 33°59,2'W	4716	ICE WORK,CTD, SED,APN,LS,MN
16/167	26.09.89	01:05	66°35,1'S 32°51,4'W	4732	CTD
16/168	26.09.89	13:45	66°36,6'S 31°29,1'W	4740	ICE WORK,CTD, LS,APN,MN, DEPL. O3,RTR
16/169	26.09.89	23:44	66°44,7'S 30°30,3'W	4726	CTD
16/170	27.09.89	08:10	66°54,3'S 29°14,8'W	4740	CTD
16/170	127.09.89	10:45	66°53,8'S 29°13,5'W	4744	XBT
16/170	227.09.89	12:15	66°59,7'S 28°52,9'W	4763	XBT
16/170	327.09.89	13:48	67°04,2'S 28°31,0'W	4771	XBT
16/171	27.09.89	17:30	67°00,3'S 28°04,7'W	4805	ICE STATION, CTD,LS,SED, APN,MN,BO, AWI-209
16/172	01.10.89	18:30	67°00,9'S 26°01,9'W	4818	CTD
16/173	02.10.89	04:19	67°13,6'S 24°47,7'W	4838	CTD
16/174	02.10.89	13:30	67°25,0'S 23°43,6'W	4864	ICE WORK,CTD, MN;SED,APN, LS;DEPL.W1
16/175	03.10.89	02:10	67°35,8'S 22°23,6'W	4890	CTD
16/176	03.10.89	12:55	67°47,8'S 21°18,3'W	4913	ICE WORK,CTD, LS,MN,SED,APN
16/177	04.10.89	00:45	68°03,4'S 20°01,0'W	4892	CTD

16/178	04.10.89	09:00	68°23,0'S 18°45,4'W	4799	ICEWORK,CTD,MN
16/179	04.10.89	18:50	68°49,5'S 17°57,5'W	4784	CTD
16/180	05.10.89	04:05	68°10,6'S 16°49,0'W	4756	CTD
16/181	05.10.89	13:45	69°38,2'S 15°42,2'W	4752	ICE WORK, CTD, MN,SED,APN, LS,AWI-210
16/182	06.10.89	04:30	70°00,3'S 14°40,3'W	4731	CTD
16/183	06.10.89	12:30	70°21,1'S 13°24,8'W	2937	ICE WORK,CTD, MN,SED,LS
16/184	06.10.89	20:28	70°26,3'S 13°00,1'W	2450	CTD
16/185	07.10.89	03:15	70°38,5'S 12°30,8'W	2153	CTD
16/186	07.10.89	09:11	70°47,8'S 12°11,7'W	1826	CTD
16/187	08.10.89	12:08	70°58,6'S 11°50,8'W	1177	CTD,MN
16/188	08.10.89	16:49	71°01,8'S 11°39,7'W	396	CTD
16/189	08.10.89	18:57	71°04,5'S 11°22,8'W	522	CTD
16/190	10.10.89	12:13	70°20,8'S 10°00,5'W	1980	DEPL.W2
16/191	11.10.89	09:00	70°30,5'S 08°09,8'W	245	ICE WORK
16/192	11.10.89	22:36	70°25,8'S 08°13,8'W	476	CTD
16/193	12.10.89	00:37	70°18,3'S 08°10,3'W	1150	CTD
16/194	12.10.89	04:00	70°07,7'S 08°12,0'W	2183	CTD
16/195	12.10.89	14:20	69°37,3'S 08°13,4'W	2373	ICE WORK,LS, CTD,SED,APN,MN
16/196	12.10.89	18:20	69°35,7'S 08°14,8'W	2426	INSTR.TEST
16/197	12.10.89	20:02	69°29,1'S 08°13,4'W	3117	CTD
16/198	13.10.89	00:57	69°14,5'S 08°12,3'W	3647	CTD
16/199	13.10.89	06:40	68°58,8'S 07°56,1'W	3490	ICE STATION, CTD,LS,MN
16/200	15.10.89	01:20	68°34,3'S 07°42,8'W	3988	CTD
16/201	15.10.89	10:55	68°09,0'S 07°11,9'W	4297	ICE WORK,CTD
16/202	16.10.89	04:41	67°22,8'S 06°09,8'W	4851	CTD
16/203	16.10..89	15:40	66°37,8'S 05°10,4'W	4792	ICE WORK,CTD, SED,APN,LS,MN
16/204	17.10.89	20:00	65°18,4'S 04°05,7'W	5020	CTD,BO
16/205	18.10.89	22:11	64°27,6'S 03°10,3'W	5150	CTD
16/206	19.10.89	12:55	63°34,1'S 02°09,6'W	5217	ICE WORK,CTD, LS,MN,SED,APN
16/207	20.10.89	04:15	62°39,5'S 01°11,0'W	5314	CTD
16/208	20.10.89	14:50	61°45,9'S 00°13,1'W	5350	ICE WORK,CTD, LS,MN,SED,APN
16/209	21.10.89	06:00	60°51,9'S 00°40,6'E	5391	ICE WORK,CTD
16/210	21.10.89	16:45	59°57,2'S 01°31,4'E	5032	ICE WORK,CTD LS,MN,SED,APN
16/211	22.10.89	06:30	59°03,7'S 02°25,3'E	5524	ICE WORK,CTD LS,MN,SED,APN
16/212	22.10.89	18:30	58°13,5'S 03°13,0'E	5176	ICE WORK,CTD
16/213	23.10.89	05:00	57°15,9'S 04°02,3'E	4385	ICE WORK,CTD LS,MN,SED,APN
16/214	23.10.89	12:42	56°48,4'S 04°30,4'E	5141	CTD
16/215	23.10.89	15:39	56°27,0'S 04°40,5'E	4557	MET STATION, CTD,MN
16/216	24.10.89	02:05	55°55,1'S 05°14,8'E	3571	CTD

16/217	24.10.89	05:18	55°28,0'S 05°38,5'E	3160	CTD,MN
16/218	24.10.89	10:24	55°00,7'S 06°01,7'E	3135	CTD
16/219	24.10.89	13:40	54°34,2'S 06°24,0'E	3215	CTD,MN
16/220	24.10.89	19:30	54°06,2'S 06°46,7'E	2615	CTD
16/221	24.10.89	23:03	53°39,9'S 07°08,1'E	3442	CTD,MN
16/222	25.10.89	04:29	53°13,0'S 07°29,6'E	2786	CTD,XBT
16/223	25.10.89	09:02	52°38,7'S 07°53,5'E	3749	CTD,XBT
16/224	25.10.89	10:00	52°37,7'S 07°54,5'E	3727	XBT
16/225	25.10.89	13:09	52°00,0'S 08°19,3'E	3925	XBT
16/226	25.10.89	15:45	51°28,3'S 08°35,6'E	4396	XBT
16/227	25.10.89	18:08	51°00,5'S 08°51,8'E	4303	XBT
16/228	25.10.89	20:50	50°30,0'S 09°10,9'E	4375	XBT
16/229	25.10.89	23:31	50°00,8'S 09°30,4'E	3955	XBT
16/230	26.10.89	02:19	49°29,8'S 09°49,5'E	4281	XBT
16/231	26.10.89	04:59	49°00,2'S 10°08,4'E	3150	XBT
16/232	26.10.89	07:38	48°30,7'S 10°28,1'E	3753	XBT
16/233	26.10.89	13:18	47°29,8'S 11°06,8'E	785	XBT
16/234	26.10.89	16:07	47°00,4'S 11°27,4'E	4689	XBT
16/235	26.10.89	18:55	46°30,4'S 11°43,6'E	4903	XBT
16/236	26.10.89	21:36	46°00,2'S 12°00,8'E	4585	XBT
16/237	27.10.89	00:20	45°29,1'S 12°16,7'E	4664	XBT
16/238	27.10.89	03:06	44°57,6'S 12°32,0'E	4964	XBT
16/239	27.10.89	06:32	44°30,7'S 12°46,8'E	4810	XBT
16/240	27.10.89	08:32	43°59,9'S 13°04,8'E	4640	DEPL NN
16/241	27.10.89	08:36	43°59,7'S 13°04,09'E	4651	XBT
16/242	27.10.89	11:15	43°30,0'S 13°20,2'E	4877	XBT
16/243	27.10.89	13:45	43°00,8'S 13°36,7'E	4553	XBT
16/244	27.10.89	17:25	42°30,6'S 13°53,2'E	4165	XBT
16/245	27.10.89	19:06	42°00,2'S 14°08,9'E	4218	XBT
16/246	27.10.89	21:47	41°30,3'S 14°25,5'E	4606	XBT
16/247	28.10.89	00:32	41°00,1'S 14°44,4'E	4154	XBT
16/248	28.10.89	05:30	40°30,3'S 15°02,1'E	2441	XBT
16/249	28.10.89	06:22	40°00,4'S 15°15,9'E	4624	XBT
16/250	28.10.89	09:55	39°30,4'S 15°28,3'E	4858	XBT
16/251	28.10.89	13:12	38°59,8'S 15°46,0'E	4803	XBT
16/252	28.10.89	18:18	38°30,2'S 16°01,5'E	4743	XBT

XBT	Expandable Bathythermograph
CTD	Conductivity-Temperature-Depth-Sonde
LS	Light Sensor
SED	Secchi Disk
APN	Apstein Net
MN	Multinet
SSS	Side Scan Sonar
ICE WORK	Routine ice measurements
ICE STATION	Longer term station including ice work, meteorology and oceanography
BO	Bongonet
AWI-NNN	Deployment of current meter mooring
DEPL NN	Deployment of drifting buoy
RTR	Ring trawl

2.6. Zeitplan / Time Table

RV Polarstern

WWGS-Work	11 September to 25 October 1989
Arrival at Cape Town (South Africa)	30 October 1989

RV Akademik Fedorov

Departure from Montevideo	12 Sptember 1989
WWGS-Work	15 September to 22 October
Arrival at Puerto Madryn	08 November 1989

2.7 Beteiligte Institute / Participating Institutions on RV "Polarstern"

Adresse Address		Teilnehmerzahl Number of participants
Federal Republic of Germany		
AWI	Alfred-Wegener-Institut für Polar- und Meeresforschung Postfach 12 01 61 2850 Bremerhaven	37
DWD	Deutscher Wetterdienst Bernhard-Nocht-Straße 76 2000 Hamburg 4	3
HSW	Helicopter Service Wasserthal GmbH Kätnerweg 43 2000 Hamburg 65	4
IfBG	Georg-August-Universität Forstwissenschaftlicher Fachbereich Institut für Bioklimatologie Büsgenweg 1 3400 Göttingen	2
IMH	Institut für Meteorologie und Klimatologie der Universität Hannover Herrenhäuserstraße 2 3000 Hannover 1	5
MPIfM	Max-Planck-Institut für Meteorologie Bundesstraße 55 2000 Hamburg 13	1
RB	Radio Bremen Heinrich-Hertz-Straße 2800 Bremen	1
RUB	Ruhr-Universität Bochum Fakultät für Chemie Lehrstuhl für Physikalische Chemie I Universitätsstraße 150 4630 Bochum 1	1
UNIB	Universität Bremen Bibliothekstraße 2800 Bremen	5

UNIK	Universität Konstanz Limnologisches Institut Mainaustraße 212 7750 Konstanz	2

Canada

AES	AES/Cress Microwave Group Petrie 014-York University 4700 Keele Street North York, Ontario Canada M3J 1P3	1

United Kingdom

SPRI	Scott Polar Research Institute Lensfield Road Cambridge CB2 1ER	3

United States of America

CRREL	US Army Cold Regions Research and Engineering Laboratory 72 Lyme Road Hanover, NH 03755	2
GSFC	NASA/Goddard Space Flight Center Lboratory for Oceans, Code 61 Greenbelt, Maryland, 20771	1
OSU	Oregon State University College of Oceanography Oceanography Admin. Bld. 104 Corvallis, Oregon 97331-5503	3
UNIM	University of Massachusetts Amherst, MA 01003	1

Union of Socialistic Soviet Republics

AARI	Arctic and Antarctic Research Institute 38 Berin Street 19226 Leningrad	2
IFB	Institute for Botany Academy of Sciences 2 Popov Street 197022 Leningrad	1
IFO	Institute of Fishery and Oceanography 17 a Verkhnyaya Krasnoselskaya 107140 Moskau	1

2.8. Fahrtteilnehmer / Participants

2.8.1 on RV "Polarstern"

Name Name	Institut Institute
Augstein, E.	AWI
Bathmann, U.	AWI
Beyer, K.	AWI
Bredemeier, M.	IfBG
Carbonell, M. C.	OSU
Casarini, M. P.	SPRI
Claffey, K.	CRELL
Comiso, J.	GSFC
Crane, D.	SPRI
Dittmer, K.-P.	DWD
Eicken, H.	AWI
Engelbart, D.	IMH
Fahl, Kirsten	AWI
Fahrbach, E.	AWI
Frieden, W.	IMH
Fromme, J.-P.	AWI
Garrity, C.	AES
Gerdes, A.	RB
St. Germain, K.	UNIM
Gradinger, R.	AWI
Hehl, O.	IMH
Helmes, L.	AWI
Helwig, A.	HSW
Heusel, R.	UNIK
Ibrahim, J.	HSW
Jennings, J.	OSU
Lange, M.	AWI
Lemke, P.	MPI, HH
Lytle, V.	CRREL
Lyeleev, M.	AARI
Mahler, G.	HSW
Mahnke, P.	AWI
Makarov, R.	IfO
Meyer, G.	AWI
Möhrke, H.	HSW
Nikolaev, V.	IfB
Nöthig, E.-M.	AWI
Ochsenhirt, W.-T.	DWD
Olf, J.	IMH
Reisemann, M.	AWI
Rohardt, G.	AWI
Ross, A.	OSU
Schenk, C.	AWI
Schröder, M.	AWI
Schütt, E.	UNIB
Surkow, R.	IMH

Viehoff, Th.	AWI
Vogeler, A.	AWI
Wadhams, P.	SPRI
Weissenberger, J.	AWI
Wicke, A.	UNIB
Wieser, Th.	UNIK
Witte, H.	AWI
Wisotzki, A.	UNIB
Wolf-Gladrow, D.	AWI
Yurganov, L.	AARI

2.8.2 German participants on RV "Akademik Fedorov"

Wamser, C.	AWI
König-Langlo, G.	AWI
Loose, B.	AWI
Stichternaht, A.	UNIB
Bosse, J.	UNIB
Genz, G.	UNIB

2.9. Schiffsbesatzung /Chip`s Crew on RV "Polarstern"

	ANT VIII/2
Kapitän	Jonas
1. Offizier	Gerber
Naut. Offizier	Schiel
1. Offizier Ladung	Fahje
Naut. Offizier	Baumhoer
Arzt	Dr. Reimers
Ltd. Ingenieur	Schulz
1. Ingenieur	Erreth
2. Ingenieur	Delff
2. Ingenieur	Simon
Elektriker	Erdmann
Elektroniker	Thonhauser
Elektroniker	Hoops
Elektroniker	Both
Elektroniker	Muhle
Funkoffizier	Butz
Funkoffizier	Müller
Koch	Klasaen
Kochsmat	Klauck
Kochsmaat	Kröger
1. Steward	Peschke
Krankenschwester/ Stewardess	Lieboner
Stewardess	Hoppe
Steward/Stewardess	Rusdam
Steward/Stewardess	Gollmann
2. Steward	Chi-Chun, Chang
2. Steward	Yiu-Sin, Chau
Wäscher	Tzyh-Shyang, Shyu
Bootsmann	Schwarz
Zimmermann	Kassubeck
Matrose	Meis Torres
Matrose	Martinez
Matrose	Willbrecht
Matrose	Novo Lovreira
Matrose	Prol Otero
Matrose	Pereira Portela
Lagerhalter	Barth
Maschinenwart	Jordan
Maschinenwart	Fritz
Maschinenwart	Heurich
Maschinenwart	Buchas
Maschinenwart	Reimann